Shallow Water Wave Correction in the OEB (Monochromatic and Bichromatic Waves)

Zaman, Hasanat; Peng, Heather; Baddour, Emile

Publisher's version / Version de l'éditeur:
https://doi.org/10.4224/17210702
Technical Report, 2010-11-01

DOCUMENTATION PAGE

REPORT NUMBER	NRC REPORT NUMBER	DATE		
TR-2010-21		September 2010		
REPORT SECURITY CLASSIFICATION		**DISTRIBUTION**		
Unclassified		Unlimited		
TITLE				
SHALLOW WATER WAVE CORRECTION IN THE OEB (Monochromatic and Bichromatic waves)				
AUTHOR (S)				
Hasanat Zaman, Heather Peng and Emile Baddour				
CORPORATE AUTHOR (S)/PERFORMING AGENCY (S)				
National Research Council, Institute for Ocean Technology and Memorial University of Newfoundland				
PUBLICATION				
SPONSORING AGENCY(S)				
IOT PROJECT NUMBER		**NRC FILE NUMBER**		
42_2298_10 Project: Wave quality (42_2414_26)				
KEY WORDS		**PAGES**	**FIGS.**	**TABLES**
Second order waves, monochromatic and bichromatic waves, unwanted free waves.		ix, 97	38	7

SUMMARY

In this work first order and second order wave generation techniques are utilized to study the correct generation of mono and bichromatic waves in the OEB. For a flat bottom wave basin when the interaction between two frequencies are considered bounded sub harmonics or bounded low frequency waves are generated at the difference frequency and bounded super harmonics or bounded high frequency waves are generated at the sum frequency and they travel locked with their generating / fundamental wave components along with some unwanted free waves. These free waves are, free waves due to first order motion of the wave boards, free wave due to displacement of the wave board from its zero position and free wave due to local disturbances. These unwanted free waves are inevitable due to the linear motion of the wave maker. The second order wave generation technique includes second order board motion and correction components of the above-mentioned unwanted free waves. In this study only sub-harmonics or low frequency wave components are considered. Total 14 wave probes are used to capture the data in the wave tank. A NRC-IOT code (LWAVE) is used to isolate the primary waves, the bounded waves and the unwanted free waves from the measured data at each wave probe. The measured data are analyzed in this paper to illustrate the differences in the waves generated by two different generation techniques.

ADDRESS National Research Council
Institute for Ocean Technology
Arctic Avenue, P. O. Box 12093
St. John's, NL A1B 3T5
Tel.: (709) 772-5185, Fax: (709) 772-2462

National Research Council Canada
Conseil national de recherches Canada

Institute for Ocean Technology
Institut des technologies océaniques

SHALLOW WATER WAVE CORRECTION IN THE OEB
(Monochromatic and Bichromatic waves)

TR-2010-21

Hasanat Zaman, Heather Peng and Emile Baddour

September 2010

TABLE OF CONTENTS

LIST OF PHOTOS

LIST OF TABLES

LIST OF FIGURES

ABSTRACT
In this work first order and second order wave generation techniques are utilized to study the correct generation of mono and bichromatic waves in the OEB. For a flat bottom wave basin when the interaction between two frequencies are considered bounded sub harmonics or bounded low frequency waves are generated at the difference frequency and bounded super harmonics or bounded high frequency waves are generated at the sum frequency and they travel locked with their generating / fundamental wave components along with some unwanted free waves. These free waves are, free waves due to first order motion of the wave boards, free waves due to displacement of the wave board from its zero position and free waves due to local disturbances. These unwanted free waves are inevitable due to the linear motion of the wave maker. The second order wave generation technique includes second order board motion and correction components of the above-mentioned unwanted free waves. In this study only sub-harmonics or low frequency wave components are considered. Total 14 wave probes are used to capture the wave data in the wave tank. A NRC-IOT code (LWAVE) is used to isolate the primary waves, the bounded waves and the unwanted free waves from the measured data at each wave probe. The measured data are analyzed in this paper to illustrate the differences in the waves generated by two different generation techniques.

INTRODUCTION
Recently, the correct generation of the second order waves and the reproduction of group-induced second order low and high frequency waves have been considered essential for physical model tests in the laboratory to understand the effects of the wave-action phenomena on, for instance, offshore structures, mooring system, floating vessels, harbour resonance, loadings, etc.

Proper understanding of the effects of the wave-action and consequent loading pattern of the primary waves along with their bounded waves are very important factors in design, implement and operation of any ocean structures, mooring system, floating vessels, harbour resonance, etc.. In an accurate physical model test in the laboratory it is crucial to choose the precise design parameters of such structures and/or vessels, etc. So the generation of spurious waves free primary waves and the reproduction of the group-induced second-order low frequency and high frequency components are essential for physical model tests in the laboratory. Please see Zaman and Mak (2007) for high frequency second-order wave components.

When bi-chromatic primary waves are generated in the wave basin the required bounded waves will also be generated naturally at the difference frequency. In addition to that several unwanted free waves are also generated. The Free wave-1, having the same frequency of the bounded wave is reproduced due to mismatch of the boundary conditions at the wave paddle. The Free wave-2 is due to the wave paddle displacement from its zero position. There is another type of free wave due to the local disturbances. The local disturbances usually disappear at some distance from the wave-makers and thus are not discussed here. Those free waves are evidently generated and propagate towards the test model and reflect from the boundaries and can cause an amplification of low frequency wave phenomena, such as harbour resonance and oscillations of moored ships and, breaking of waves on floating or fixed structures. In this experiment second order wave generation technique is also successfully used to reproduce the correct bounded waves along with elimination of the unwanted free waves from the wave profiles. This experiment is implemented by means of compensating free waves imposed on the system by second-order paddle motion. The control signal for this motion has to be introduced along with the primary waves. If the wave basin is not unconditionally flat then there might be some other types of unwanted free waves in the basin in addition to the aforesaid three categories.

When there are two waves (*i.e.* Bichromatic wave) of frequencies f_1 and f_2 form a group, the group-induced second-order low and high frequency waves (bounded) are generated along with other unwanted free waves. A low frequency wave or long wave will be produced due to the difference (f_1 - f_2) of the frequencies and a high frequency or short wave would be generated due to the summation (f_1 + f_2) of the frequencies. Fig. 1 shows an example of a typical wave group and its locked bounded high and low frequency waves.

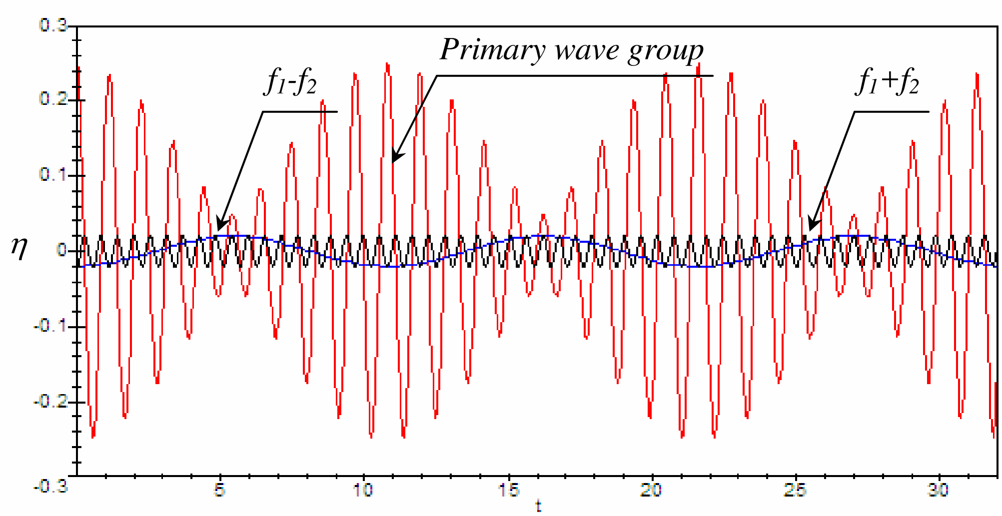

Fig. 1 An example: A primary wave group formed by two different wave frequencies. [H=0.2m and f1 =0.833 Hz, and H=0.28m and f2 =0.926 Hz]

In this report we only concentrated on the low frequency (f_1 - f_2) wave components and high frequency components (f_1 + f_2) will not be discussed here. Please refer to Zaman and Mak (2006) for high frequency waves components. The profile of the long wave having frequency (f_1 - f_2) is generally termed as the set-down in the larger wave zone and the set-up in the smaller wave zone (*see* Figure 1).

These set-down and set-up phenomena were first investigated and reported by Longuet-Higgins and Stewart (1961, 1962, 1963, 1964 and 1977) in a series of papers. They introduced the radiation stress concept, which explained that in a wave group individual wave components exerted an internal compressive force in the direction of the wave propagation. To balance this force the mean water level goes down in the region of larger waves known as set-down and goes up in the region of smaller waves known as set-up. Bowen et al (1968) later explained the set-up and set-down phenomena with experimental data.

The theoretical and experimental descriptions of such natural low frequency waves along with their various unwanted free waves were given by many researchers. Hansen (1978), Sand (1982), Barthel et al (1983), Sand and Mansard (1986), Mansard (1991), Mansard et al (1987), Schaffer (1993), Stansberg (2006), Zaman and Mak (2006, 2007), Spinneken and Swan (2009), Zaman et al (2010) are a few who described the methods for curtailing these unavoidable free waves in the resulting surface elevations in the wave basin.

In our present experiments the first-order and the second-order wave generation techniques for the monochromatic and bichromatic waves were used. In the experiment water depths are varied in the range of 0.3m to 0.8m. The wave periods also have varied from 1.0s to 4.105s for monochromatic waves and 0.9s to 2.22s for bichromatic waves. However in this paper several cases of monochromatic waves of different water depths and periods are discussed (Table-2). Bichromatic waves in the water depth of 0.4m and period 1.25s to 2.22s are also shown and discussed (Table-3). Comparisons are made between data obtained from the first-order wave generation and the second-order wave generation technique.

In this experiments first order and second order wave generation techniques are employed to measure data in the wave basin. LWAVE code is then used to isolate various wave components from the measured wave profiles at different probe locations. The relevant component waves obtained from the first and the second order wave generation techniques are compared.

THEORY

A wave group would be generated with the presence of at least two frequencies (bi-chromatic wave). The difference of these two frequencies would generate a long period bounded wave with a period equal to the period of the wave group. This long wave is also known as 'set-up' at the high waves zone and 'set-down' at the low waves zone.

A pair of regular waves with frequencies f_n and f_m and, surface elevations η_n and η_m respectively would constitute a wave group as follows (Sand 1982):

$$\begin{aligned} \eta_{nm}(t) &= \eta_n(t) + \eta_m(t) \\ &= a_n \cos(\omega_n t - k_n x) + b_n \sin(\omega_n t - k_n x) \\ &+ a_m \cos(\omega_m t - k_m x) + b_m \sin(\omega_m t - k_m x) \end{aligned} \tag{1}$$

where, ω_n and ω_m are the wave angular frequencies, k_n and k_m the wave numbers, x the spatial distance, t the time and a_n, b_n, a_m and b_m are the Fourier coefficients.

The first-order control signal for only two frequencies can be derived as follows [see also Barthel et al (1983)]:

$$X_1 = \frac{\cosh(k_1 h)\sinh(k_1 h) + k_1 h}{2\sinh^2(k_1 h)}(a_1 \sin\omega_1 t - b_1 \cos\omega_1 t) + \frac{\cosh(k_2 h)\sinh(k_2 h) + k_2 h}{2\sinh^2(k_2 h)}(a_2 \sin\omega_2 t - b_2 \cos\omega_2 t) \quad (2)$$

By means of Laplace equations, the second order contributions due to difference frequency can be given as follows:

$$\eta_2^-(x,t) = G_{mn}^-(a_m a_n - b_m b_n)\cos(\Delta\omega_{mn}^- t - \Delta k_{mn}^- x) + G_{mn}^-(a_m b_n + a_n b_m)\sin(\Delta\omega_{mn}^- t - \Delta k_{mn}^- x) \quad (3)$$

where, G_{mn}^- is a second order quadratic transfer function, $\Delta\omega_{mn}^- = \omega_n - \omega_m$ and $\Delta k_{mn}^- = k_n - k_m$.

The quadratic transfer function is given by the following equation:

$$G_{mn}^- = \left(\frac{A_{nm}^-(\omega_n - \omega_m)}{2g} - \frac{k_m k_n g}{4\omega_m \omega_n}(1 + \tanh k_m h \tanh k_n h) + \frac{1}{4}(k_m \tanh k_m h + k_n \tanh k_n h)\right)\delta \quad (4)$$

where,

$$A_{nm}^- = \frac{1}{2}\frac{B_{mn}^- + C_{mn}^-}{(\omega_n - \omega_m)^2 - (k_n - k_m)g\tanh(k_n - k_m)h}g^2 \quad (5)$$

$$B_{mn}^- = \frac{k_m^2}{\omega_m \cosh^2 k_m h} - \frac{k_n^2}{\omega_n \cosh^2 k_n h} \quad (6)$$

$$C_{mn}^- = \frac{2k_m k_n(\omega_n - \omega_m)(1 + \tanh k_m h \tanh k_n h)}{\omega_m \omega_n} \quad (7)$$

where, h is the water depth and g is the acceleration due to gravity and

$$\delta = \begin{cases} 1 & n \neq m \\ 0.5 & n = m \end{cases}$$

The second order control signal for a correct reproduction of the wave train up to second order takes the following form:

$$X_2^-(t) = ((a_n b_m - a_m b_n)F_1^- + (a_n a_m + b_m b_n)F_{23}^-)*$$
$$\cos(\Delta\omega_{mn}^- t) + ((a_n a_m + b_m b_n)F_1^- + \quad (8)$$
$$(a_m b_n - a_n b_m)F_{23}^-)\sin(\Delta\omega_{mn}^- t)$$

The function F_1 is written as:

$$F_1^- = F_{11}^- + F_{12}^- \quad (9)$$

$$F_{11}^- = \left[G_{mn}^- \Delta k_f^- h \begin{Bmatrix} (\Delta k_{mn}^- h - \Delta k_f^- h)\sinh(\Delta k_{mn}^- h + \Delta k_f^- h) + \\ (\Delta k_{mn}^- h + \Delta k_f^- h)\sinh(\Delta k_{mn}^- h - \Delta k_f^- h) \end{Bmatrix} \right] / \left[2((\Delta k_{mn}^- h)^2 - (\Delta k_f^- h)^2)\sinh(\Delta k_{mn}^- h)\sinh(\Delta k_f^- h) \right] \quad (10)$$

$$F_{12}^- = \frac{f_m \Delta k_f^- k_m h(1+H_n)[\delta k_m^- h \sinh(\delta k_m^+ h) + \delta k_m^+ h \sinh(\delta k_m^- h)]}{8(f_n - f_m)((k_m h)^2 - (\Delta k_f^- h)^2)\sinh(\Delta k_f^- h)\sinh(k_m h)\tanh(k_n h)} + \frac{f_n \Delta k_f^- k_n h(1+H_m)[\delta k_n^- h \sinh(\delta k_n^+ h) + \delta k_n^+ h \sinh(\delta k_n^- h)]}{8(f_n - f_m)((k_n h)^2 - (\Delta k_f^- h)^2)\sinh(\Delta k_f^- h)\sinh(k_n h)\tanh(k_m h)} \quad (11)$$

The free long wave number Δk_f^- is computed from the dispersion relation given as:

$$(\Delta\omega_{mn}^-)^2 = g\Delta k_f^- \tanh(\Delta k_f^- h) \quad (12)$$

where,

$$\delta k_m^\pm = k_m \pm \Delta k_f^- \quad (13)$$

$$\delta k_n^\pm = k_n \pm \Delta k_f^- \quad (14)$$

$$H_m = \frac{2k_m h}{\sinh(2k_m h)}; H_n = \frac{2k_n h}{\sinh(2k_n h)} \quad (15)$$

$$F_{23}^- = F_2^-(F_{3,m}^- - F_{3,n}^-) \quad (16)$$

$$F_2^- = \frac{\Delta k_f^-(1+H_m)(1+H_n)}{8\tanh(k_m h)\tanh(k_n h)} \quad (17)$$

$$F_{3,m}^{-} = \frac{f_m}{(f_n - f_m)} \sum_{j=1}^{\infty} \frac{2k_j h \sin(k_j h)[k_j h \sin(k_j h) \coth(\Delta k_f^{-} h) + \Delta k_f^{-} h \cos(k_j h)]}{((k_j h)^2 + (\Delta k_f^{-} h)^2)(\sin(k_j h)\cos(k_j h) + k_j h)} \quad (18)$$

where, $k_j h$ is computed from the following expression:

$$\frac{4\pi^2 h f_m^2}{g} = -k_j h \tan(k_j h), \text{ with } (j - \tfrac{1}{2})\pi < k_j h < j\pi \quad (19)$$

EXPERIMENTS

In the present experiment various water depths such as, 0.3m, 0.4m, 0.5m, 0.6m and 0.8m were used. The experiments were carried out for monochromatic and bichromatic waves. For both wave cases first order and second order generation techniques are used.

Software

In IOT bichromatic waves are generated using BIWAVE computer code. This is a first order wave generation code. The second order bichromatic wave generation code SOWG is developed using Sand's (1982) formula. We used these two codes to generate waves in the OEB. When surface elevations are measured a computer code called LWAVE is used to isolate the component waves.

Experimental setup

Total fourteen (14) wave probes were employed to record the experimental data in the OEB. Figure 2 shows the experimental setup and red circles are the locations of the wave probes. The distances of the wave probes from the wave paddle are shown in Table 1.

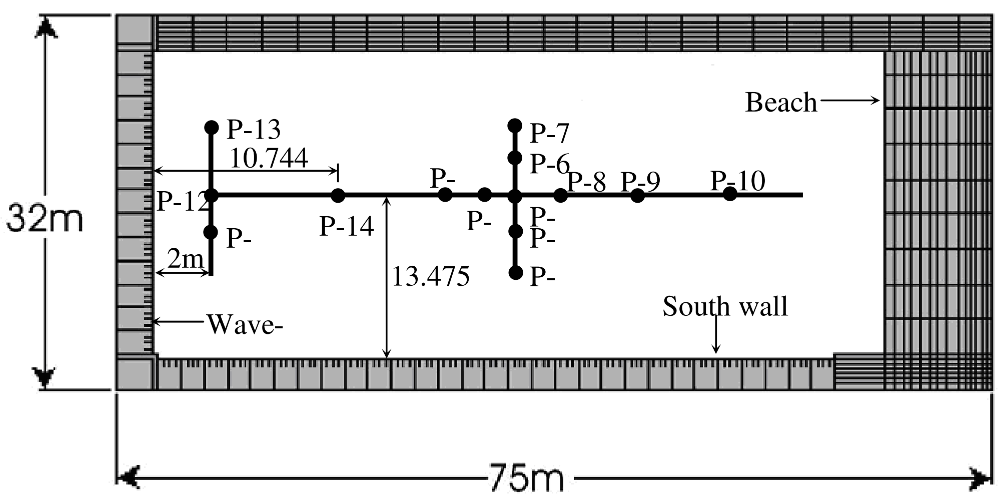

Fig. 2 Top view of the experimental setup in the OEB

Photo 1: Setup of 14 wave probes in the OEB.

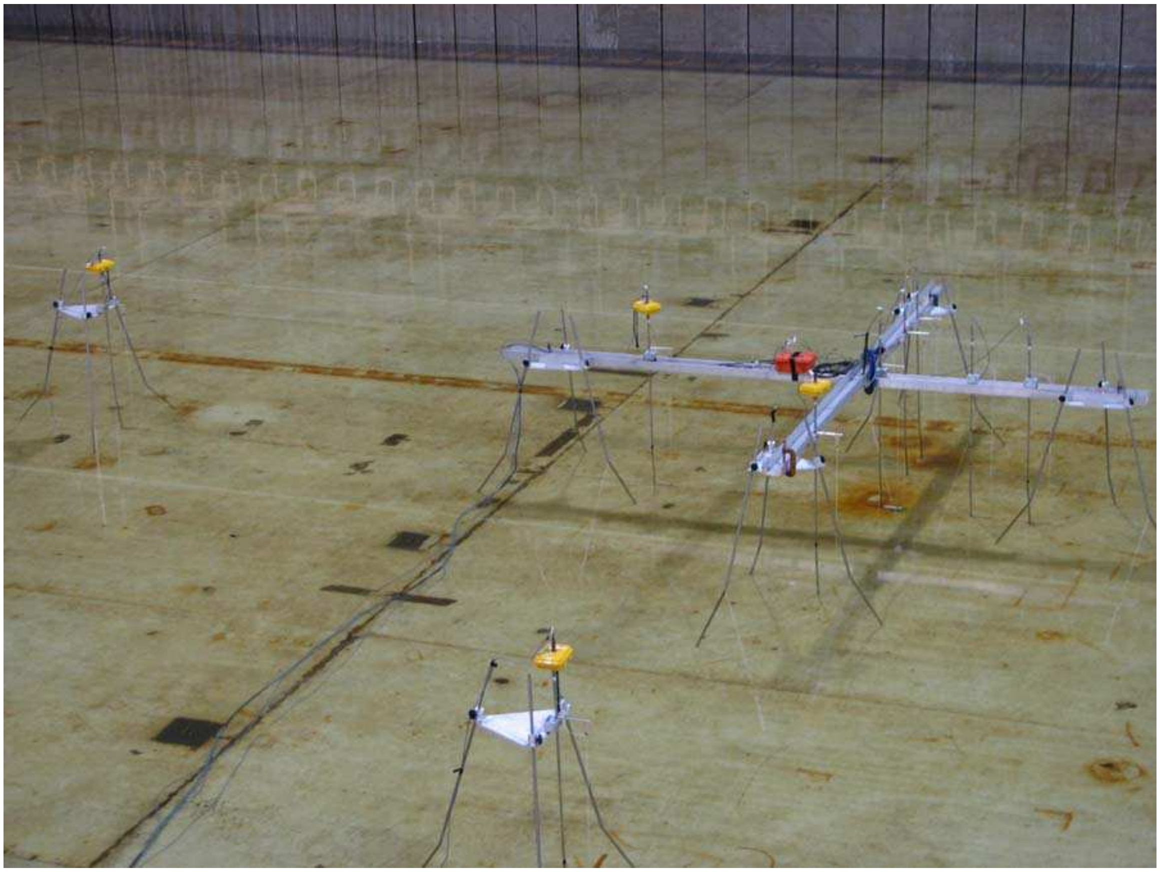

Photo 2: 8 wave probes are set over the cross

Table 1 Location of the wave probes in the OEB

No of the probe	Distance from the east wave paddle (m)	Distance from the south wall (m)
1	26.891	13.475
2	27.221	13.475
3	27.731	13.475
4	27.731	12.955
5	27.731	12.635
6	27.731	14.825
7	27.731	18.365
8	29.081	13.475
9	32.621	13.475
10	41.621	13.475
11	2.0	12.635
12	2.0	13.475
13	2.0	18.365
14	10.744	13.475

The bottom of the basin was flat and the blanking plates were deployed to cover the north beach.

CASE STUDY - 1: Monochromatic waves

In this experiment monochromatic waves of different wave periods, wave heights and water depths are used. Table 2 shows the wave conditions for 0.4m water depths. Table 3 shows the wave parameters that we used in the experiments for 0.5m water depth while Table 4 shows the same parameters for 0.8m water depth. For all water depths first order and second order wave generation techniques are utilized. Some comparisons of the wave profiles obtained from two different wave generation techniques are also shown.

Table 2 Incident wave parameters (*h=0.4m*)

	T_1 (s)	H_1 (m)	h(m)	h/L
C4-1	1.228	0.02	0.4	0.20
C4-2	1.0	0.04	0.4	0.27
C4-3	1.228	0.04	0.4	0.20
C4-4	2.145	0.04	0.4	0.10
C4-5	1.0	0.08	0.4	0.27
C4-6	2.145	0.08	0.4	0.10
C4-7	4.105	0.08	0.4	0.05
C4-8	3.116	0.12	0.4	0.07
C4-9	4.105	0.16	0.4	0.05

Figs. 3 to 11 show surface elevations for the wave conditions mentioned in Table 2. Measured surface elevations at probes 14, 1, 2, 3 and 8 are plotted to show wave propagation along the longitudinal direction of the wave tank while probes 3, 4, 5, 6 and 7 illustrate wave profiles along the transverse direction of the wave tank. Figs. 11 to 13 show wave profiles in the transverse direction and just 2m away from the wave maker

Table 3 Incident wave parameters (*h=0.5m*)

	T_1 (s)	H_1 (m)	h(m)	h/L
C5-1	1.182	0.02	0.5	0.25
C5-2	1.0	0.04	0.5	0.33
C5-3	1.182	0.04	0.5	0.25
C5-4	1.977	0.04	0.5	0.13
C5-5	1.0	0.08	0.5	0.33
C5-6	1.977	0.08	0.5	0.13
C5-7	3.704	0.08	0.5	0.06
C5-8	2.829	0.12	0.5	0.08
C5-9	3.704	0.16	0.5	0.06

Figs. 12 to 20 demonstrate surface elevations for the wave conditions mentioned in Table 3. In this case also probes 14, 1, 2, 3 and 8 and, probes 3, 4, 5, 6 and 7 are plotted separately to illustrate wave profiles in the longitudinal and transverse directions of the tank.

Table 4 Incident wave parameters (*h=0.8m*)

	T_1 (s)	H_1 (m)	h(m)	h/L
C8-1	3.035	0.08	0.8	0.25
C8-2	4.105	0.08	0.8	0.33

Figs. 21 to 22 show similar descriptions of the wave profiles for wave conditions expressed in Table 4

Figs. 23 to 25 show some comparisons of the measured wave profiles obtained from first- and second-order wave generation techniques for water depth 0.5m as mentioned in Table 3.

Comparing the results of the shallowest case C5-7, it may be observed that the amplitudes of the wave profiles measured close to the blanking wall (Probe-7) are relatively small for both first-order (Fig. 25a) and second-order cases (Fig. 25b). The amplitudes of the measured wave profiles and wave heights for both first- and second-order cases of run C5-7 are shown in Table 5.

Table 5 Measured wave parameters for C5-7 case. First-order and Second-order runs

Probe No.	First-order generation			Second-order generation			(Hs-Hf)*100 / H1 %
	Crest	Trough	Wave height (Hf)	Crest	Trough	Wave height (Hs)	
1	0.0644	-0.0316	0.0961	0.0636	-0.0370	0.1007	5.71
2	0.0634	-0.0301	0.0947	0.0663	-0.0362	0.0996	6.09
3	0.0597	-0.0343	0.0941	0.0623	-0.0331	0.0955	1.76
8	0.0612	-0.0316	0.0928	0.0616	-0.0325	0.0941	1.63
Fig. 25a				**Fig. 25b**			
3	0.0597	-0.0343	0.0941	0.0623	-0.0331	0.0955	1.76
4	0.0554	-0.0334	0.0888	0.0642	-0.0280	0.0922	4.24
5	0.0558	-0.0327	0.0885	0.0611	-0.0280	0.0891	0.65
6	0.0608	-0.0368	0.0977	0.0611	-0.0354	0.0965	-1.43
7	0.0429	-0.0242	0.0672	0.0431	-0.0302	0.0733	7.62
Fig. 25c				**Fig. 25d**			
11	0.0373	-0.0334	0.0708	0.0517	-0.0245	0.0762	6.64
12	0.0373	-0.0344	0.0717	0.0491	-0.0235	0.0726	1.07
13	0.0331	-0.0311	0.0642	0.0424	-0.0260	0.0684	5.24
Fig. 25e				**Fig. 25f**			

Table 5 shows the crests, troughs and the wave heights obtained from run C5-7 for both first-order and second-order generation techniques. The comparisons [(Hs-Hf)/H1*100] of the wave heights are done with respect to the incident wave height (H1). Where Hf is the wave height obtained from the first-order generation and Hs is the wave height for second-order generation.

CASE STUDY - 2: Bichromatic waves

In this report, bichromatic waves are considered on a 0.4m water depth. The aim of this study was to investigate and compare the propagation of the primary and the bounded waves and quantify the hereditary spurious waves in the OEB. In this category of experiments our focus would be to understand and use the first order and the second order wave generation techniques to generate correct primary and bounded waves and to isolate the spurious waves.

As we already stated above, several cases of the 0.4m water depth experiments are reported. Table 6 summarizes the incident wave parameters of the three different wave conditions examined in this work.

Table 6 Incident wave parameters

	T_1 (s)	h(m)	H_1 (m)	T_2 (s)	H_2 (m)	h/L
Case-1	1.25	0.4	0.06	1.17	0.06	0.195
Case-2	1.55	0.4	0.06	1.45	0.06	0.146
Case-3	2.22	0.4	0.06	2.00	0.06	0.096

For each case, there were two runs, one used the first-order generation technique and the other one used the second-order wave generation technique. Figs. 26 and 27 show the comparisons of the spectrums at 6 different locations in the wave basin between first-order and second-order wave generation techniques for Case-1 and Case-2, respectively. This 6 locations are at Probe-14, Probe-1, Probe-2, Probe-3, Probe-8 and Probe-9. These probes are on the same line down the wave tank, see Fig. 1. No big differences in the results are observed in these comparisons, especially in the components of the low frequency second order waves.

Fig. 28 shows the same comparisons for Case-3. In this figure one can perceive the differences in low frequency second order wave components between two different generation techniques.

LWAVE utilization

A NRC-IOT computer code LWAVE that can split a surface elevation data set into its component waves is used to isolate the primary waves, bounded second order waves and unwanted free waves from the raw measured data at every probe location. For First-order wave generation technique, Figs. 29 show the isolated component waves for Case-2 at 6 different probe locations, Probe-14, Probe-1, Probe-2, Probe-3, Probe-8 and Probe-9. Among the five figures, the first one represents the incident wave, the second one is the bounded wave, the third is the Free-wave-1 having the same frequency of the bounded wave and is reproduced due to mismatch of the boundary conditions at the wave paddle, the fourth one is the Free- wave-2 due to the wave paddle displacement from its zero position and the last one is the summation of all the above four waves. Figs. 30 show the similar results for Case-3.

For Second-order wave generation technique, Figs. 31 show the isolated component waves for Case-2 at 6 different probe locations, Probe-14, Probe-1, Probe-2, Probe-3, Probe-8 and Probe-9 while Figs. 32 demonstrate alike results for Case-3.

Comparing Figs. 26 and 27 no big differences in the results of energy density is observed especially in the components of the low frequency second order waves. Fig. 28

shows the same comparisons for Case-3. In this figure one can perceive the differences in the low frequency second order wave components between two different generation techniques. So from now on we will concentrate on Case-3 only to identify the spurious wave components.

For Case-3, Figs. 33 to 36 show the comparisons of the measured raw bi-chromatic waves and separated, primary waves, corresponding bounded waves and unwanted free waves between the first-order and the second-order wave generation techniques. The comparisons are done at Probe-1, Probe-2, Probe-3 and Probe-8 locations

Figs. 33a, 33b, 33c and 33d, respectively, show the comparisons of the measured raw waves, comparisons of the separated primary waves, comparisons of the separated bounded second order waves and the comparisons of the isolated unwanted free waves at Probe-1. Similar comparisons are shown in Figs. 34, 35 and 36 for Probe-2, Probe-3 and Probe-8.

From Figs. 33d, 34d, 35d and 36d, it may be observed that Free wave-2 which is due to the wave paddle displacement differ insignificantly for both generation techniques. On the other hand, the Free wave-1 which is due to mismatch of the boundary conditions at the wave paddle differ at a low magnitude. Table 7 shows the comparisons of the bounded waves and free waves at different probe locations for both first-order and second-order generation techniques. The comparisons [%= (FW1 / MWH1)*100] or [%= (FW2 / MWH1)*100] are done with respect to the measured wave height at Probe-1 (MWH1=0.0864m) obtained in first-order wave generation method.

Table 7 Comparisons of Free waves and Bounded waves

	FW1 (FOG) %	FW1 (SOG) %	FW2 (FOG) %	FW2 (SOG) %	BW (FOG) %	BW (SOG) %
P-1	9.50	7.70	2.30	2.30	11.30	9.68
P-2	8.64	7.84	2.13	2.19	10.38	9.49
P-3	9.28	9.68	2.60	2.61	10.62	11.17
P-8	10.36	9.88	2.90	2.89	12.30	11.74

In the table P-1, P-2, P-3 and P-8 respectively, represent Probe-1, Probe-2, Probe-3 and Probe-8. FW1, FW2 and BW correspond to Free wave-1, Free wave-2 and Bounded wave, respectively. On the other hand, FOG and SOG stand for **F**irst-**O**rder wave **G**eneration technique and **S**econd-**O**rder wave **G**eneration technique.

Fig. 37a shows the comparisons of different wave spectrums at Probe-14 and at Probe-1 after when the reflection analysis is carried over. In this analysis we have separated the reflected wave components from the measured wave profiles and then comparisons are made between relevant wave components generated by both first- and second-order generation techniques. Again Case-3 is only used for this analysis. Fig. 37a shows the comparisons of the primary waves at Probe-1 and at Probe-14 for the first-order wave generation method. On the other hand, Fig. 37d shows the same comparisons for the second-order wave generation method. Fig. 37b shows the comparisons of the reflected waves at Probe-1 and at Probe-14 for the first-order wave generation method. Fig. 37e shows the similar comparisons for the second-order wave generation method. Figs. 37c and 37f show the comparisons of the reflected waves at Probe-1 and at Probe-

14 for the first-order and the second-order wave generation technique. It may be observed from Figs. 37 that the primary and the reflected waves are not exactly the same at Probe-1 and at Probe-14. The reflected low frequency wave components obtained from the first-order method are a little larger than that obtained from the second-order method at Probe-1 and at Probe-14.

Figs. 38 show different comparisons and analysis of wave components for Case-3 at Probe-1. Fig. 38a shows the comparisons between the First- and the Second-order incident waves energies. Fig. 38*b* describes the comparisons of First-order incident wave and reflected wave energies. Fig. 38c illustrates Second-order incident wave and reflected wave energies. Fig. 38*d* shows surface elevation from First-order incident wave spectrum and obtained by inverse FFT. Fig. 38*e* shows surface elevation from Second-order incident wave spectrum and obtained by inverse FFT. Fig. 38*f* shows wave profiles of the primary waves, bounded waves, Free wave-1 and Free wave-2 obtained using LWAVE on the surface elevation shown in Fig. 37*d* (First-order generation). For Second order generation case, Fig. 38*g* gives similar wave componenets mentioned in Fig. 37*f* but only difference is surface elevation shown in Fig. 38*e* is used in LWAVE analysis.

METHODOLOGY

The FORTRAN code BIWAVE is used to generate eta-file for a given two sets of wave parameters (wave periods and wave heights). Another FORTRAN code DWREP2 will produce necessary drive signal from the above eta-file to generate waves in the OEB. This is we call first-order-generation technique. On the other hand, from the given two sets of wave parameters, a FORTRAN code SOG (not in GEDAP) will predict primary and bounded waves' profiles that later transformed into drive signal using another FORTRAN code CONVERT and then generate waves in the OEB.

RESULTS

In this experiment 5 different water depths (*d=0.3m, 0.4m, 0.5m, 0.6m* and *0.8m*) were used. However results of 4 different depths (*d=0.4m, 0.5m* and *0.8m*) are shown and described here. The incident wave parameters are shown in Table 2 to Table 4 for monochromatic waves and in Table 6 for bi-chromatic waves. In this experiment relative water depths (*d/L*) were varied from shallow to intermediate water depth limits.

Both First-Order and Second-Order wave generation techniques were employed in the present experiments.

Appendix-I shows results of regular waves for both First-order and Second-order generation techniques. Comparisons of the measured wave profiles for the water depth of 0.5m are shown for both cases.

Appendix-II shows results of bichromatic waves for both First-order and Second-order generation techniques.

APPENDIX-I : results for monochromatic waves.
APPENDIX-II : results for bichromatic waves.

CONCLUSIONS

First-order and second-order wave generation techniques are used to generate and study the propagation of the primary waves, bounded waves and unwanted free waves in the Offshore Engineering Basin of NRC-IOT. This study is carried out for various mono- and bi-chromatic waves over different water depths in the basin. It is observed that for moderately shallow water for Case-1 and Case-2 as shown in Figs. 26 and 27, the differences in low frequency wave components are insignificant. This difference becomes moderate for Case-3 shown in Fig. 28 where the wave is extremely shallow. Comparing the obtained data from first-order and second-order wave generation techniques, it is observed that the differences between unwanted free waves are minimal. So the available facts show that the first order wave generation technique is still suitable to generate waves in the OEB.

ACKNOWLEDGEMENT

The authors highly acknowledge the help from Don Spencer of Oceanic Consultants Corporation and Shane Mckay of the Facilities Department at the Institute for Ocean Technology, National Research Council of Canada.

REFERENCES

Barthel V., Mansard, E.P.D., Sand, S.E. and Vis, F.C. (1983): Group bounded long waves in physical models, *Ocen Eng.* **10**(4).

Bowen, A. J., Inman, D. L. and Simmons, V. P. (1968): Wave set-down and set-up, *J. of Geophy. Res*. **73**(8), 2569-2577.

Longuet-Higgins, M. S. and R. W. Stewart (1961): The changes in amplitude of short gravity waves on steady non-uniform currents, *J. Fluid Mech.*, **10**, 529-549.

Longuet-Higgins, M. S. and R. W. Stewart (1962): Radiation stress and mass transport in gravity waves with application to surf beats, *J. Fluid Mech.*, **13**, 481.

Longuet-Higgins, M. S. and R. W. Stewart (1963): A note on wave set-up, *J. Marine Res.*, **21**, 9.

Longuet-Higgins, M. S. and R. W. Stewart (1964): Radiation stress in water waves, a physical discussion with application, *Deep-Sea Res.*, **11**, 529.

Sand, S. E. (1982): Long wave problems in laboratory models, *Proceedings of the ASCE, J. of Waterway, Port, coast. And Ocn. Div*. **198** (WW4).

Zaman, M. H. and L. Mak (2006): Second order wave generation in the OEB-1, IOT-Report, TR-2006-13.

Zaman, M. H. and L. Mak (2007): Second order wave generation technique in the laboratory, 26th Int. Conf. on offshore Mech. and Arctic Eng. (OMAE-2007), American Society of Mechanical Engineers (ASME), San Diego, USA, on CD-ROM.

Zaman, M. H., Peng, H., Baddour, E., Spencer, D. and Mckay, S. (2010): Identifications of spurious waves in the wave tank with shallow water, 29th Int. Conf. on offshore Mech. and Arctic Eng. (OMAE-2010), American Society of Mechanical Engineers (ASME), Shanghai, China, on CD-ROM.

APPENDIX – I

Figures for Monochromatic waves

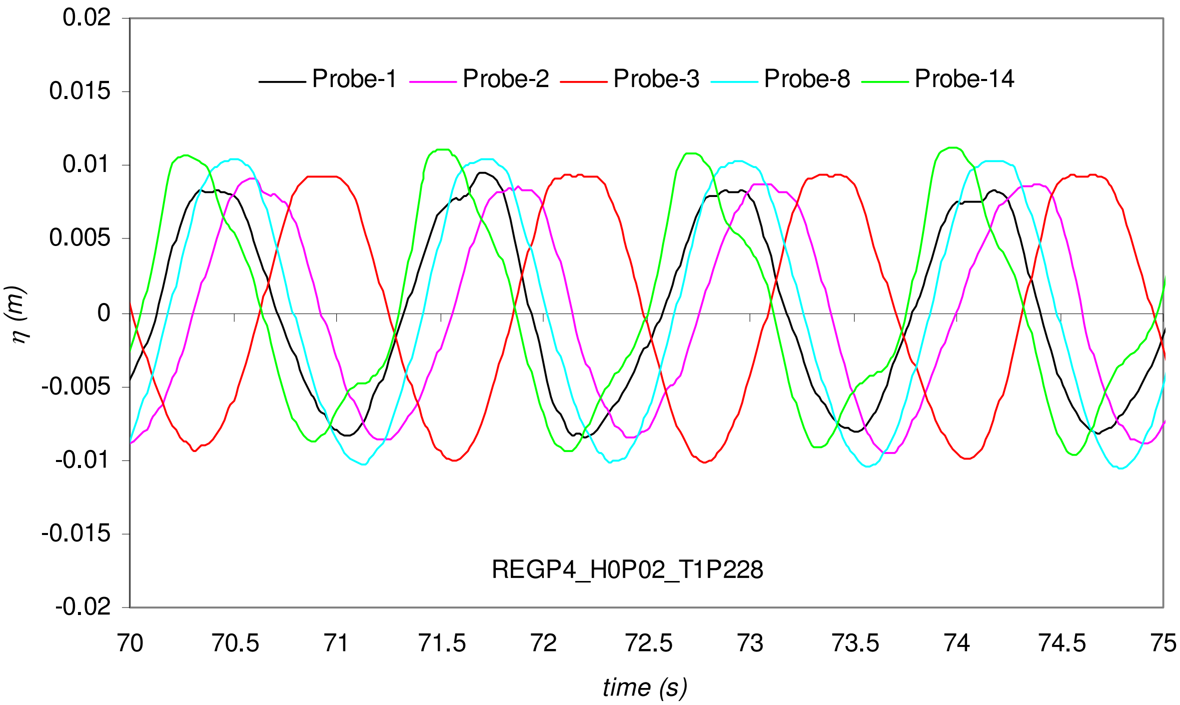

Fig. 3a Comparisons of the wave profile at Probes 14, 1, 2, 3 and 8
(C4-1, *h = 0.4m, T = 1.228s and H = 0.02m*)

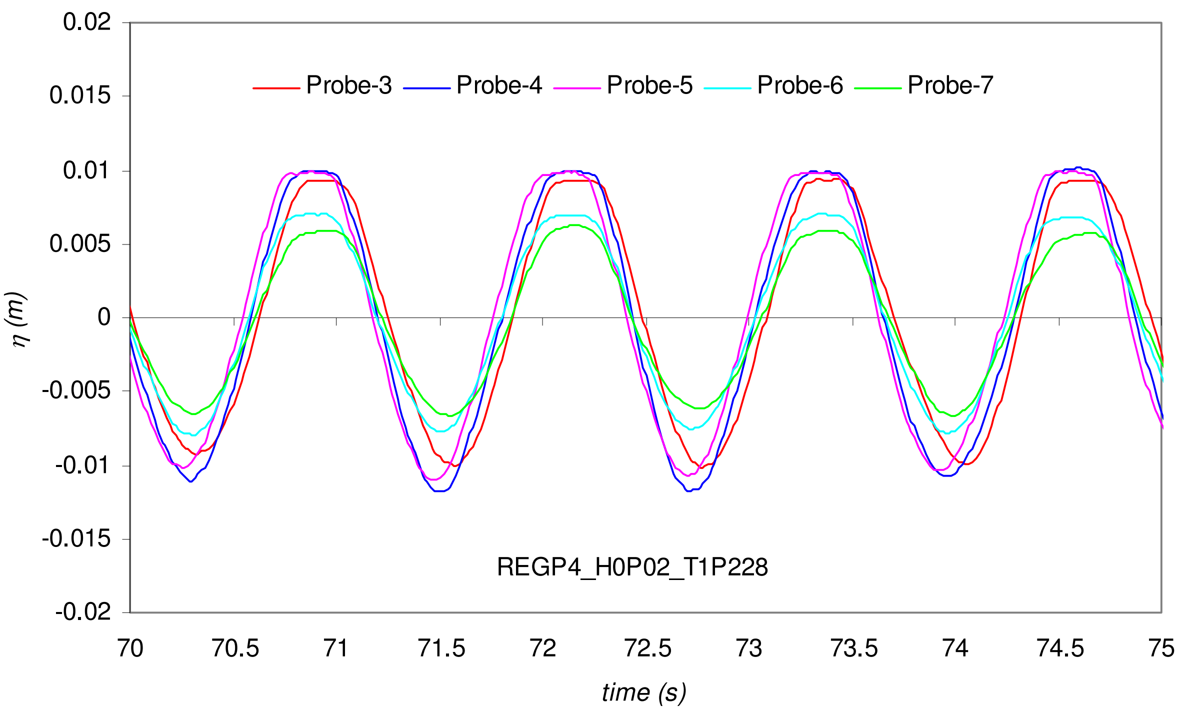

Fig. 3b Comparisons of the wave profile at Probes 3, 4, 5, 6 and 7
(C4-1, *h = 0.4m, T = 1.228s and H = 0.02m*)

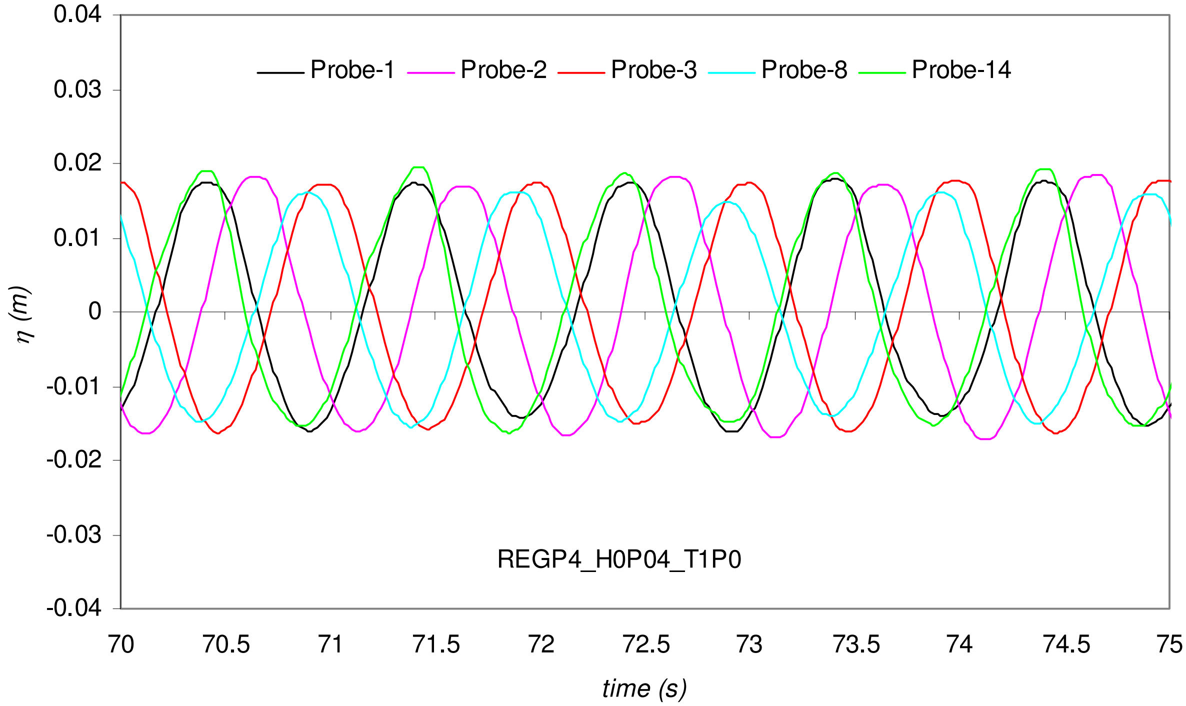

Fig. 4a Comparisons of the wave profile at Probes 14, 1, 2, 3 and 8
(C4-2, *h = 0.4m, T = 1.0s and H = 0.04m*)

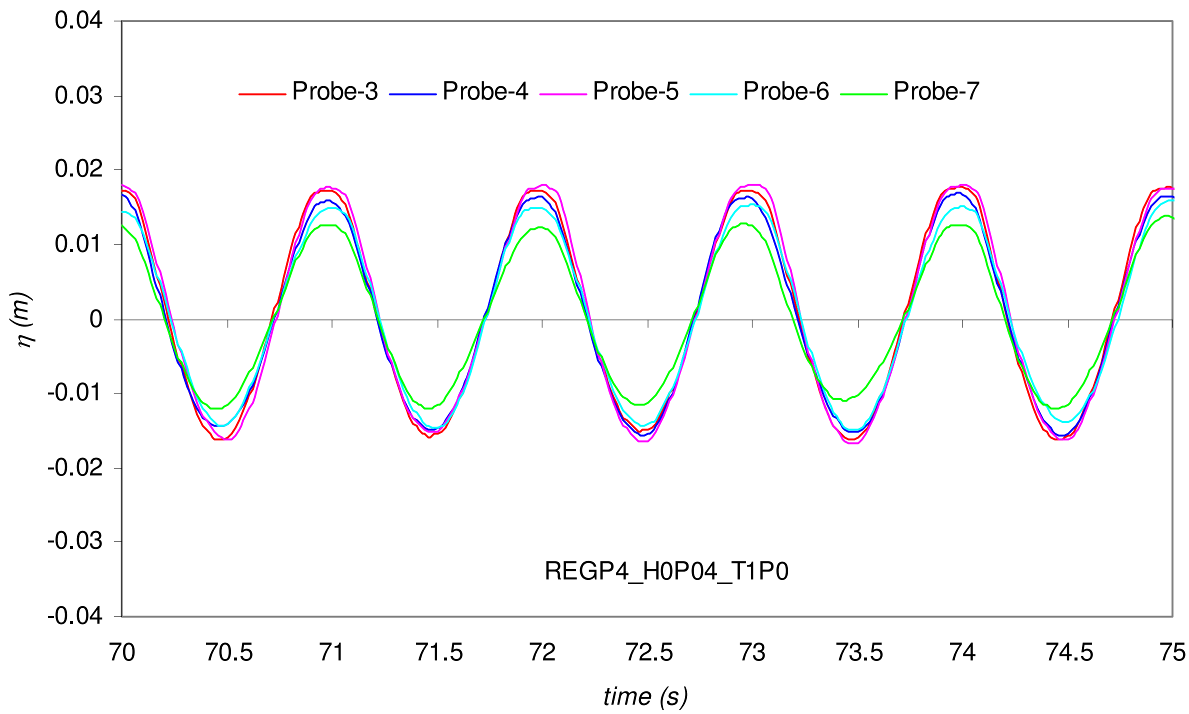

Fig. 4b Comparisons of the wave profile at Probes 3, 4, 5, 6 and 7
(C4-2, *h = 0.4m, T = 1.0s and H = 0.04m*)

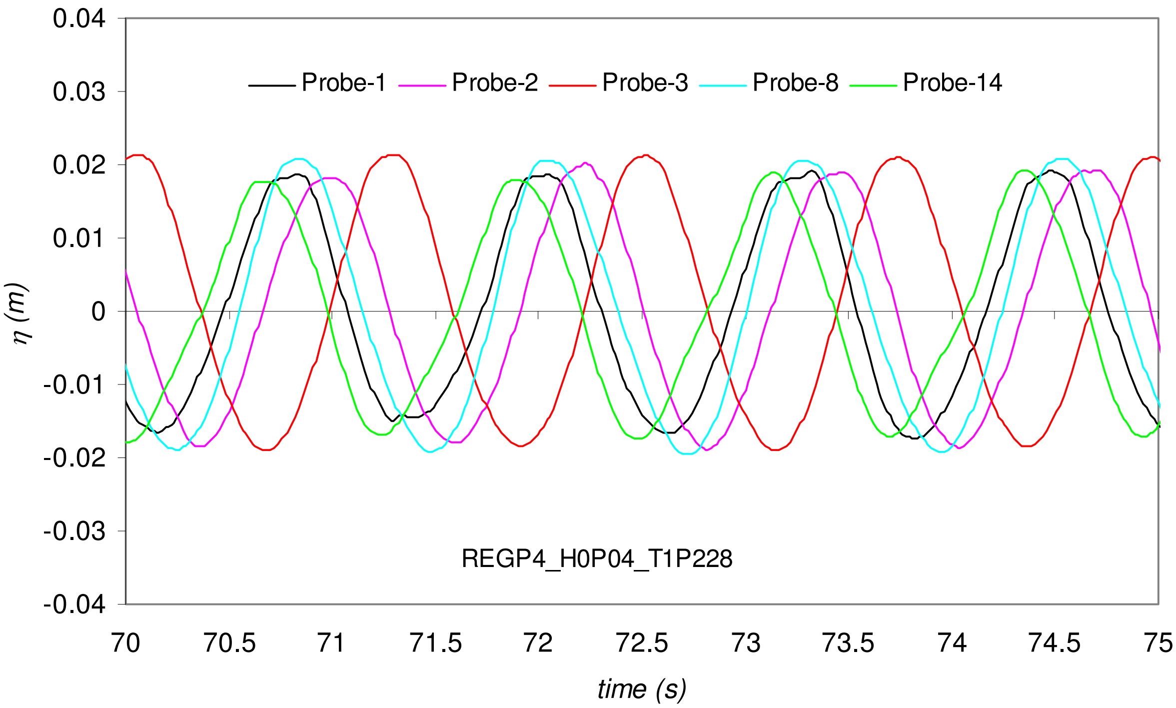

Fig. 5a Comparisons of the wave profile at Probes 14, 1, 2, 3 and 8
(C4-3, *h = 0.4m, T = 1.228s and H = 0.04m*)

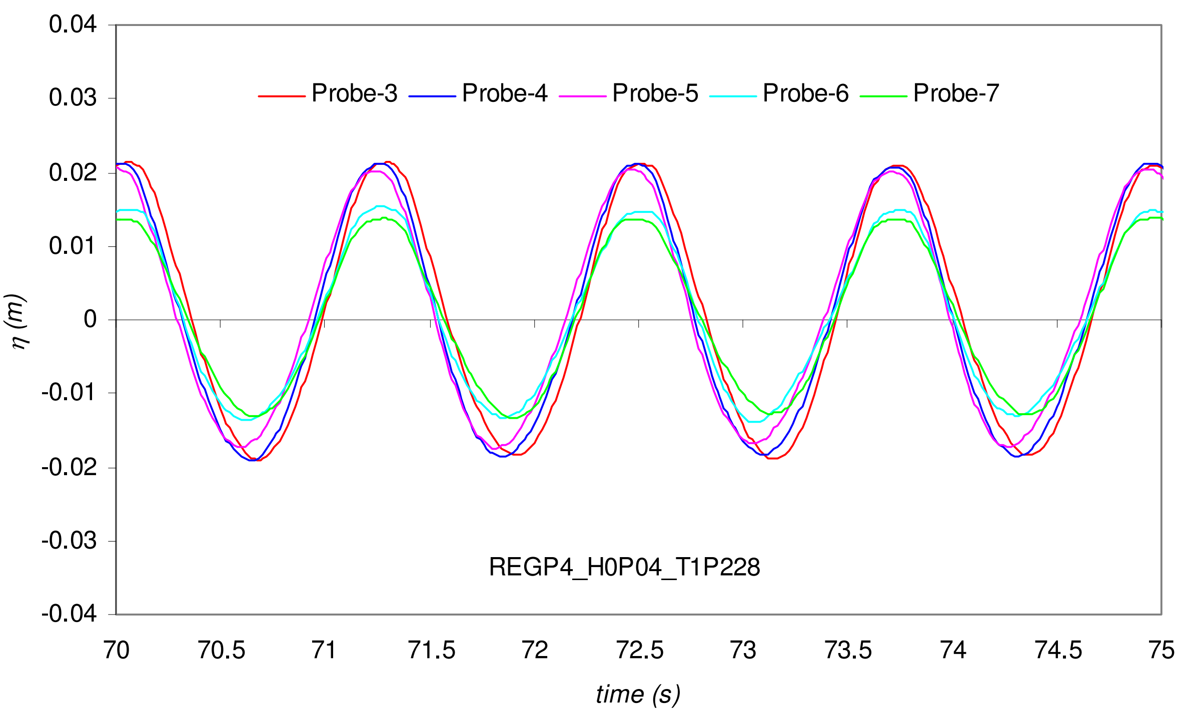

Fig. 5b Comparisons of the wave profile at Probes 3, 4, 5, 6 and 7
(C4-3, *h = 0.4m, T = 1.228s and H = 0.04m*)

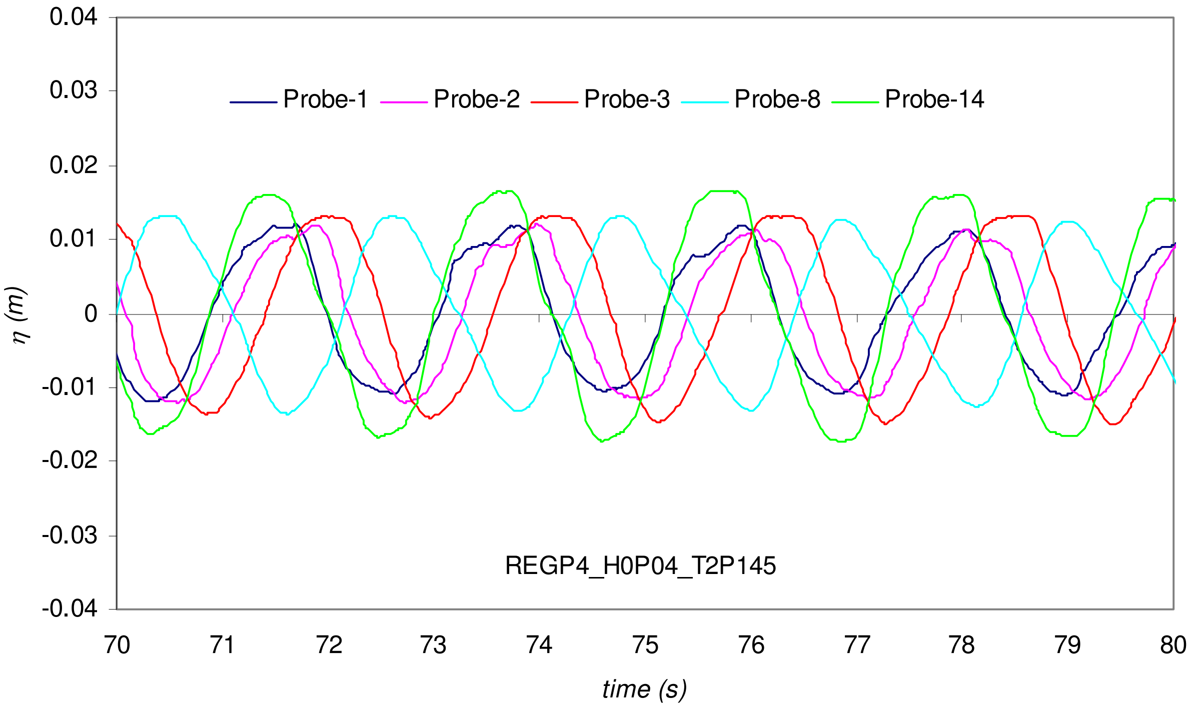

Fig. 6a Comparisons of the wave profile at Probes 14, 1, 2, 3 and 8
(C4-4, $h = 0.4m$, $T = 2.145s$ and $H = 0.04m$)

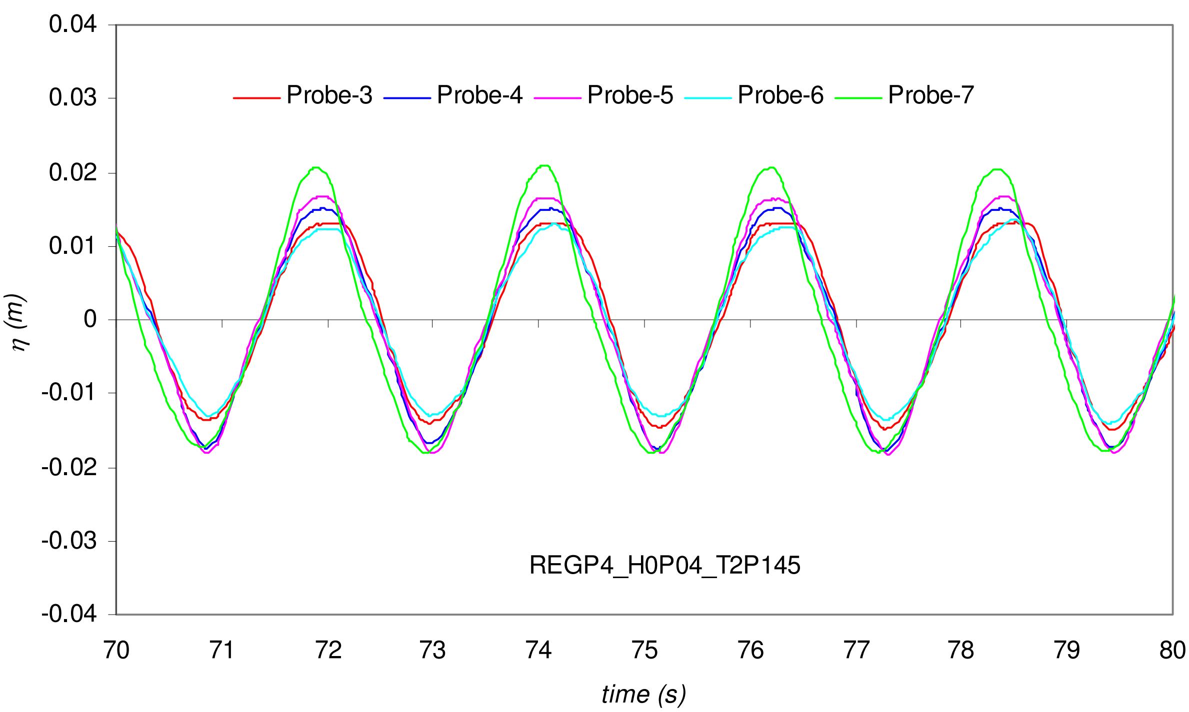

Fig. 6b Comparisons of the wave profile at Probes 3, 4, 5, 6 and 7
(C4-4, $h = 0.4m$, $T = 2.145s$ and $H = 0.04m$)

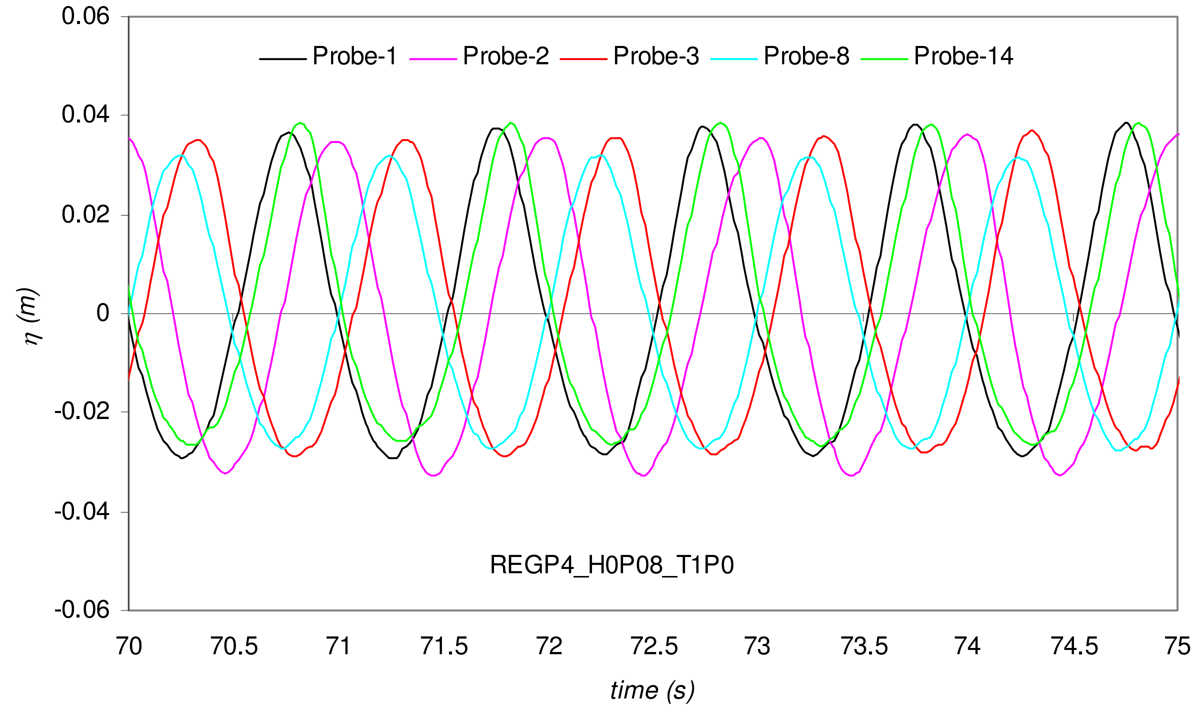

Fig. 7a Comparisons of the wave profile at Probes 14, 1, 2, 3 and 8
(C4-5, *h = 0.4m, T = 1.0s and H = 0.08m*)

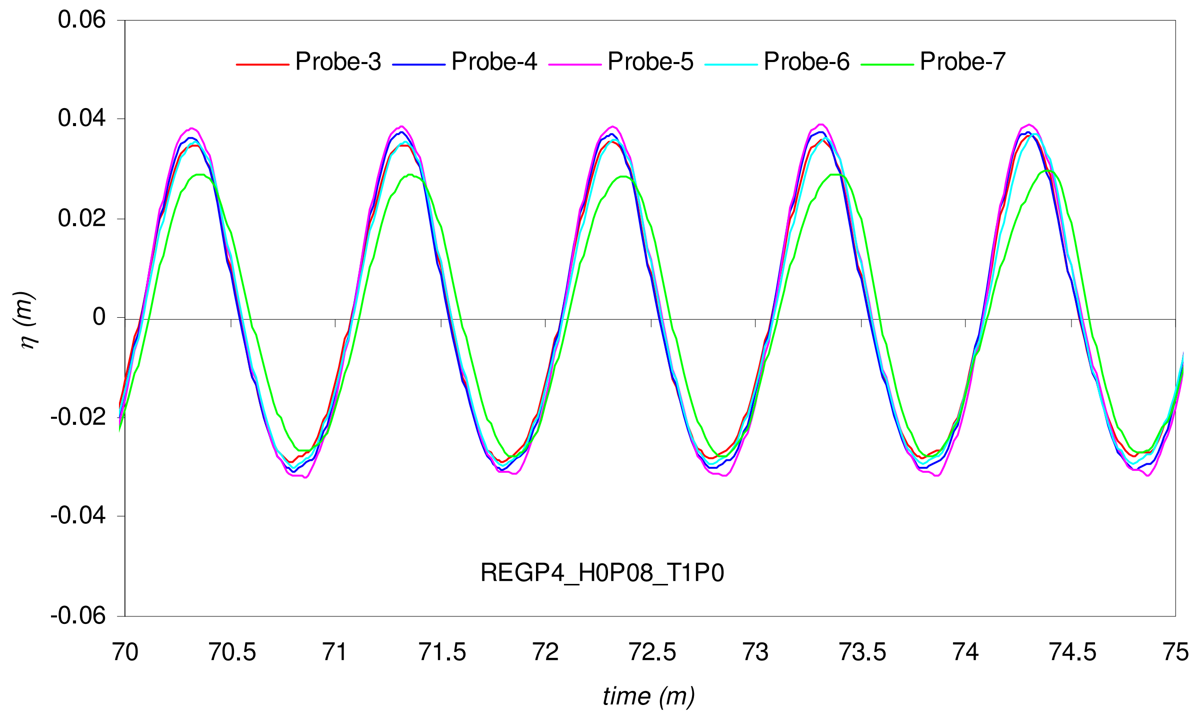

Fig. 7b Comparisons of the wave profile at Probes 3, 4, 5, 6 and 7
(C4-5, *h = 0.4m, T = 1.0s and H = 0.08m*)

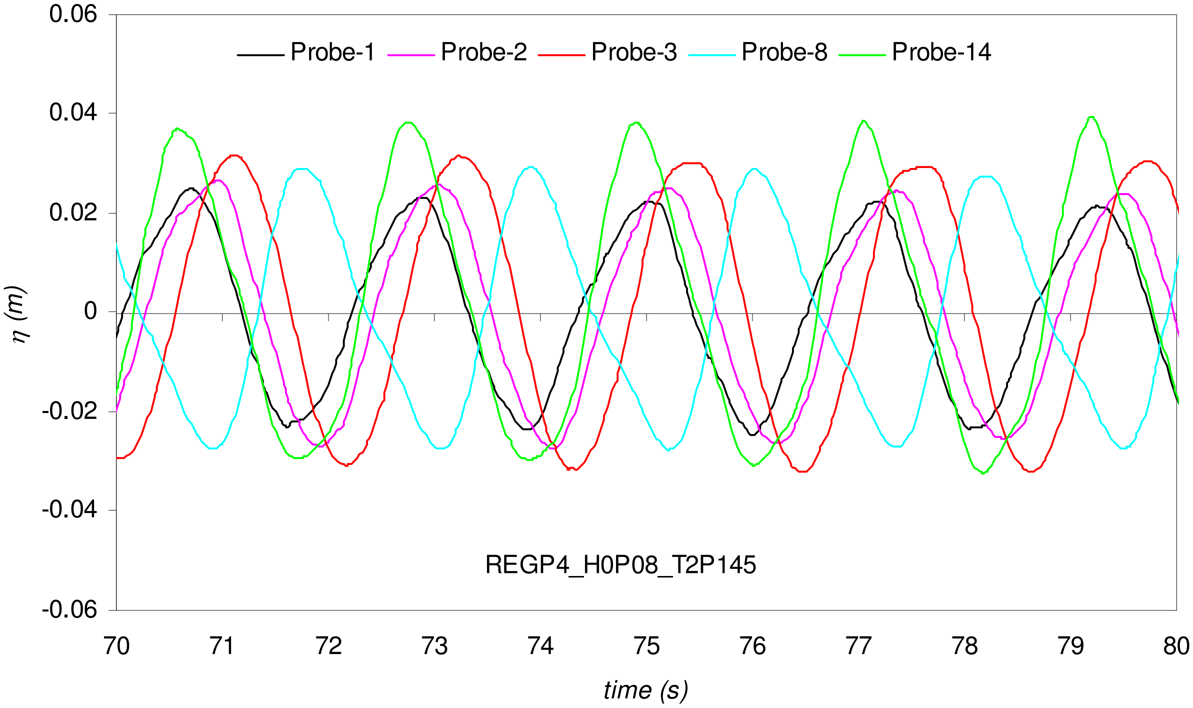

Fig. 8a Comparisons of the wave profile at Probes 14, 1, 2, 3 and 8
(C4-6, *h = 0.4m, T = 2.145s and H = 0.08m*)

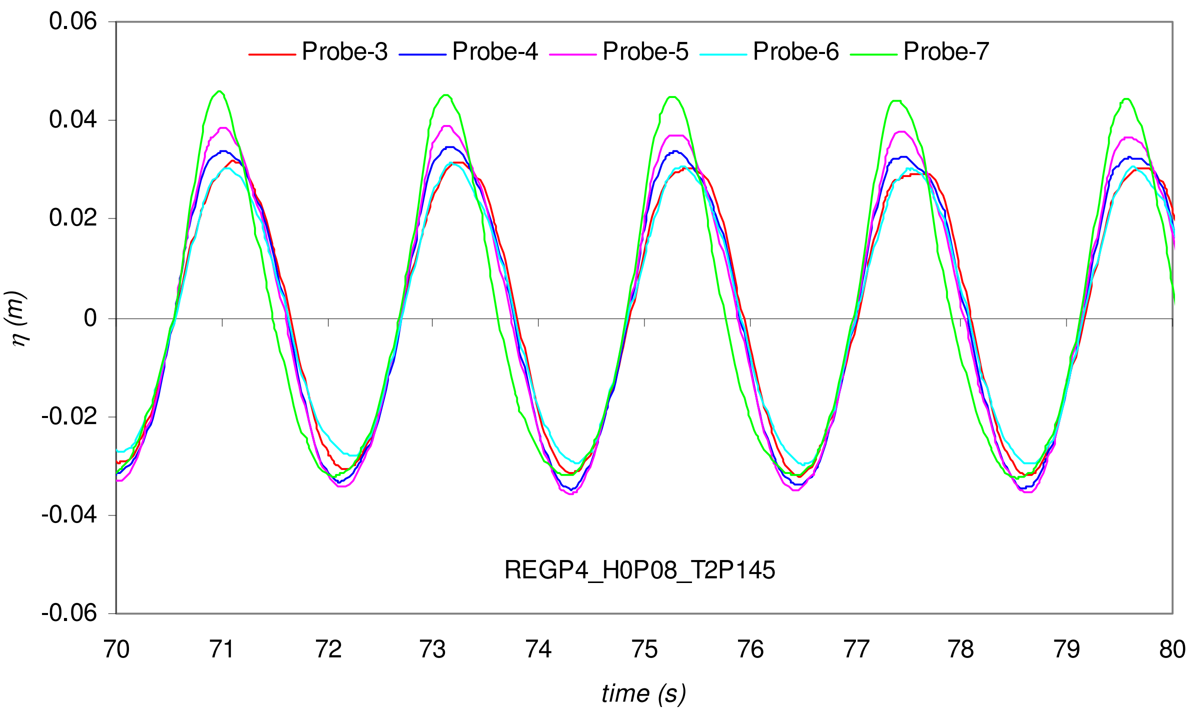

Fig. 8b Comparisons of the wave profile at Probes 3, 4, 5, 6 and 7
(C4-6, *h = 0.4m, T = 2.145s and H = 0.08m*)

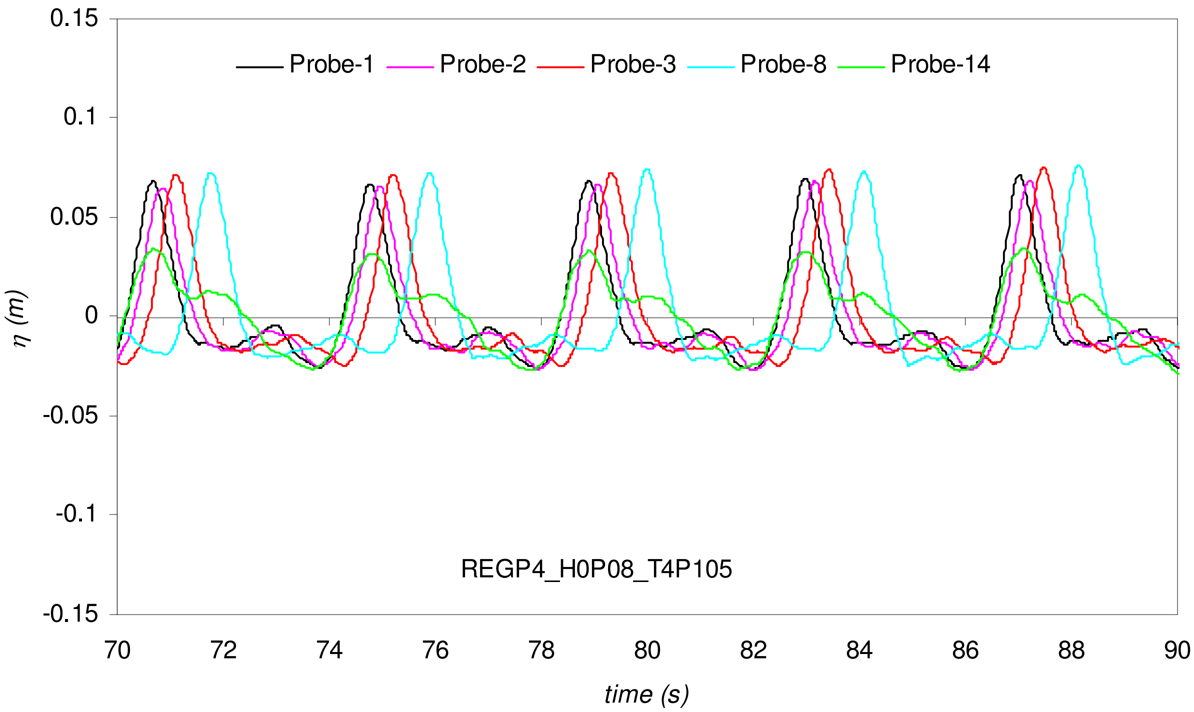

Fig. 9a Comparisons of the wave profile at Probes 14, 1, 2, 3 and 8
(C4-7, $h = 0.4m$, $T = 4.105s$ and $H = 0.08m$)

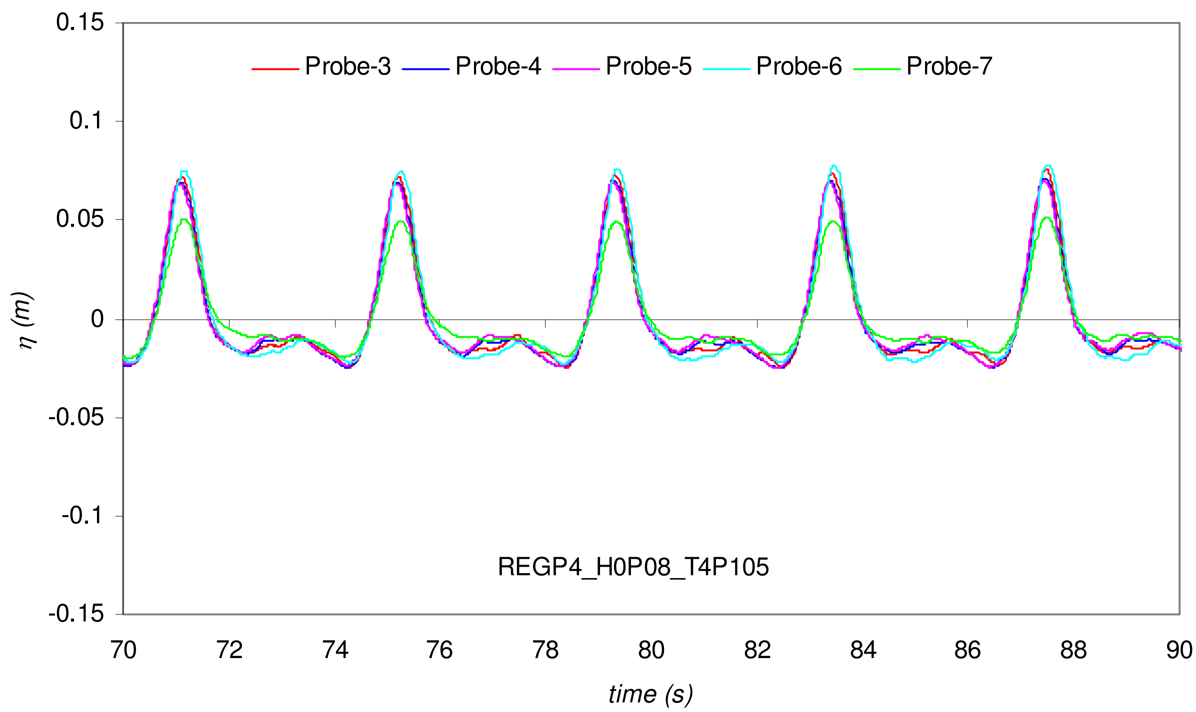

Fig. 9b Comparisons of the wave profile at Probes 3, 4, 5, 6 and 7
(C4-7, $h = 0.4m$, $T = 4.105s$ and $H = 0.08m$)

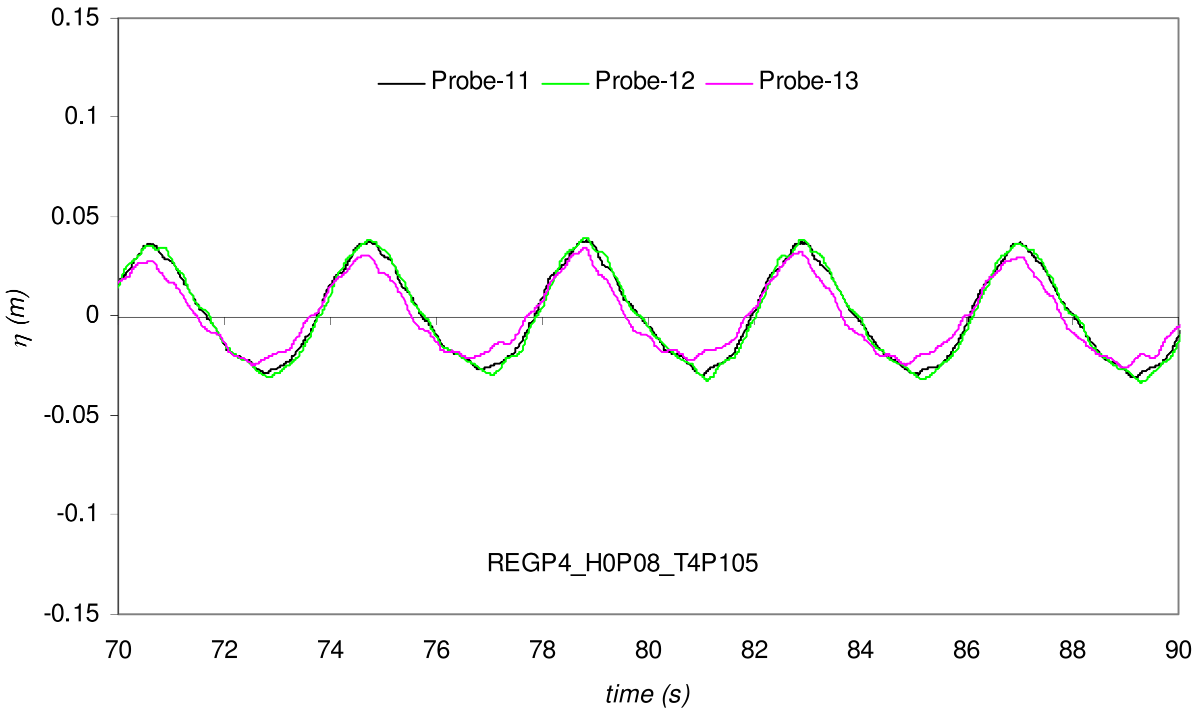

Fig. 9c Comparisons of the wave profile at Probes 11, 12 and 13
(C4-7, $h = 0.4m$, $T = 4.105s$ and $H = 0.08m$)

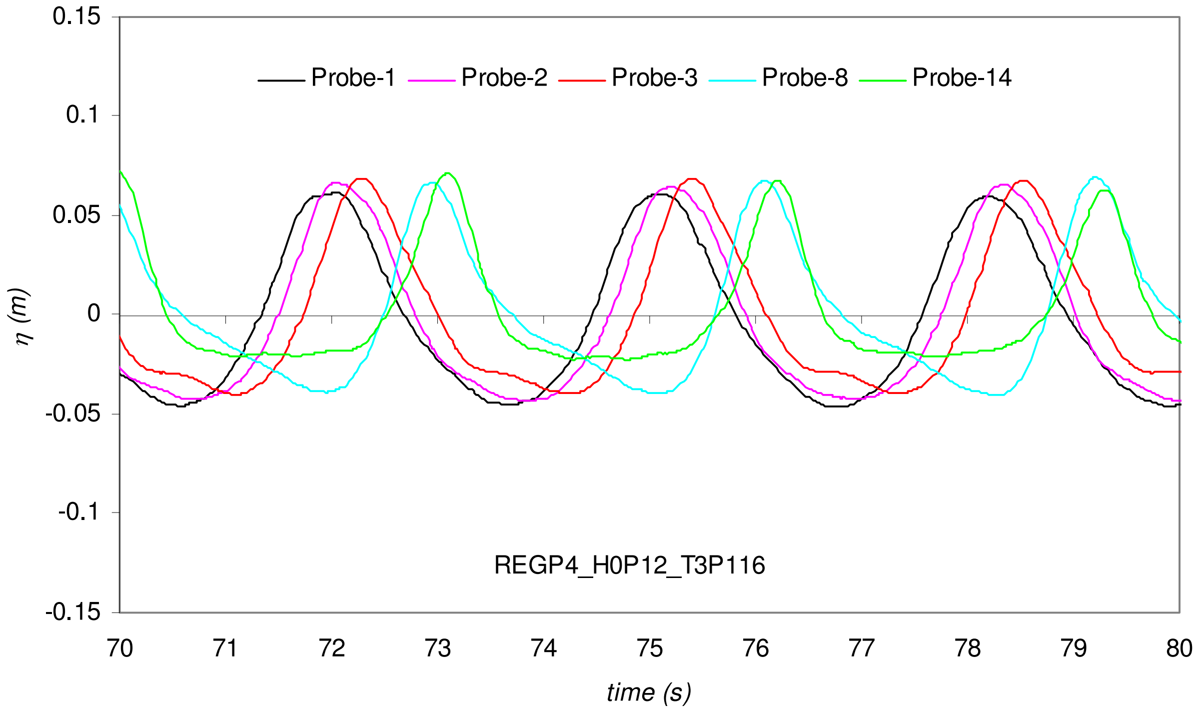

Fig. 10a Comparisons of the wave profile at Probes 14, 1, 2, 3 and 8
(C4-8, *h = 0.4m, T = 3.116s and H = 0.12m*)

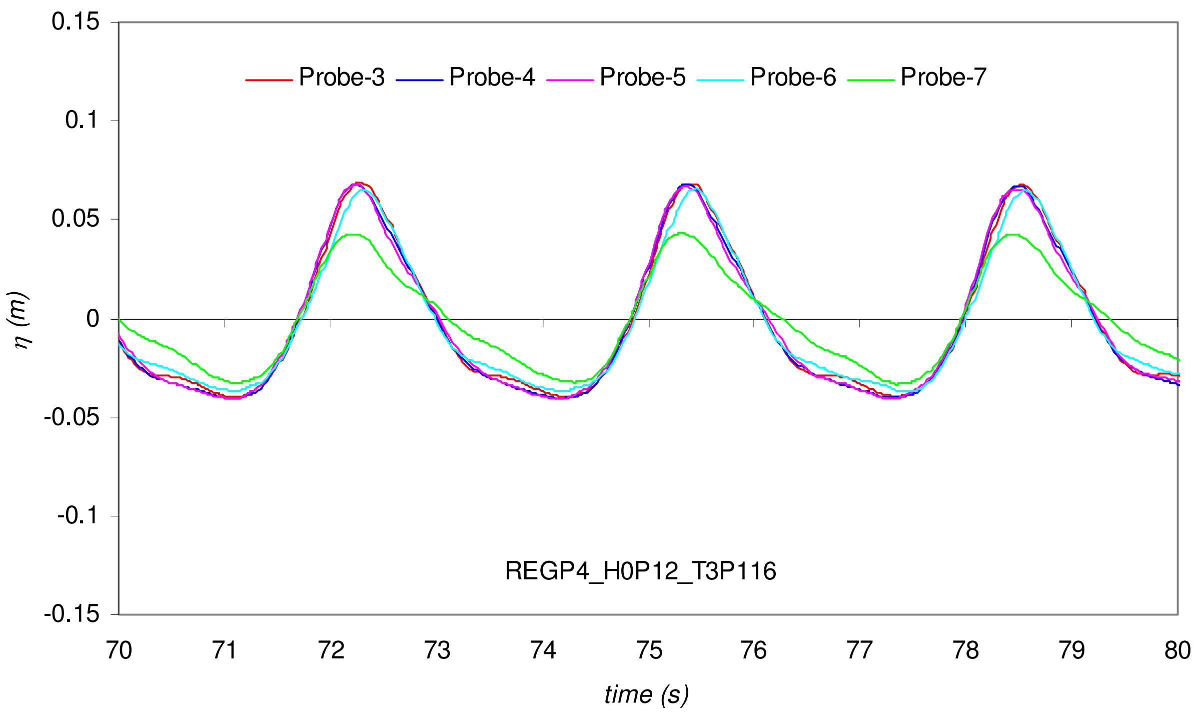

Fig. 10b Comparisons of the wave profile at Probes 3, 4, 5, 6 and 7
(C4-8, *h = 0.4m, T = 3.116s and H = 0.12m*)

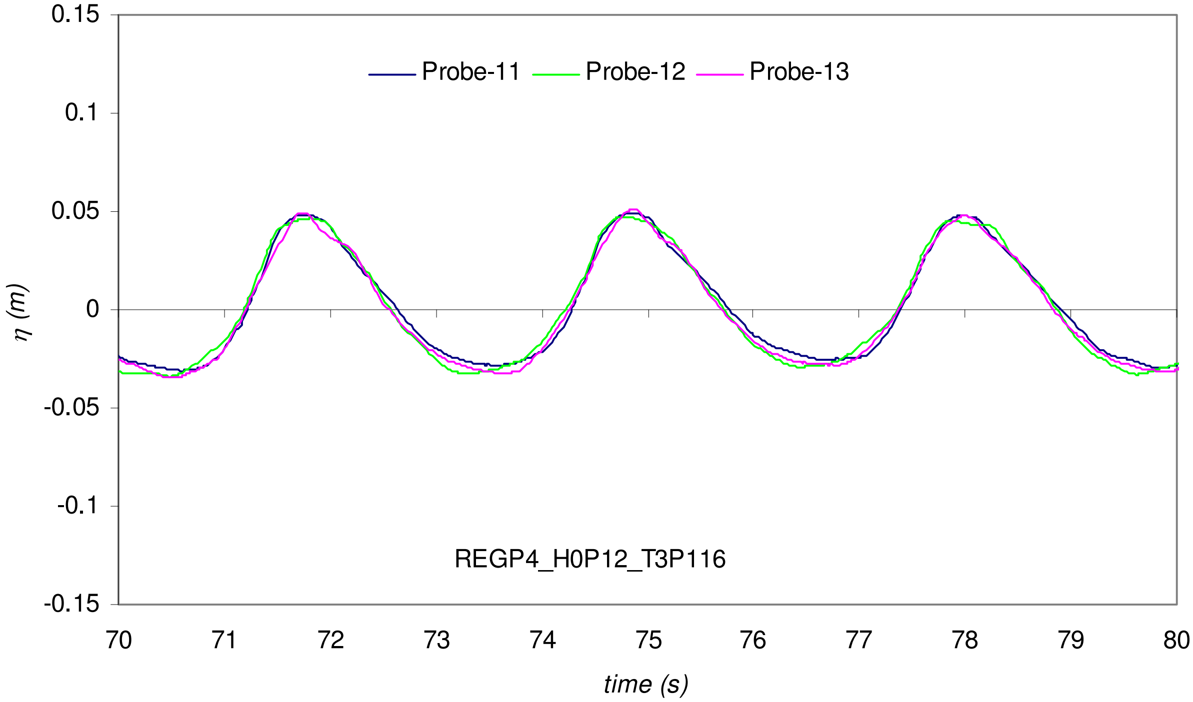

Fig. 10c Comparisons of the wave profile at Probes 11, 12 and 13
(C4-8, $h = 0.4m$, $T = 3.116s$ and $H = 0.12m$)

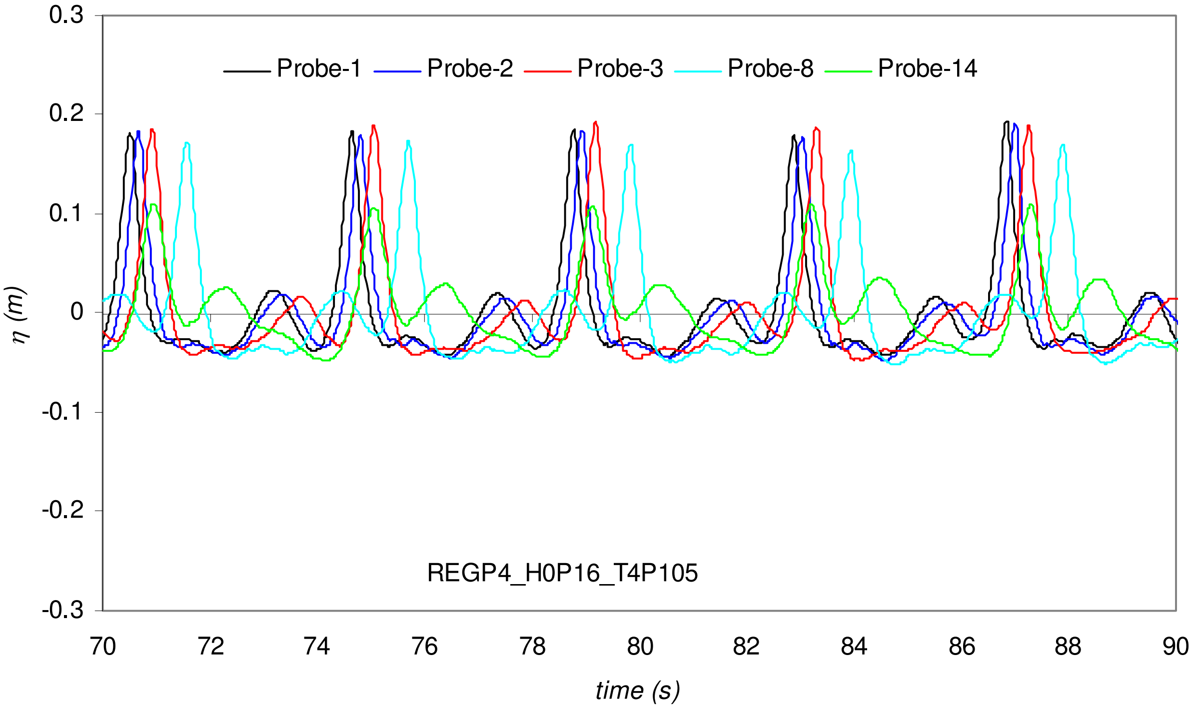

Fig. 11a Comparisons of the wave profile at Probes 14, 1, 2, 3 and 8
(C4-9, *h = 0.4m, T = 4.105s and H = 0.16m*)

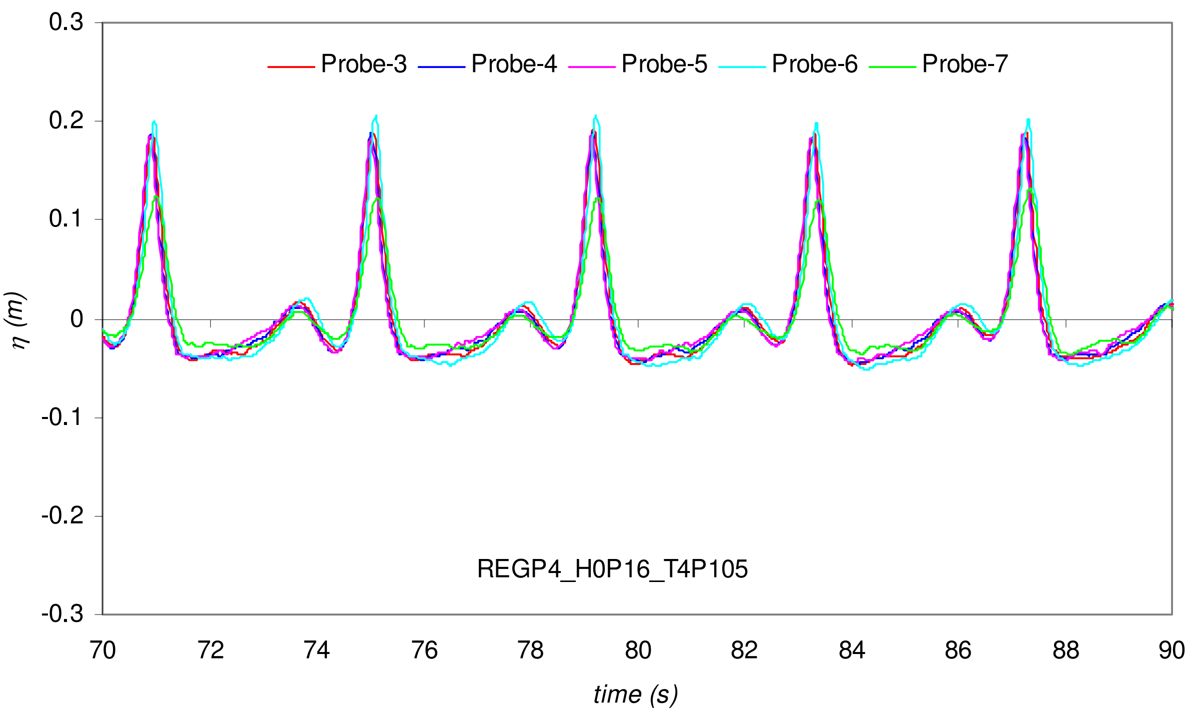

Fig. 11b Comparisons of the wave profile at Probes 3, 4, 5, 6 and 7
(C4-9, *h = 0.4m, T = 4.105s and H = 0.16m*)

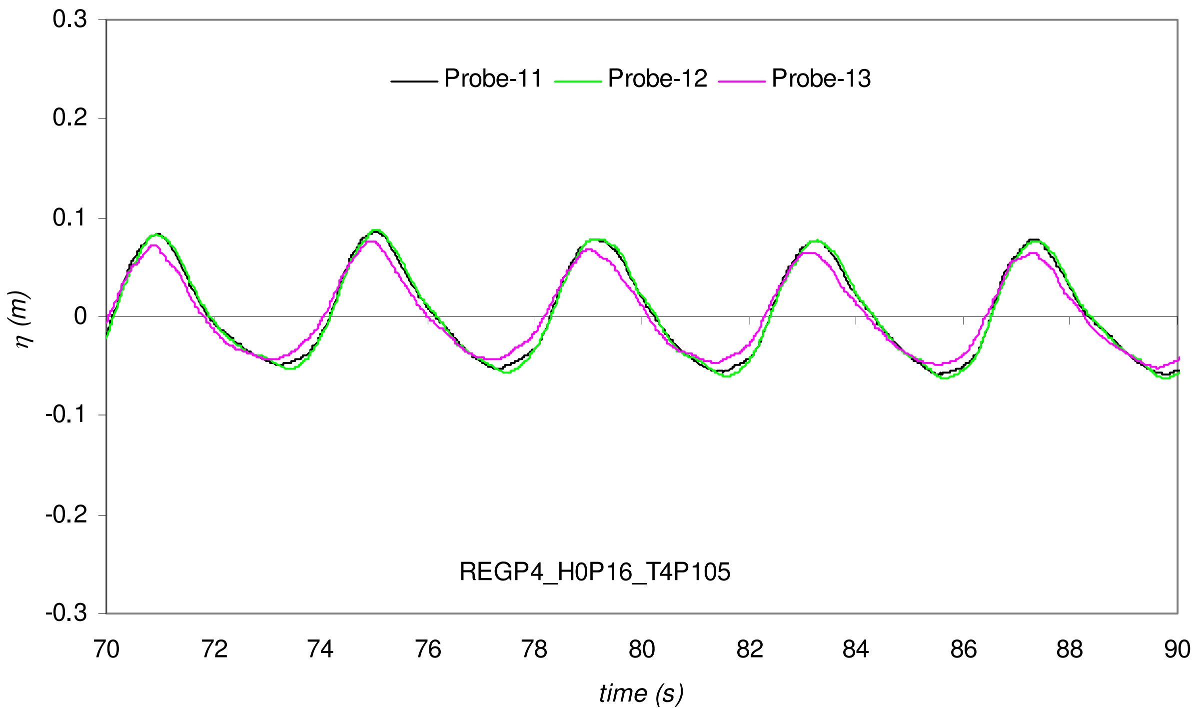

Fig. 11c Comparisons of the wave profile at Probes 11, 12 and 13
(C4-9, *h = 0.4m, T = 4.105s and H = 0.16m*)

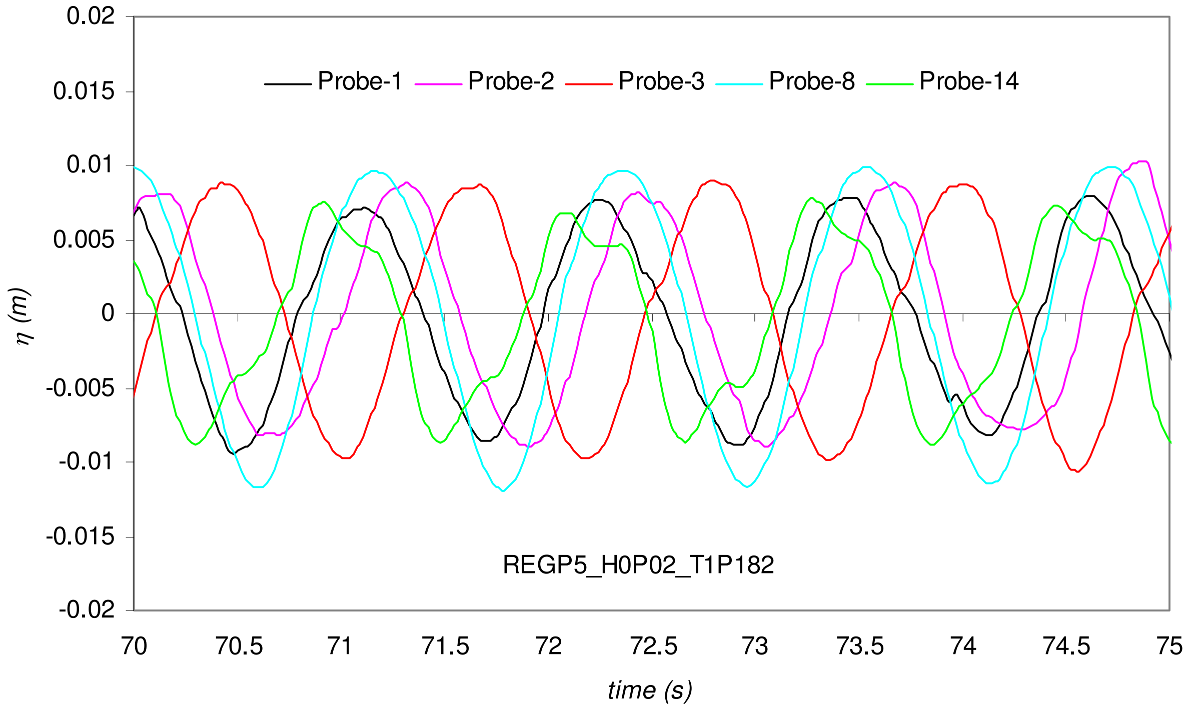

Fig. 12a Comparisons of the wave profile at Probes 14, 1, 2, 3 and 8
(C5-1, *h = 0.5m, T = 1.182s and H = 0.02m*)

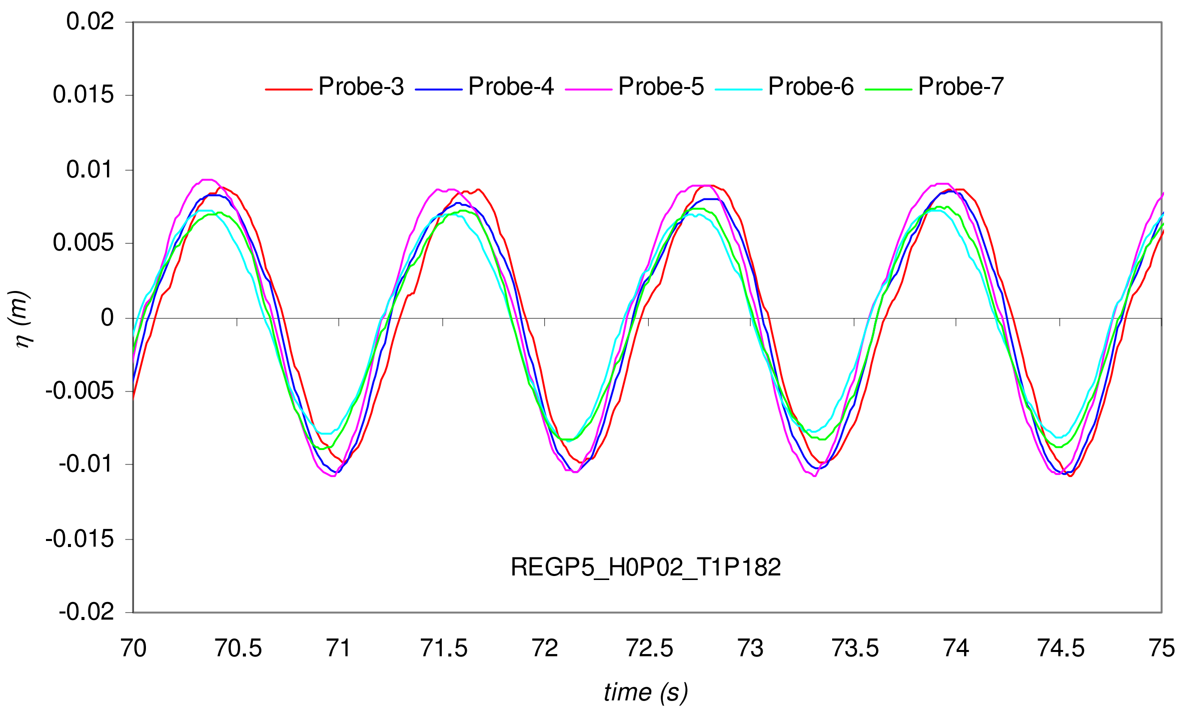

Fig. 12b Comparisons of the wave profile at Probes 3, 4, 5, 6 and 7
(C5-1, *h = 0.5m, T = 1.182s and H = 0.02m*)

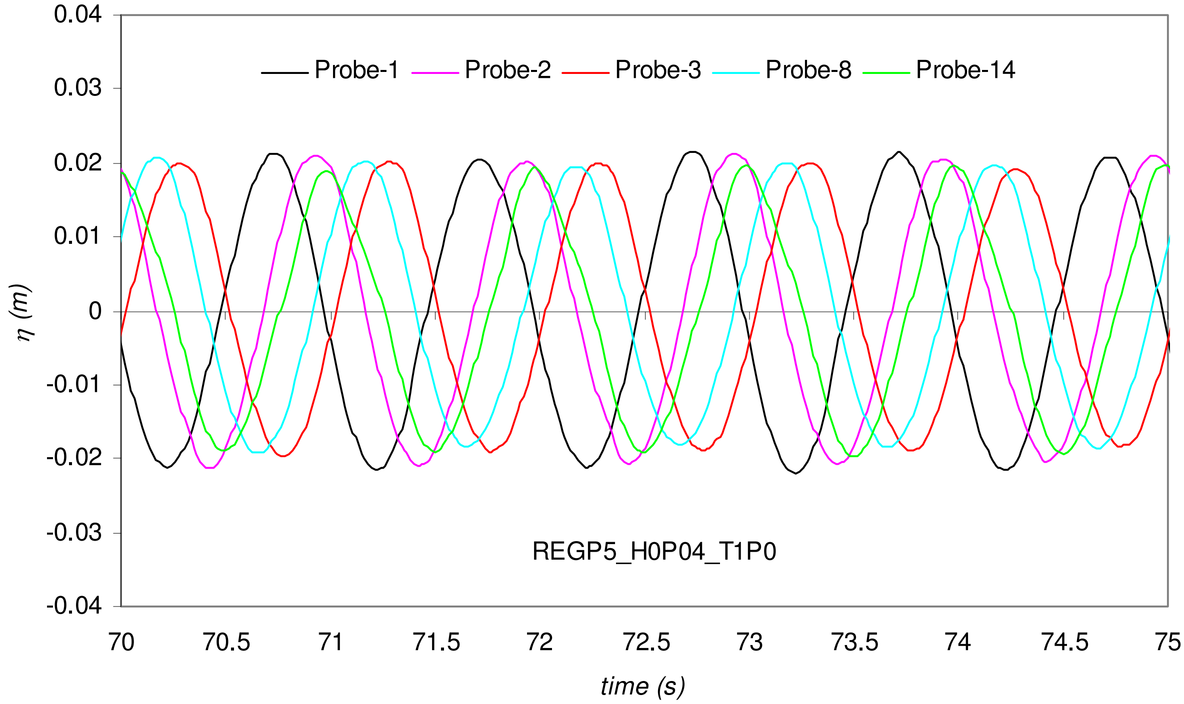

Fig. 13a Comparisons of the wave profile at Probes 14, 1, 2, 3 and 8
(C5-2, *h = 0.5m, T = 1.0s and H = 0.04m*)

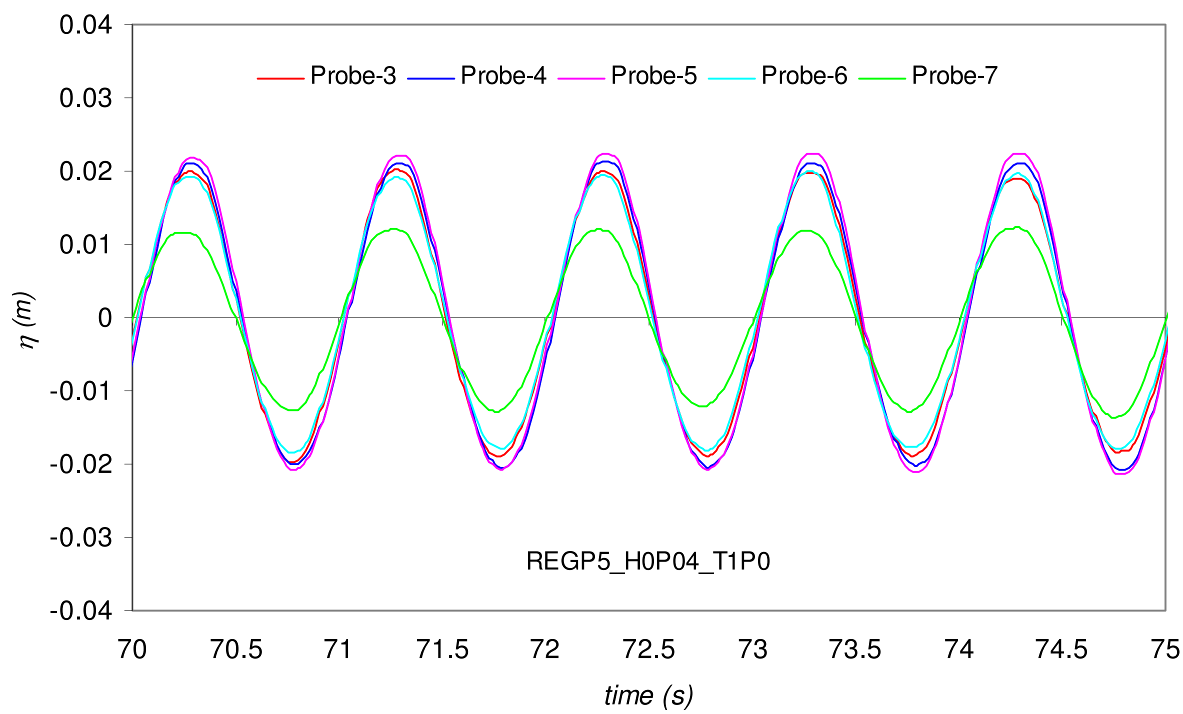

Fig. 13b Comparisons of the wave profile at Probes 3, 4, 5, 6 and 7
(C5-2, *h = 0.5m, T = 1.0s and H = 0.04m*)

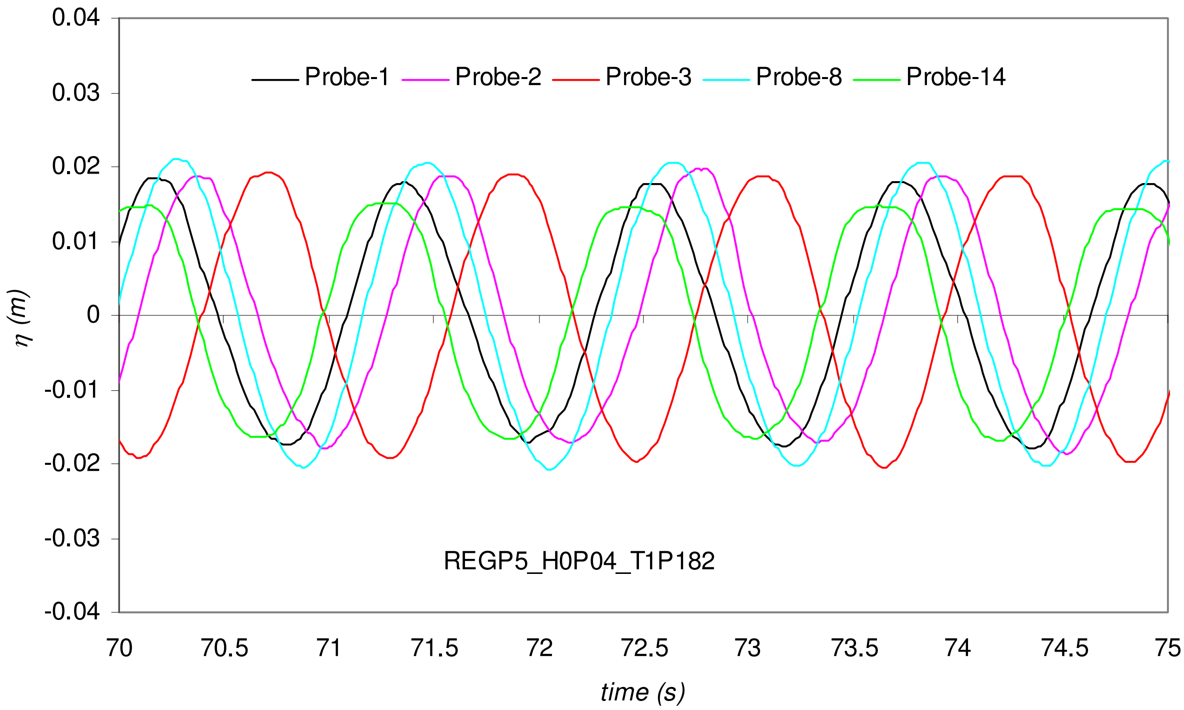

Fig. 14a Comparisons of the wave profile at Probes 14, 1, 2, 3 and 8
(C5-3, $h = 0.5m$, $T = 1.182s$ *and* $H = 0.04m$)

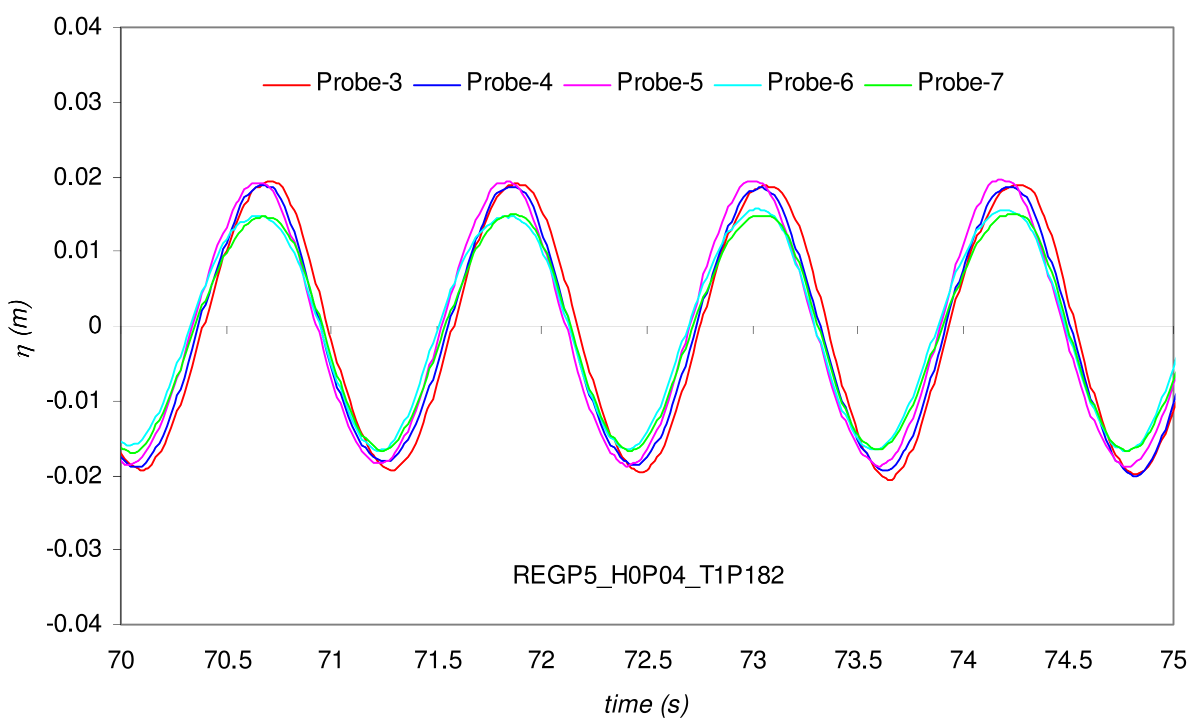

Fig. 14b Comparisons of the wave profile at Probes 3, 4, 5, 6 and 7
(C5-3, $h = 0.5m$, $T = 1.182s$ *and* $H = 0.04m$)

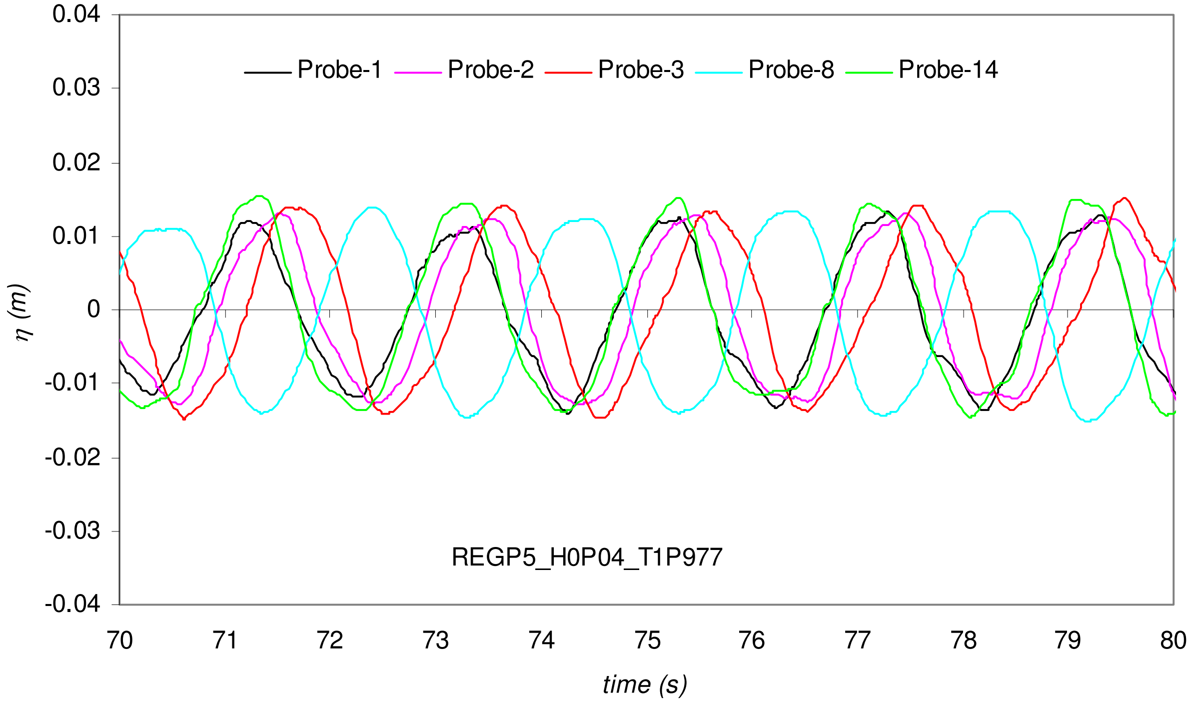

Fig. 15a Comparisons of the wave profile at Probes 14, 1, 2, 3 and 8
(C5-4, *h = 0.5m, T = 1.977s and H = 0.04m*)

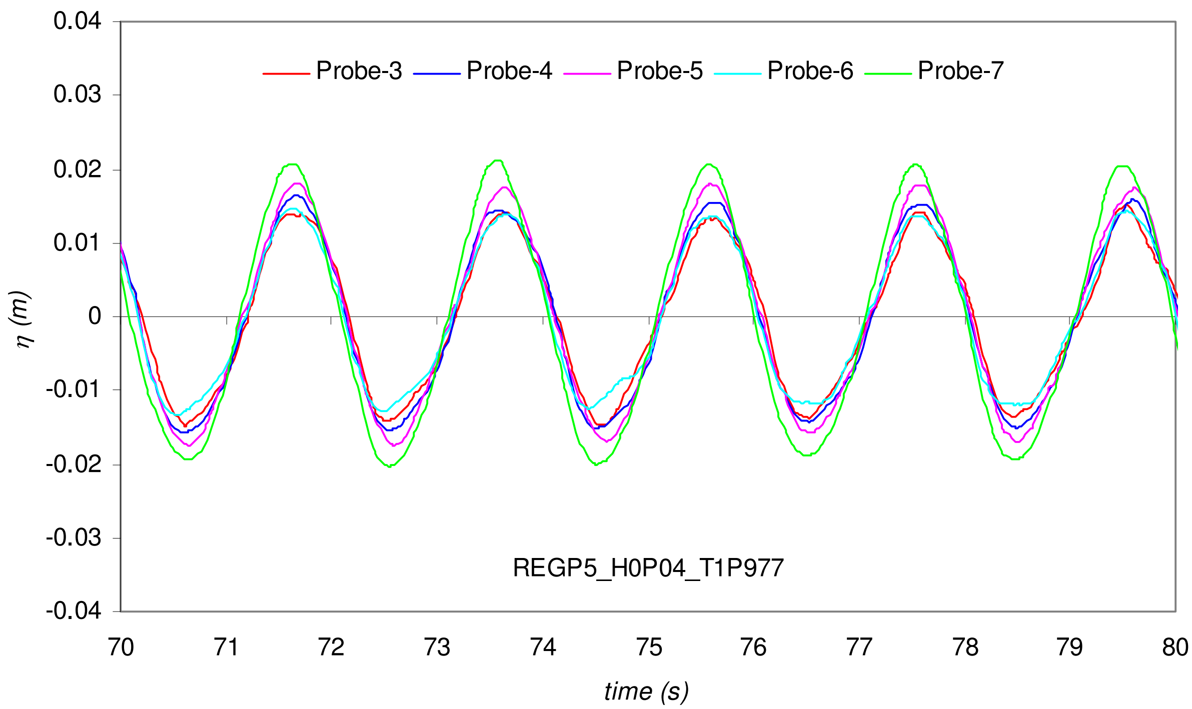

Fig. 15b Comparisons of the wave profile at Probes 3, 4, 5, 6 and 7
(C5-4, *h = 0.5m, T = 1.977s and H = 0.04m*)

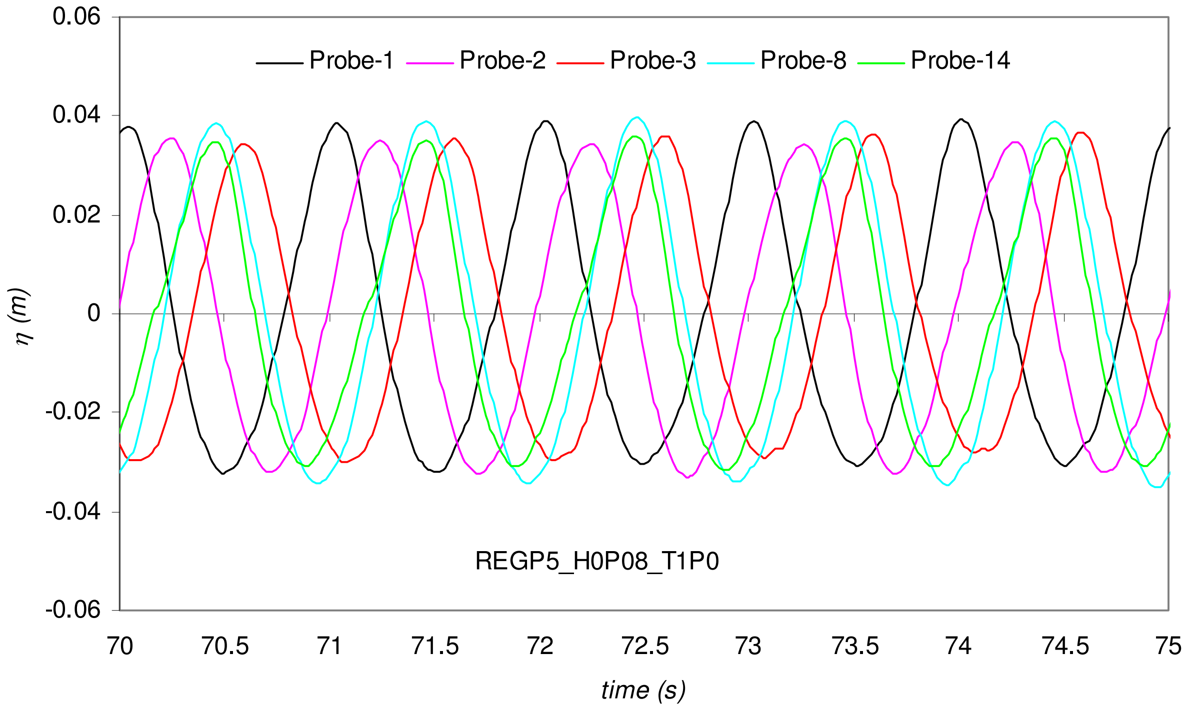

Fig. 16a Comparisons of the wave profile at Probes 14, 1, 2, 3 and 8
(C5-5, *h = 0.5m, T = 1.0s and H = 0.08m*)

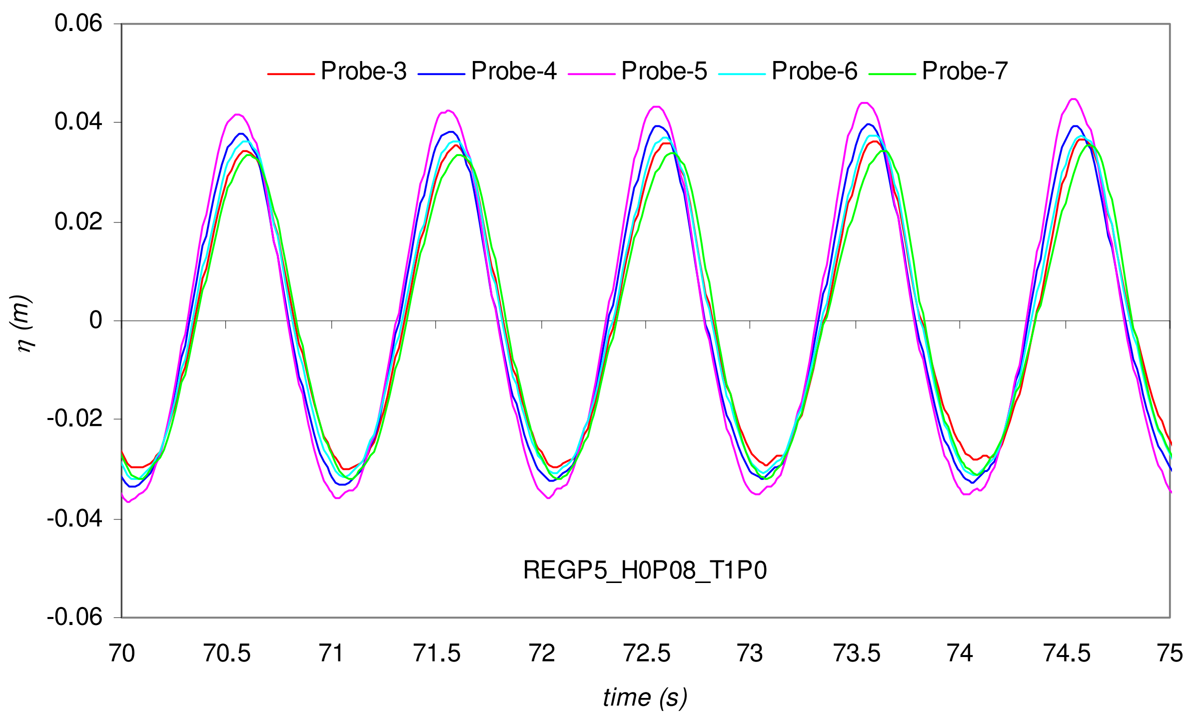

Fig. 16b Comparisons of the wave profile at Probes 3, 4, 5, 6 and 7
(C5-5, *h = 0.5m, T = 1.0s and H = 0.08m*)

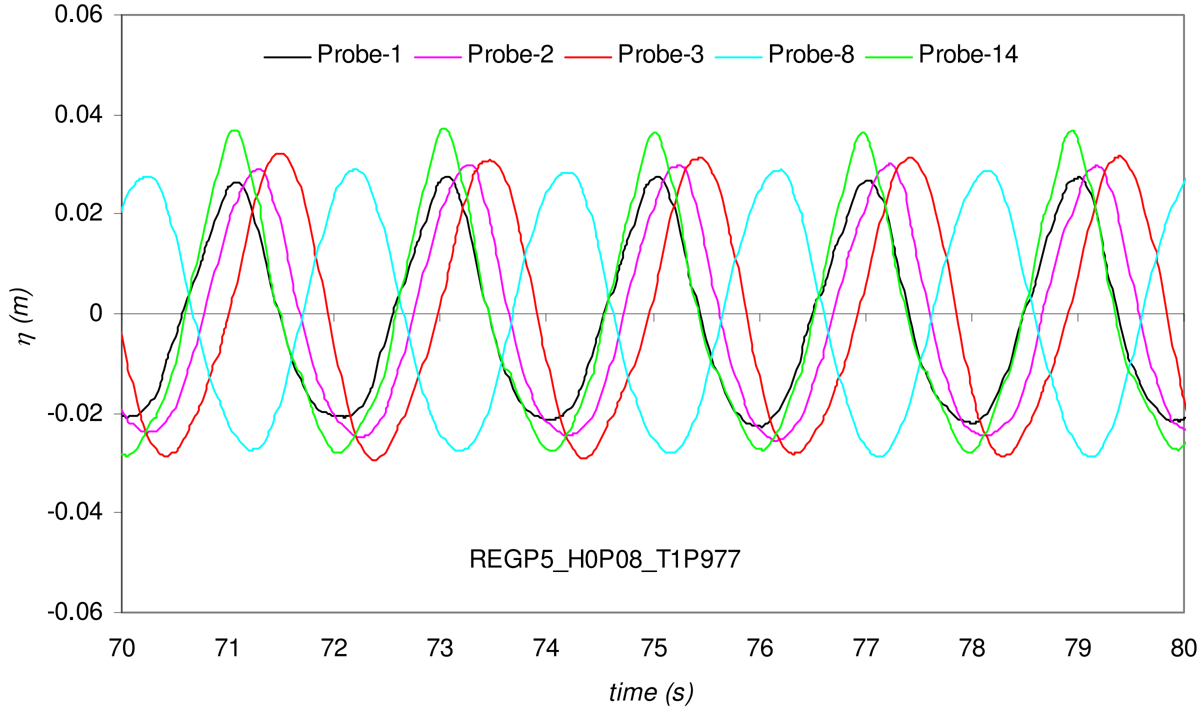

Fig. 17a Comparisons of the wave profile at Probes 14, 1, 2, 3 and 8
(C5-6, *h = 0.5m, T = 1.977s and H = 0.08m*)

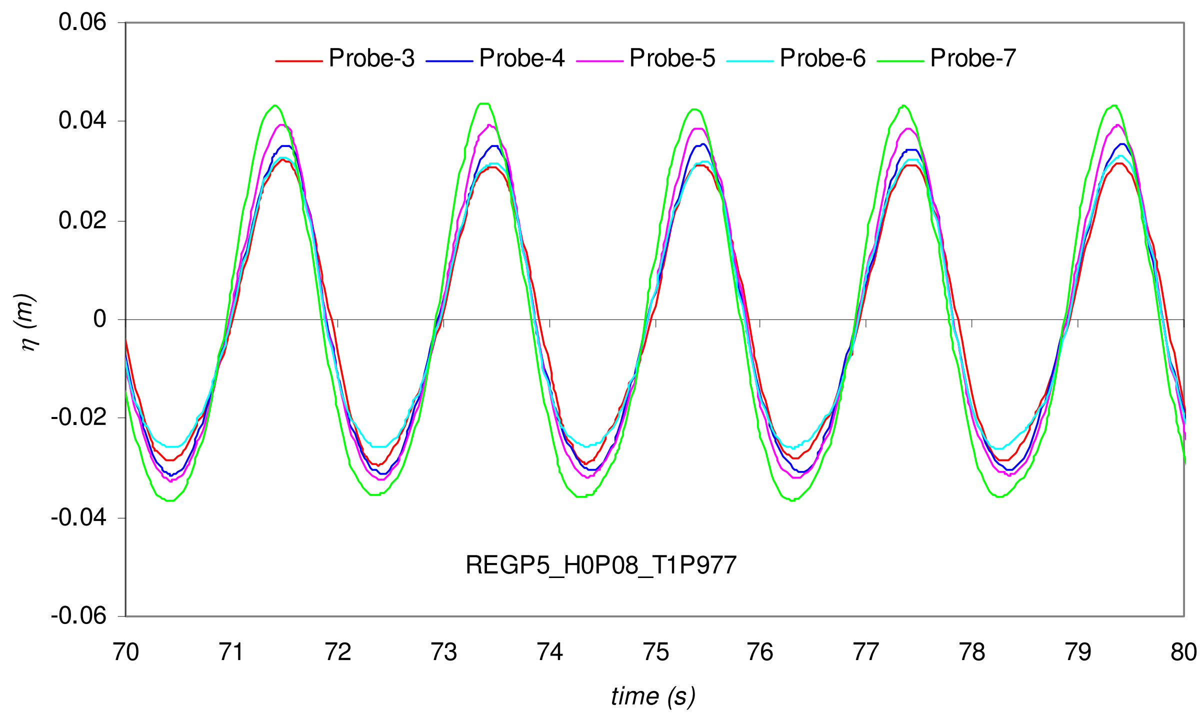

Fig. 17b Comparisons of the wave profile at Probes 3, 4, 5, 6 and 7
(C5-6, *h = 0.5m, T = 1.977s and H = 0.08m*)

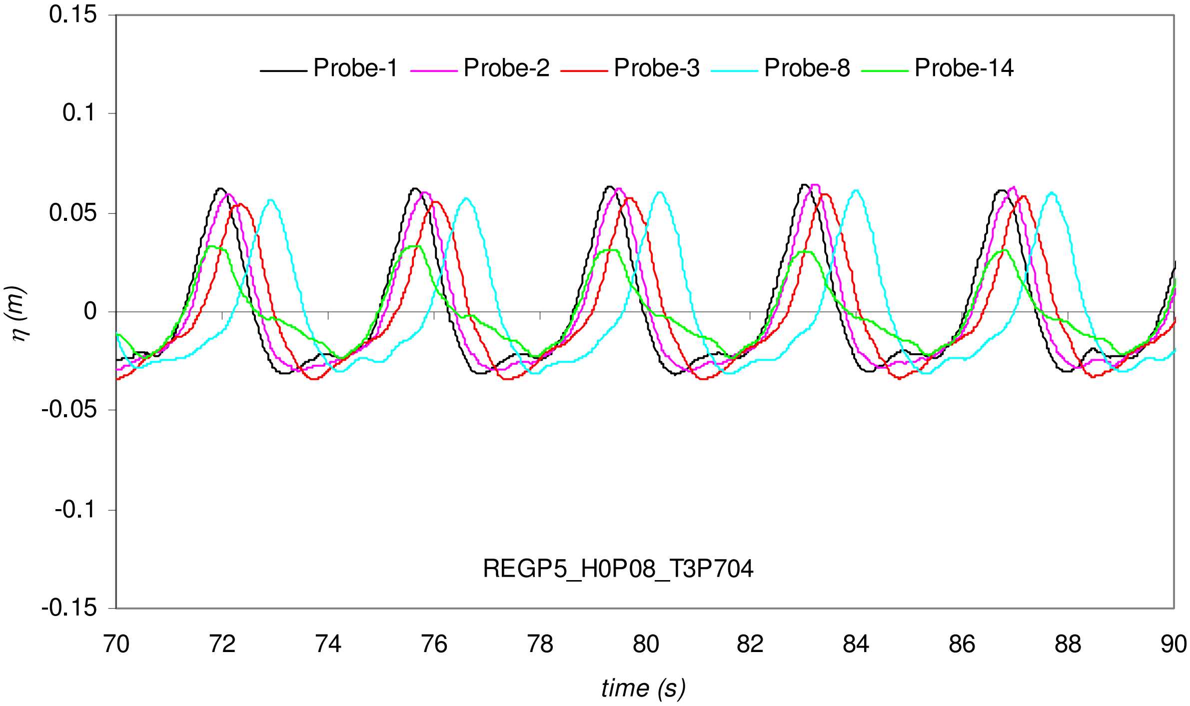

Fig. 18a Comparisons of the wave profile at Probes 14, 1, 2, 3 and 8
(C5-7, *h = 0.5m, T = 3.704s and H = 0.08m*)

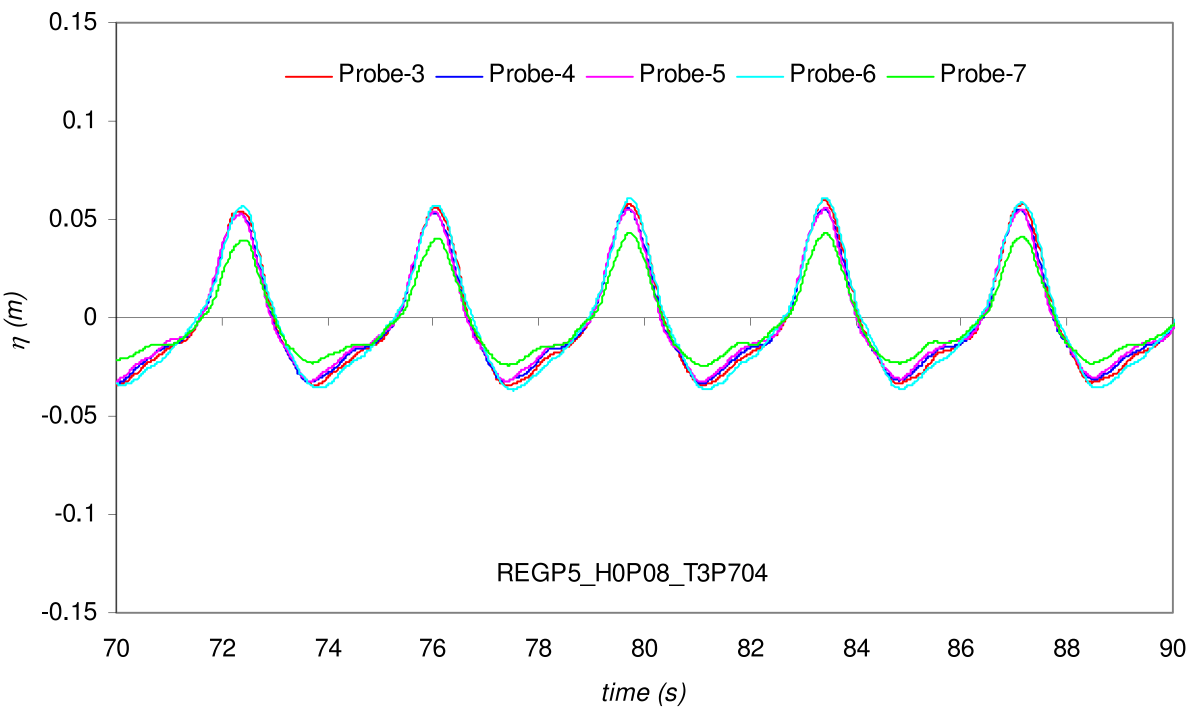

Fig. 18b Comparisons of the wave profile at Probes 3, 4, 5, 6 and 7
(C5-7, *h = 0.5m, T =3.704s and H = 0.08m*)

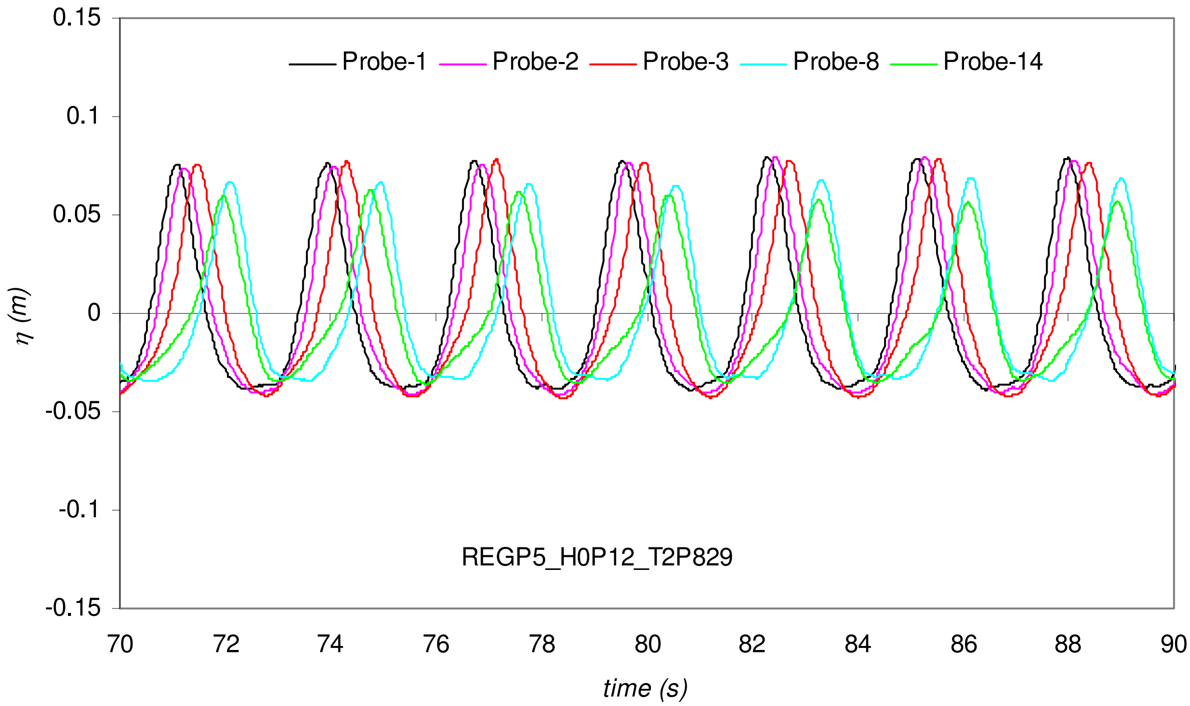

Fig. 19a Comparisons of the wave profile at Probes 14, 1, 2, 3 and 8
(C5-8, *h = 0.5m, T = 2.829s and H = 0.12m*)

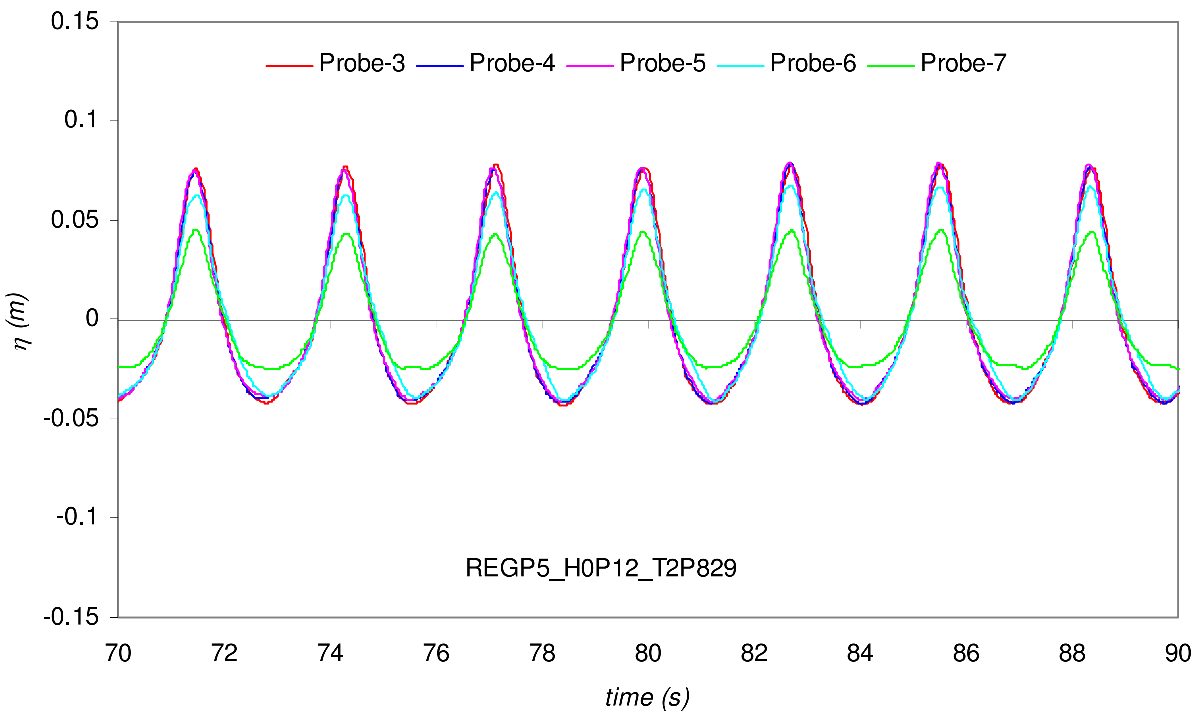

Fig. 19b Comparisons of the wave profile at Probes 3, 4, 5, 6 and 7
(C5-8, *h = 0.5m, T =2.829s and H = 0.12m*)

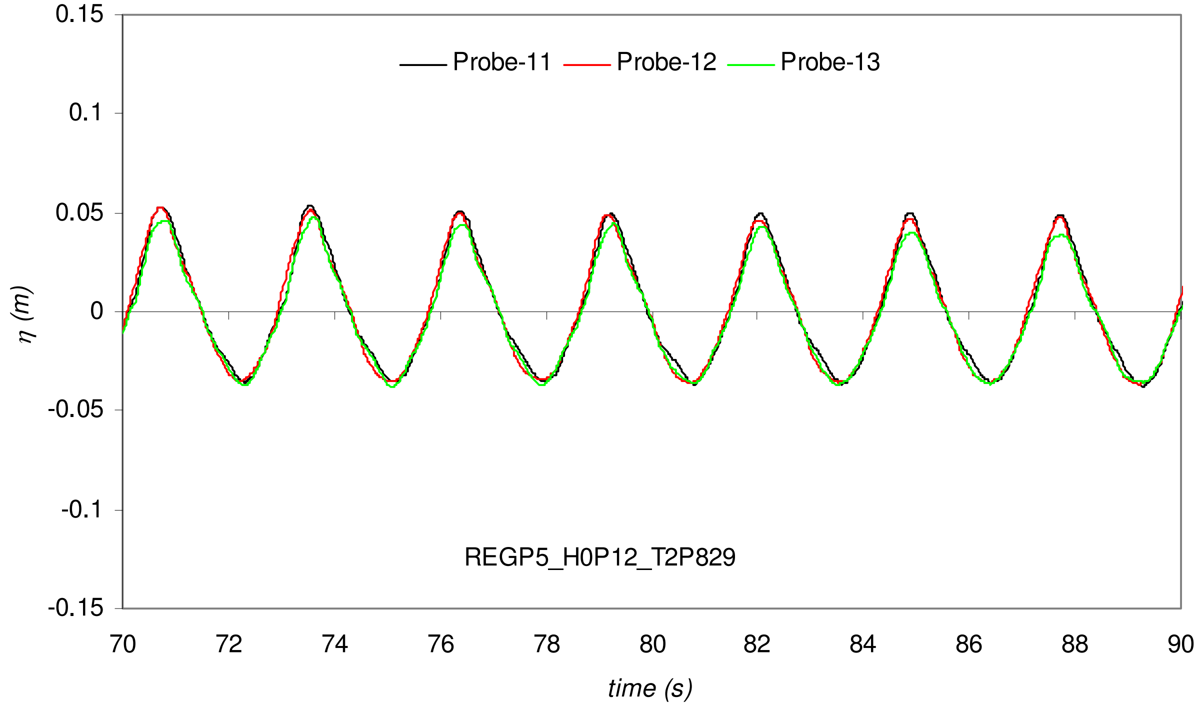

Fig. 19c Comparisons of the wave profile at Probes 11, 12 and 13
(C5-8, *h = 0.5m, T =2.829s and H = 0.12m*)

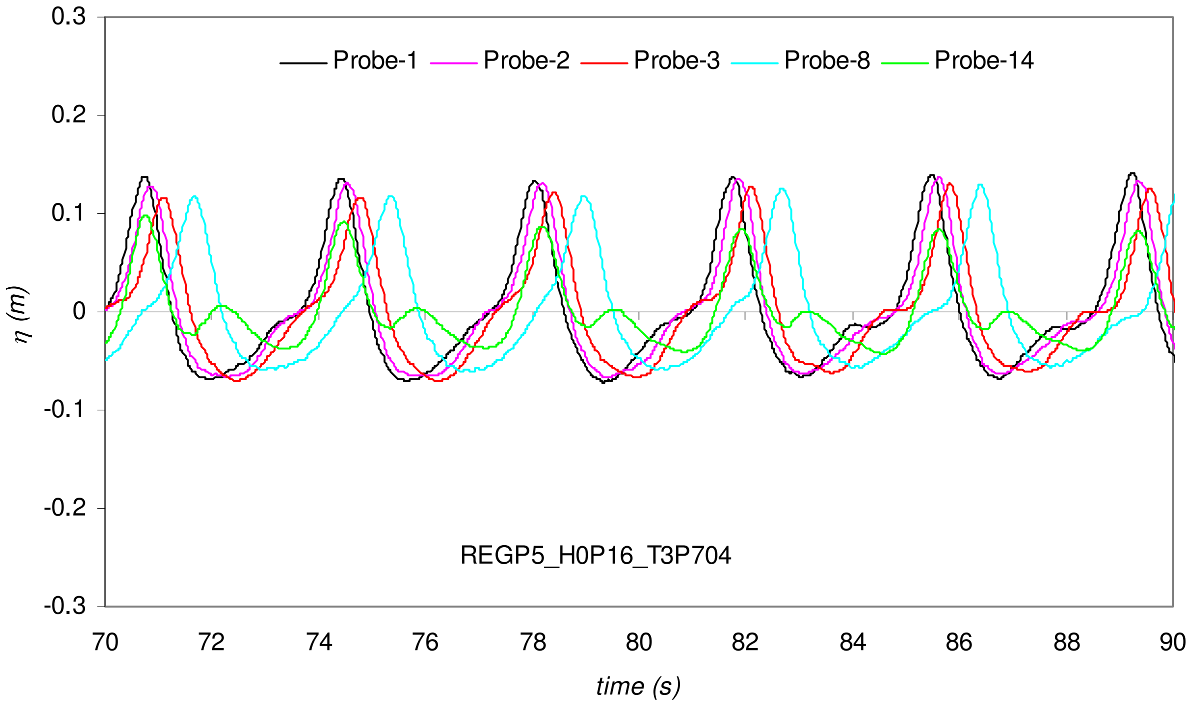

Fig. 20a Comparisons of the wave profile at Probes 14, 1, 2, 3 and 8
(C5-9, *h = 0.5m, T = 3.704s and H = 0.16m*)

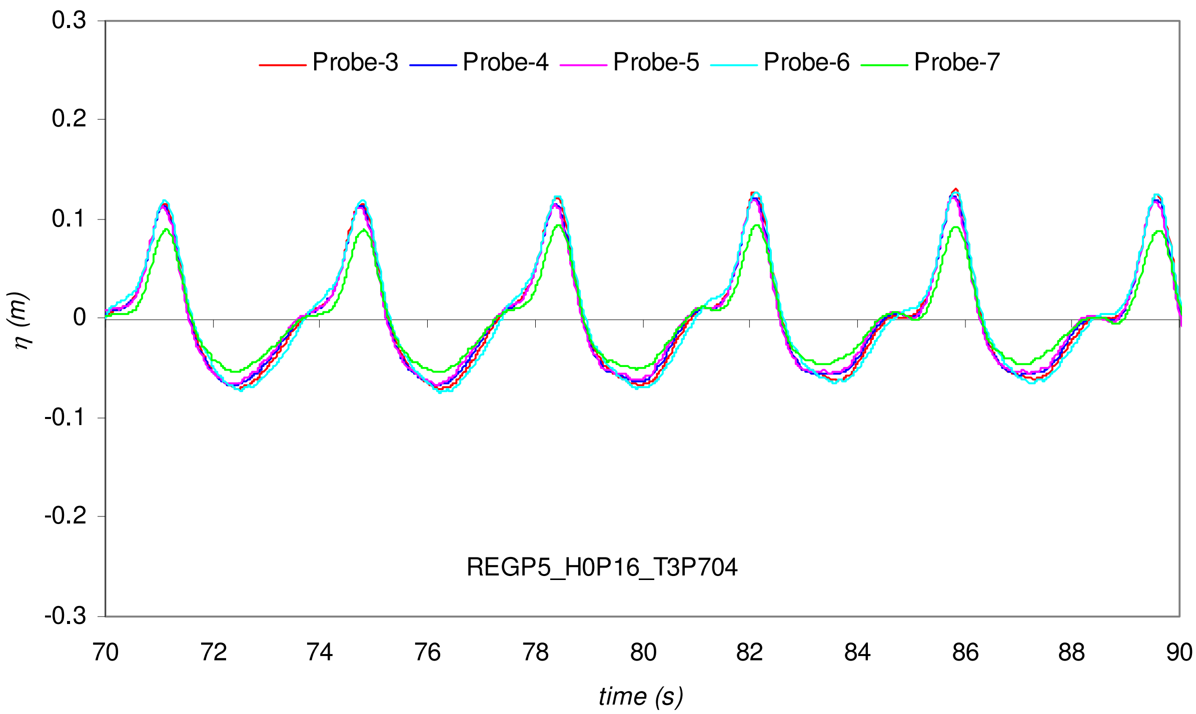

Fig. 20b Comparisons of the wave profile at Probes 3, 4, 5, 6 and 7
(C5-9, *h = 0.5m, T =3.704s and H = 0.16m*)

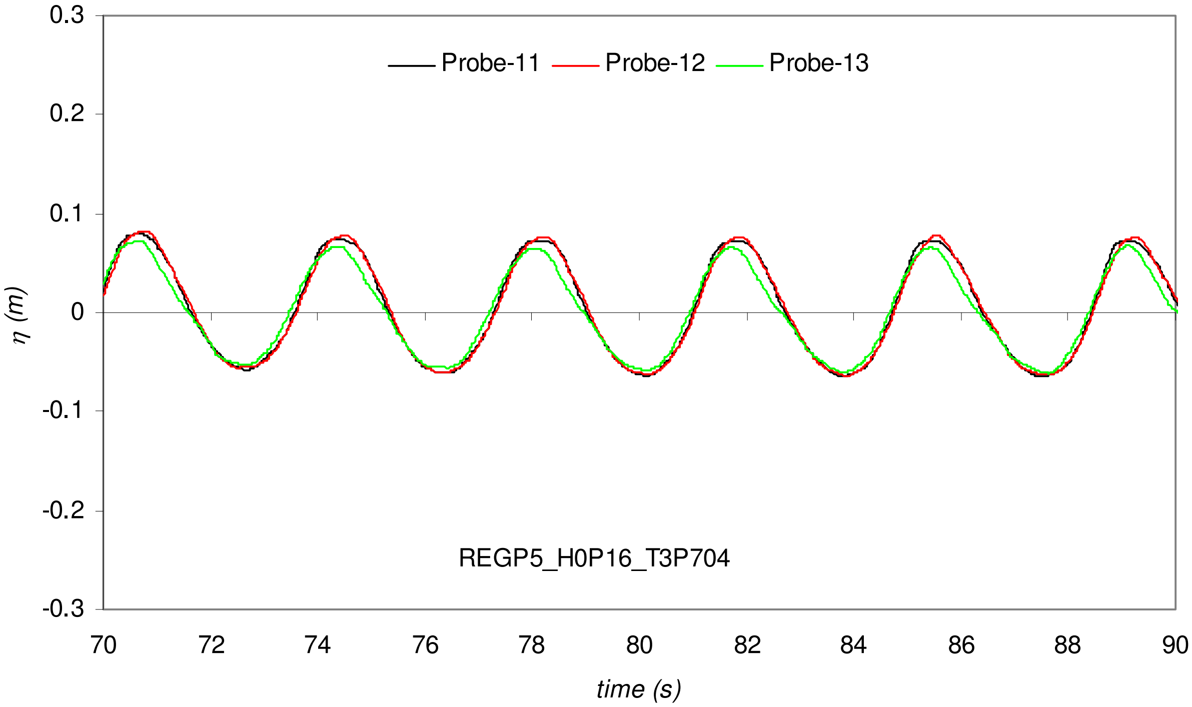

Fig. 20c Comparisons of the wave profile at Probes 11, 12 and 13
(C5-9, *h = 0.5m, T =3.704s and H = 0.16m*)

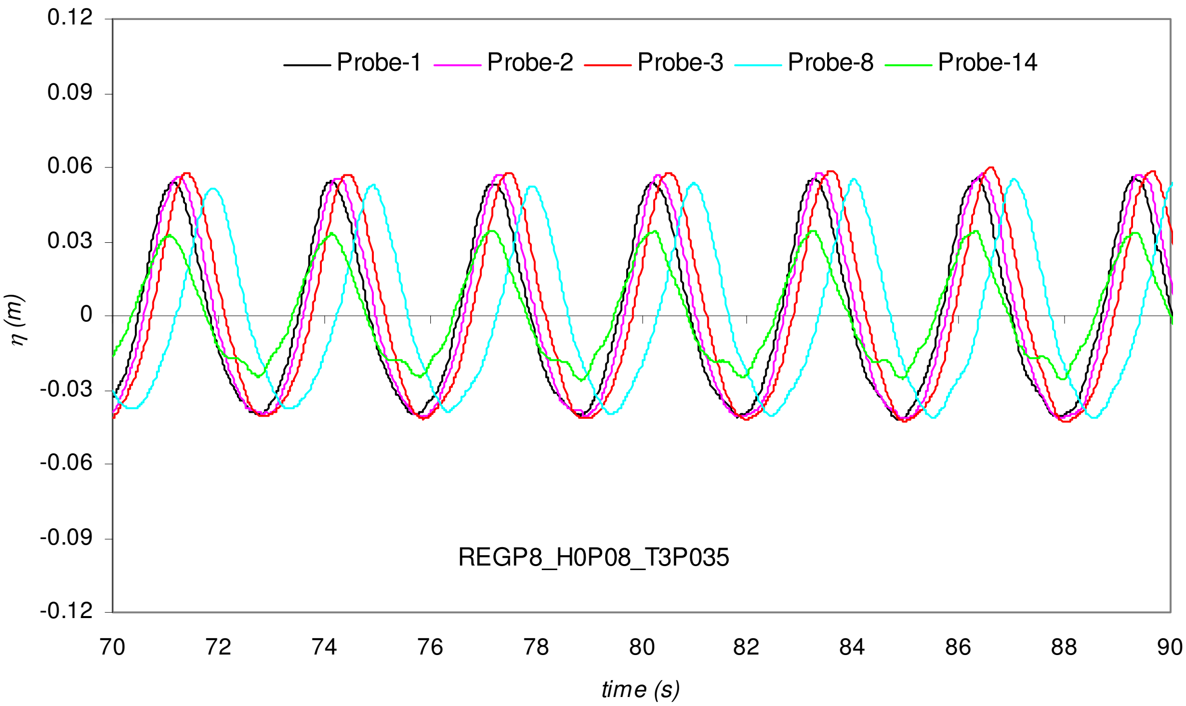

Fig. 21a Comparisons of the wave profile at Probes 14, 1, 2, 3 and 8
(C8-1, $h = 0.8m$, $T = 3.035s$ and $H = 0.08m$)

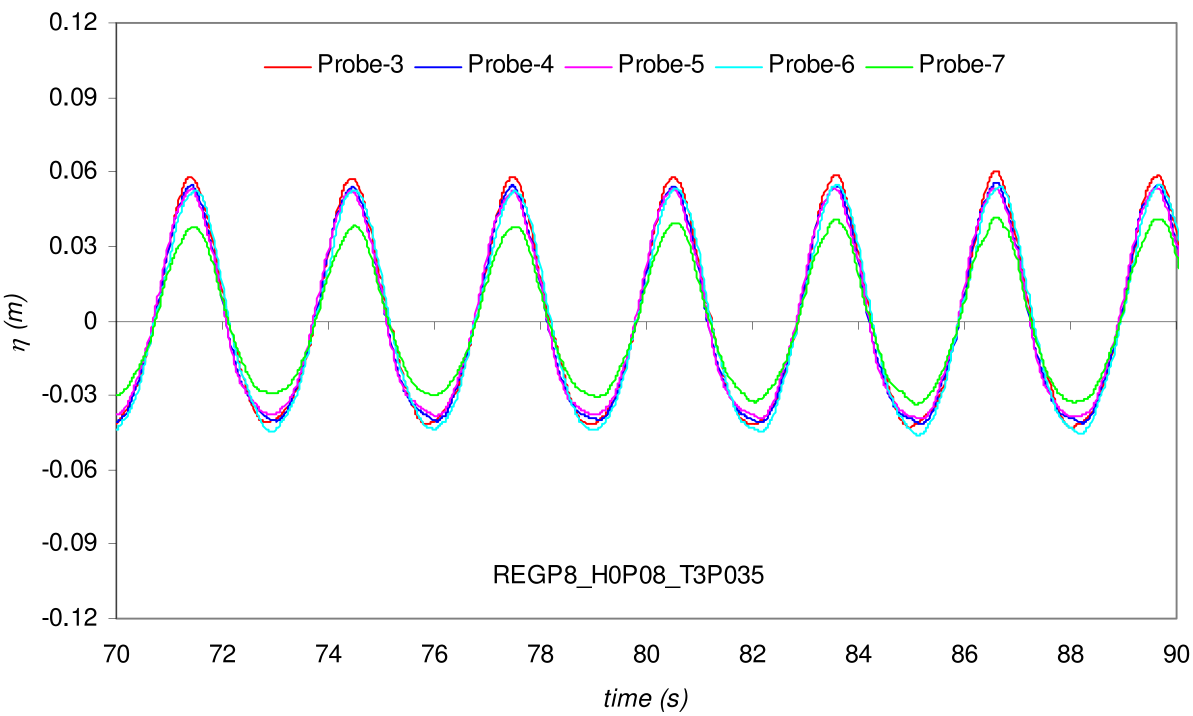

Fig. 21b Comparisons of the wave profile at Probes 3, 4, 5, 6 and 7
(C8-1, $h = 0.8m$, $T = 3.035s$ and $H = 0.08m$)

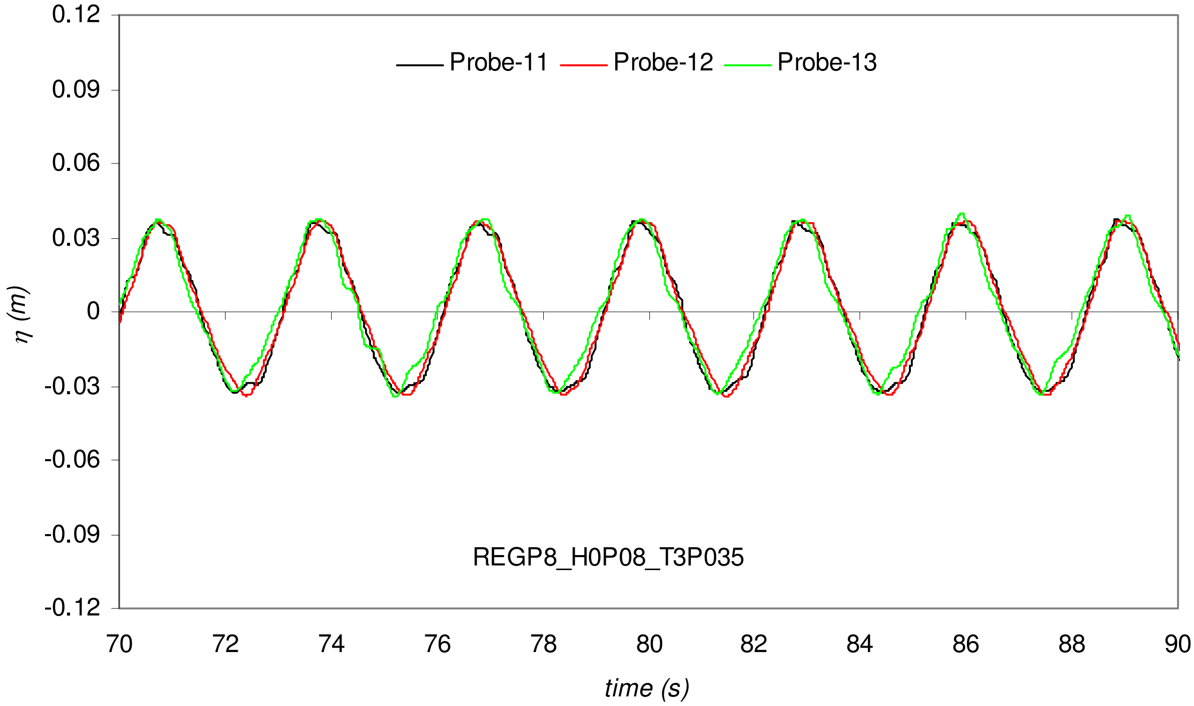

Fig. 21c Comparisons of the wave profile at Probes 11, 12 and 13
(C8-1, *h = 0.8m, T = 3.035s and H = 0.08m*)

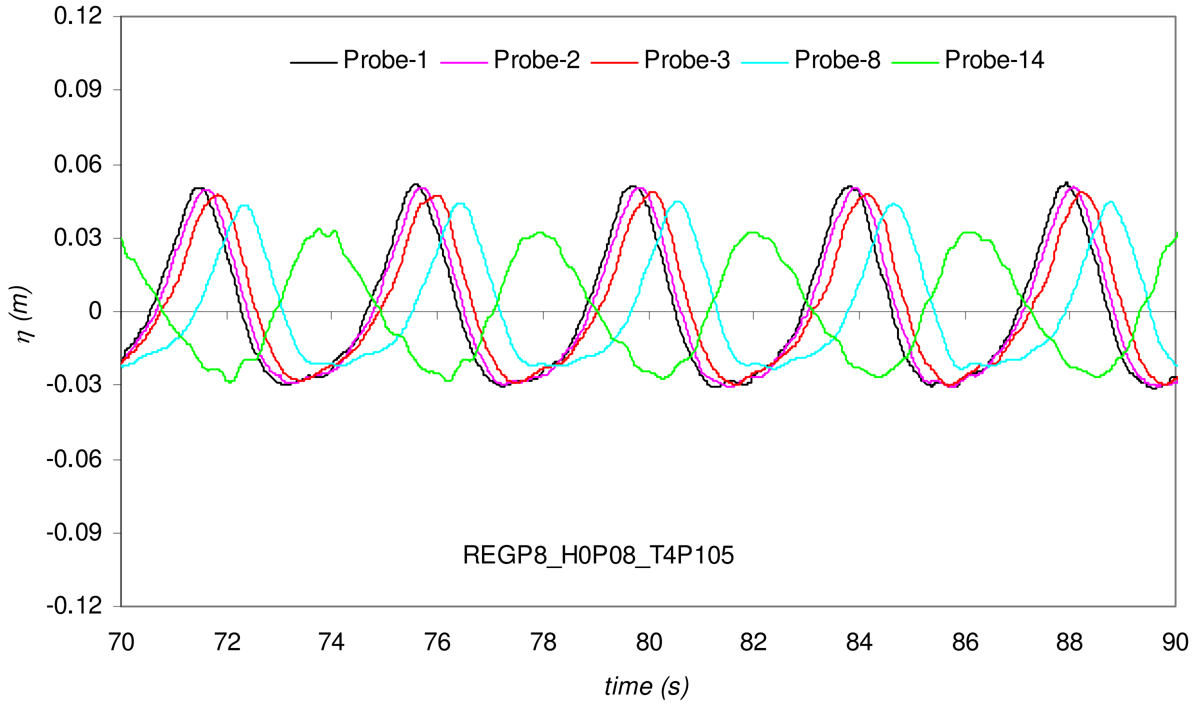

Fig. 22a Comparisons of the wave profile at Probes 14, 1, 2, 3 and 8
(C8-2, $h = 0.8m$, $T = 4.105s$ *and* $H = 0.08m$)

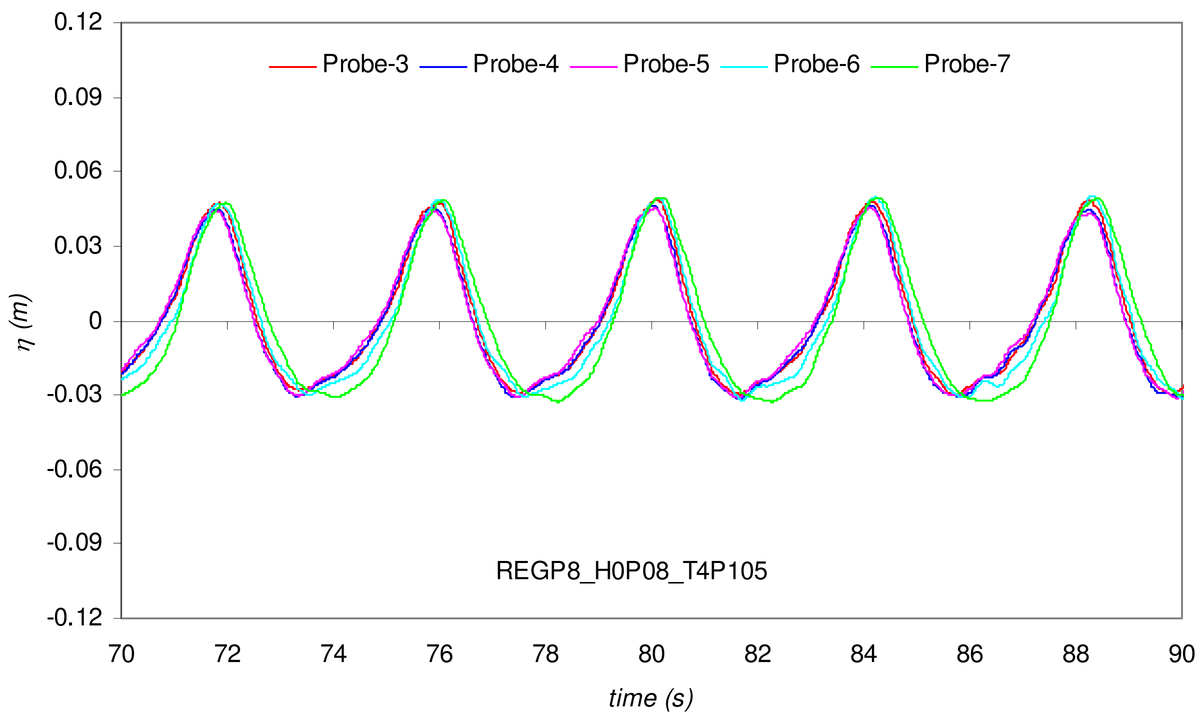

Fig. 22b Comparisons of the wave profile at Probes 3, 4, 5, 6 and 7
(C8-2, $h = 0.8m$, $T = 4.105s$ *and* $H = 0.08m$)

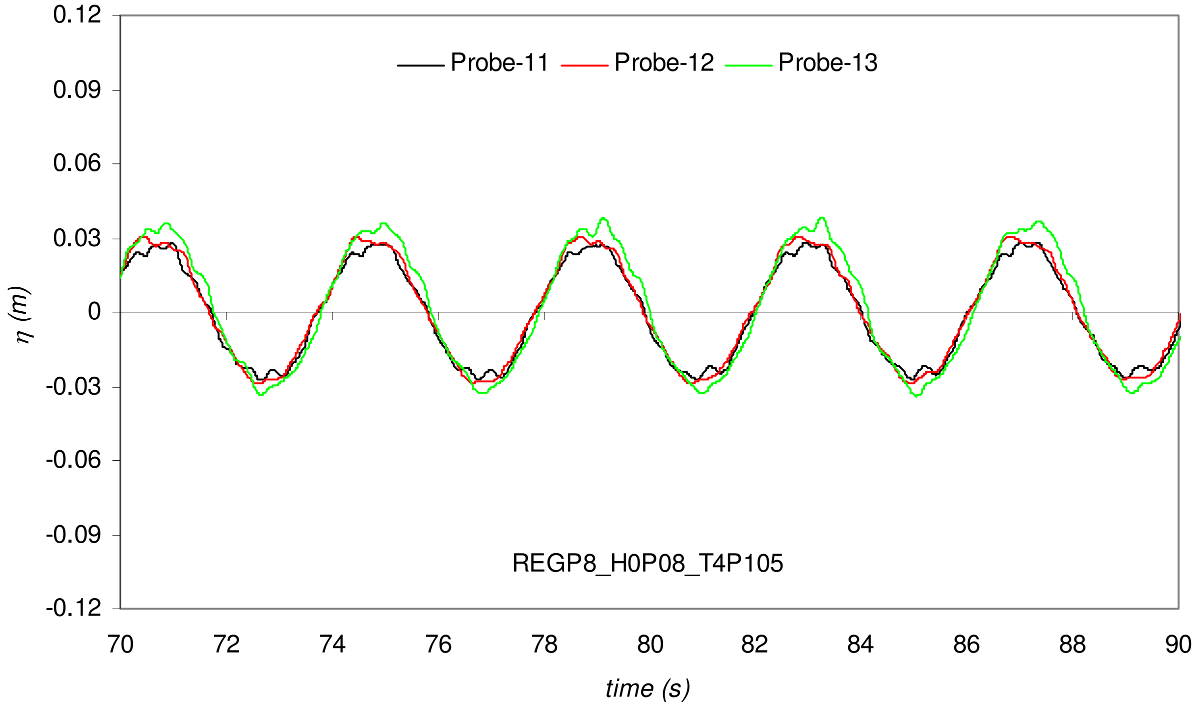

Fig. 22c Comparisons of the wave profile at Probes 11, 12 and 13
(C8-2, *h = 0.8m, T = 4.105s and H = 0.08m*)

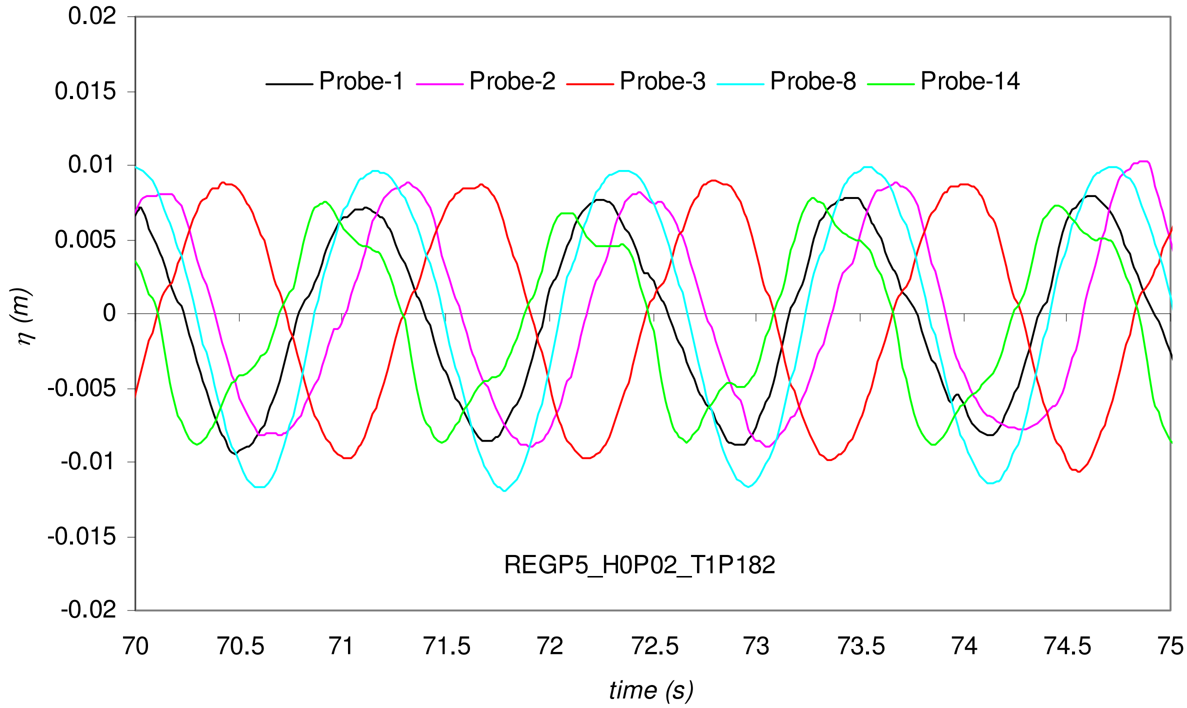

Fig. 23a Wave profile at Probes 14, 1, 2, 3 and 8 for First-order generation
(C5-1, *h = 0.5m, T = 1.182s and H = 0.02m*)

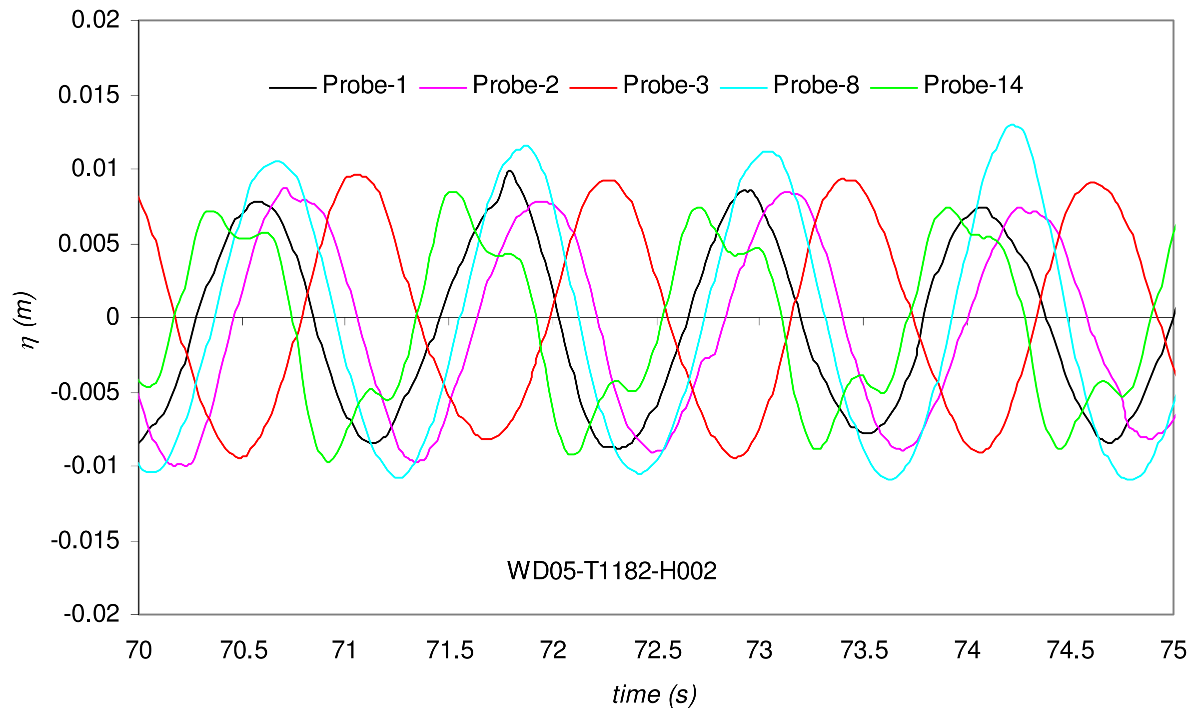

Fig. 23b Wave profile at Probes 14, 1, 2, 3 and 8 for Second-order generation
(C5-1, *h = 0.5m, T = 1.182s and H = 0.02m*)

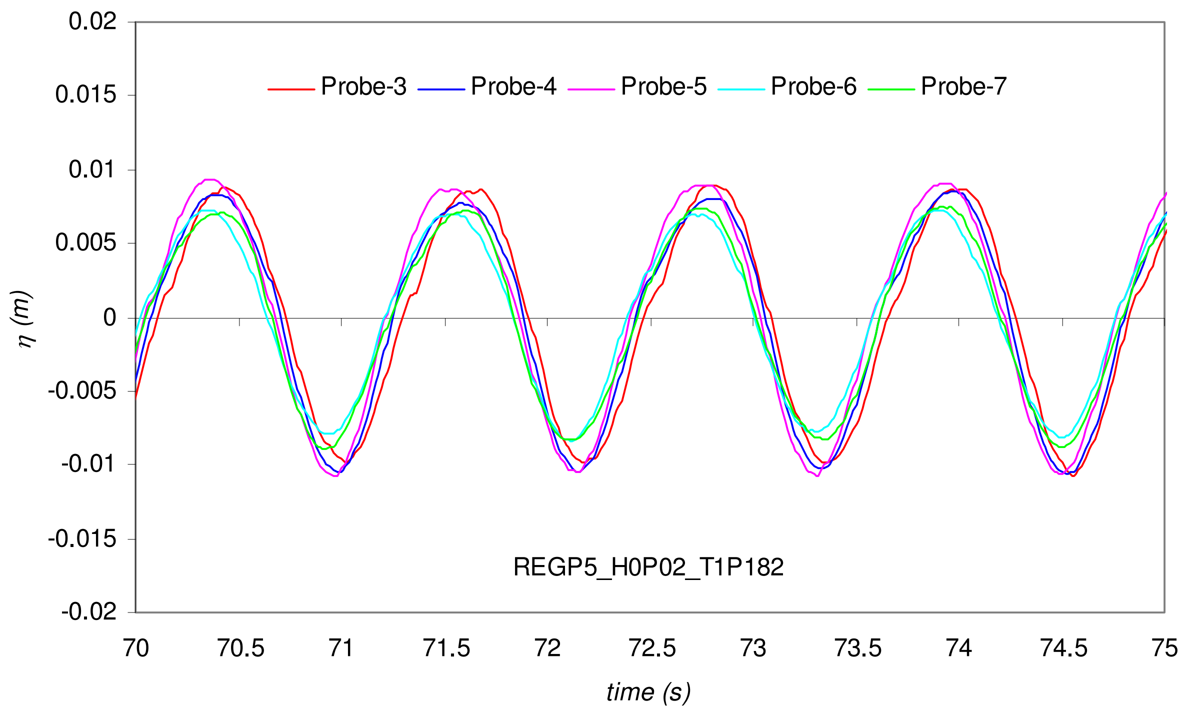

Fig. 23c Wave profile at Probes 3, 4, 5, 6 and 7 for First-order generation
(C5-1, $h = 0.5m$, $T = 1.182s$ and $H = 0.02m$)

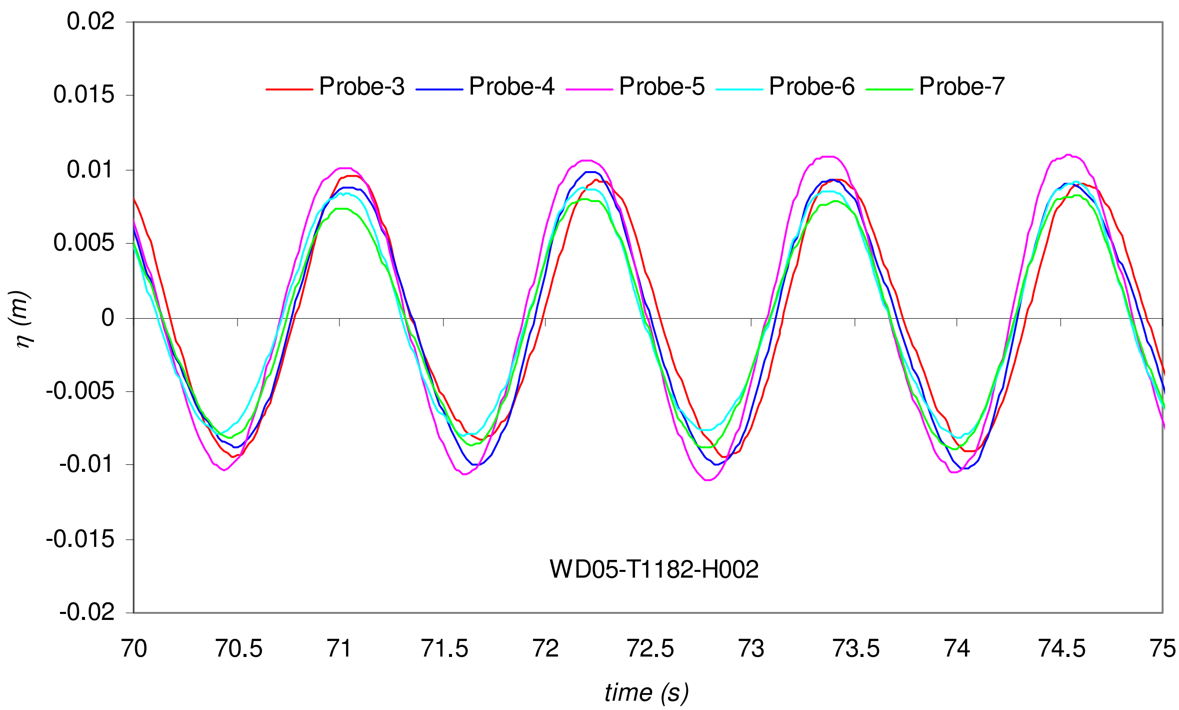

Fig. 23d Wave profile at Probes 3, 4, 5, 6 and 7 for Second-order generation
(C5-1, $h = 0.5m$, $T = 1.182s$ and $H = 0.02m$)

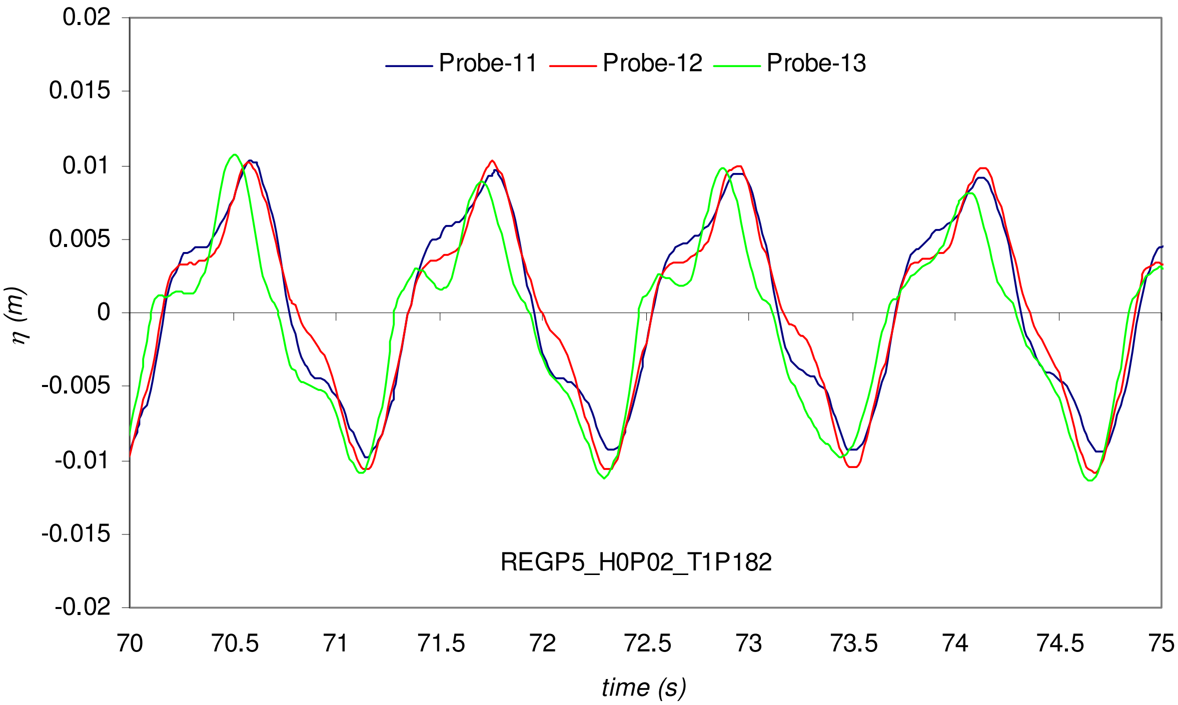

Fig. 23e Wave profile at Probes 11, 12 and 13 for First-order generation
(C5-1, *h = 0.5m, T = 1.182s and H = 0.02m*)

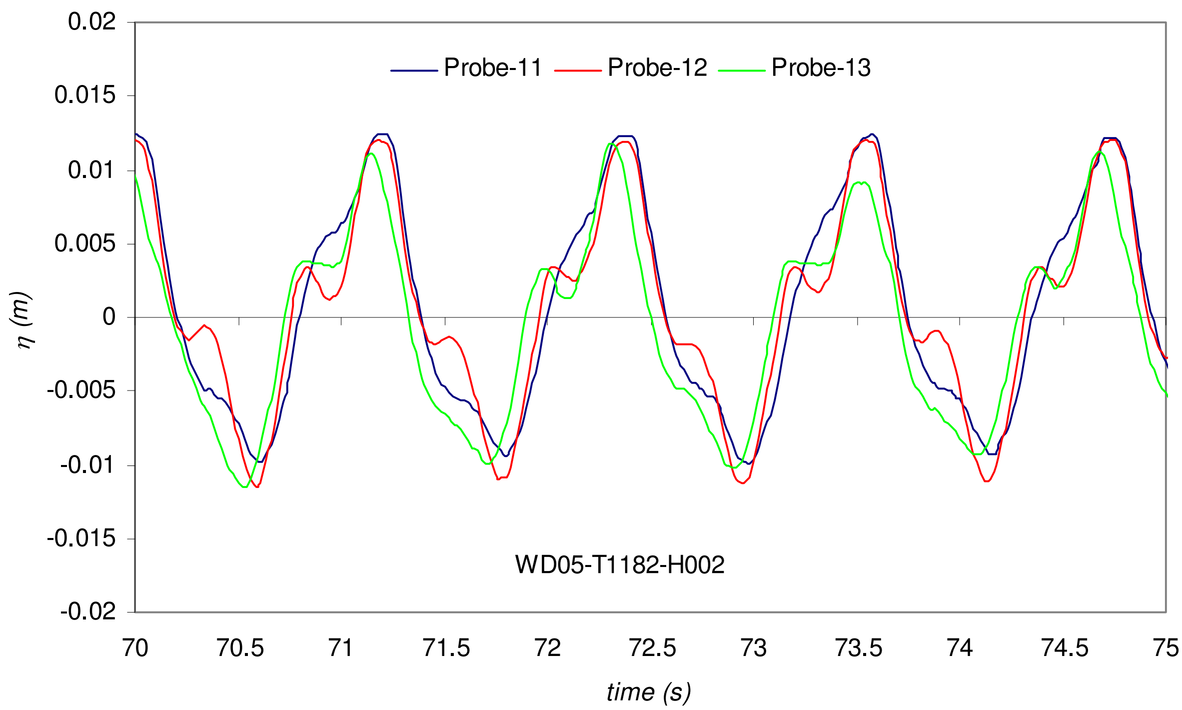

Fig. 23f Wave profile at Probes 11, 12 and 13 for Second-order generation
(C5-1, *h = 0.5m, T = 1.182s and H = 0.02m*)

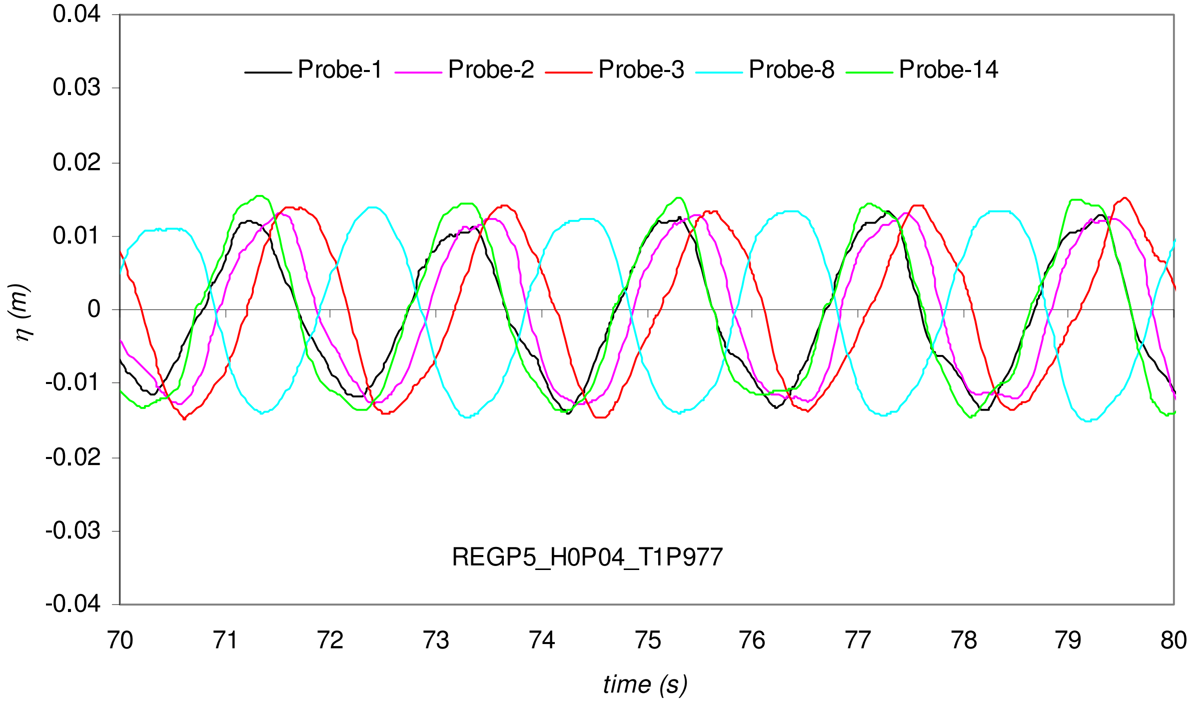

Fig. 24a Wave profile at Probes 14, 1, 2, 3 and 8 for First-order generation
(C5-4, $h = 0.5m$, $T = 1.977s$ and $H = 0.04m$)

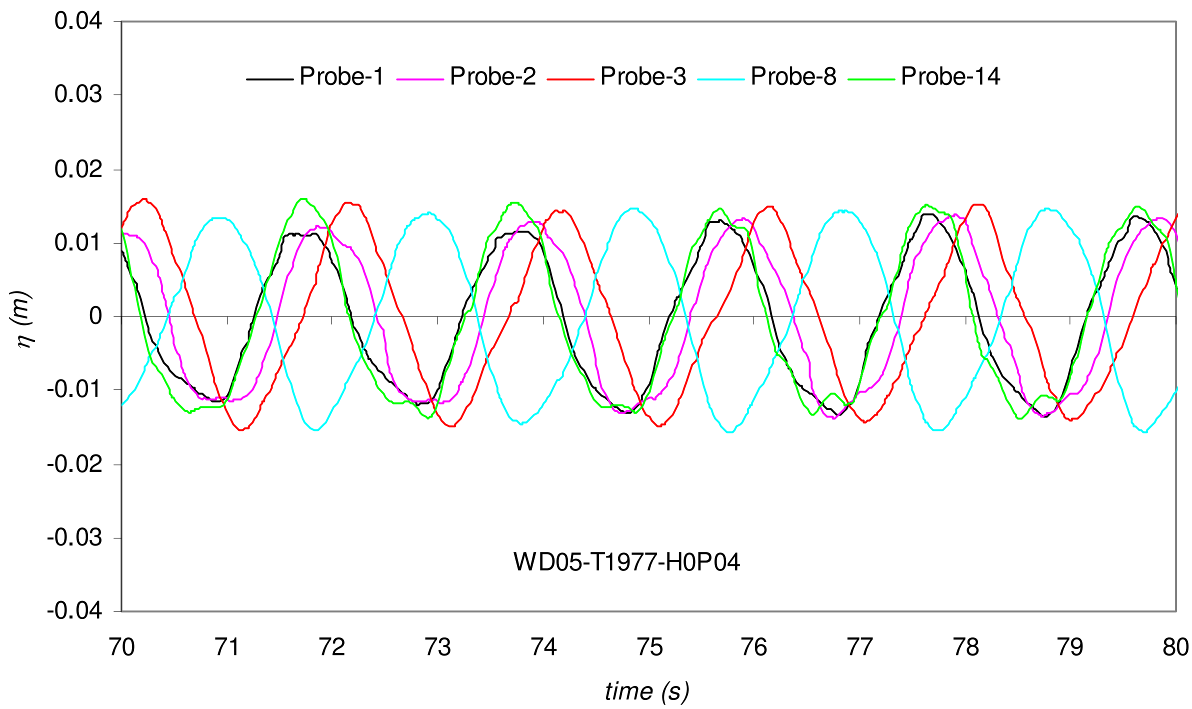

Fig. 24b Wave profile at Probes 14, 1, 2, 3 and 8 for Second-order generation
(C5-4, $h = 0.5m$, $T = 1.977s$ and $H = 0.04m$)

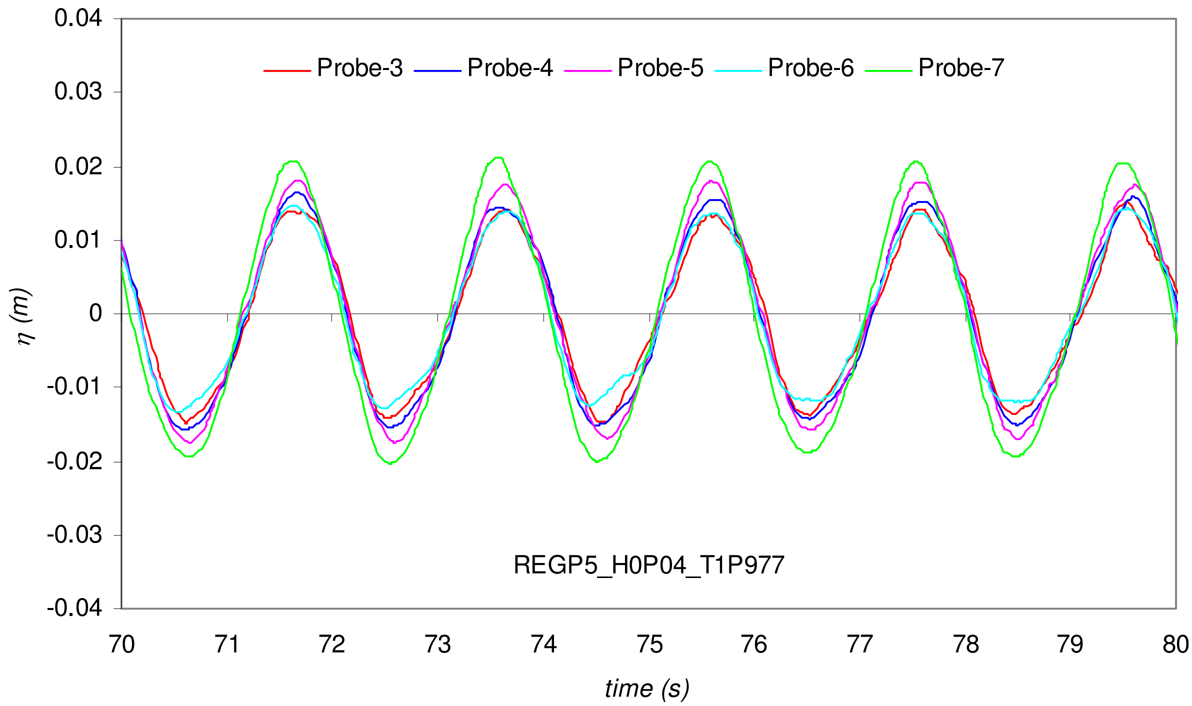

Fig. 24c Wave profile at Probes 3, 4, 5, 6 and 7 for First-order generation
(C5-4, *h = 0.5m, T = 1.977s and H = 0.04m*)

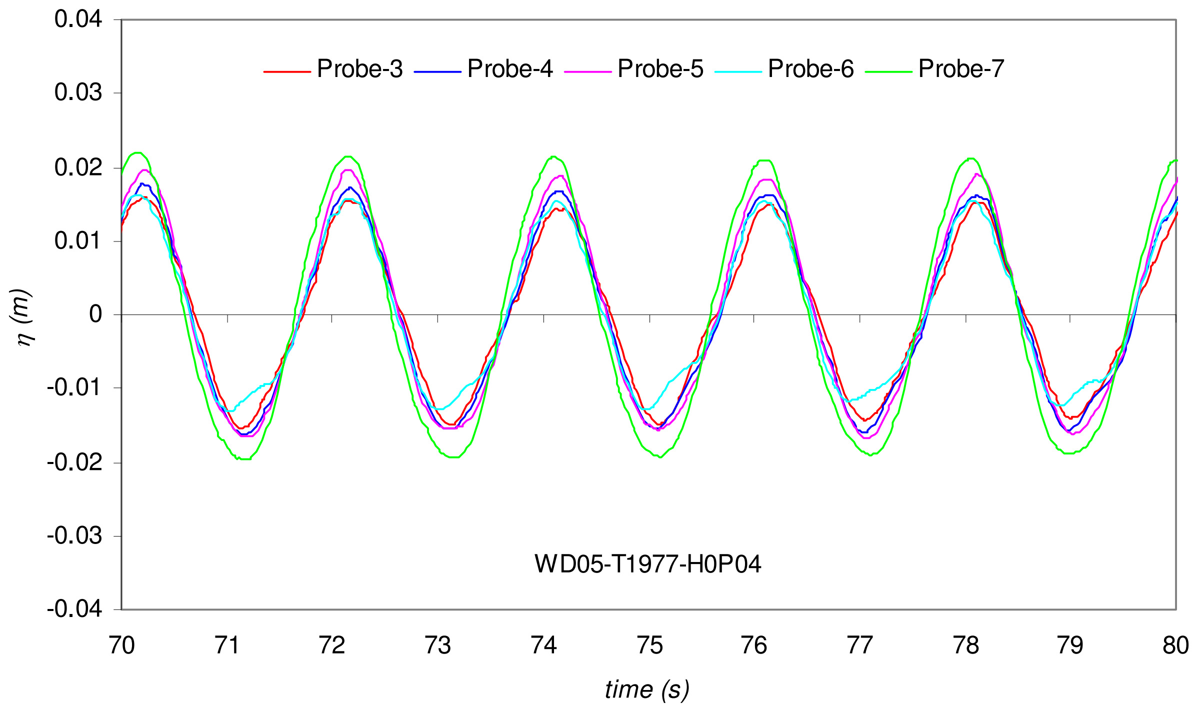

Fig. 24d Wave profile at Probes 3, 4, 5, 6 and 7 for Second-order generation
(C5-4, *h = 0.5m, T = 1.977s and H = 0.04m*)

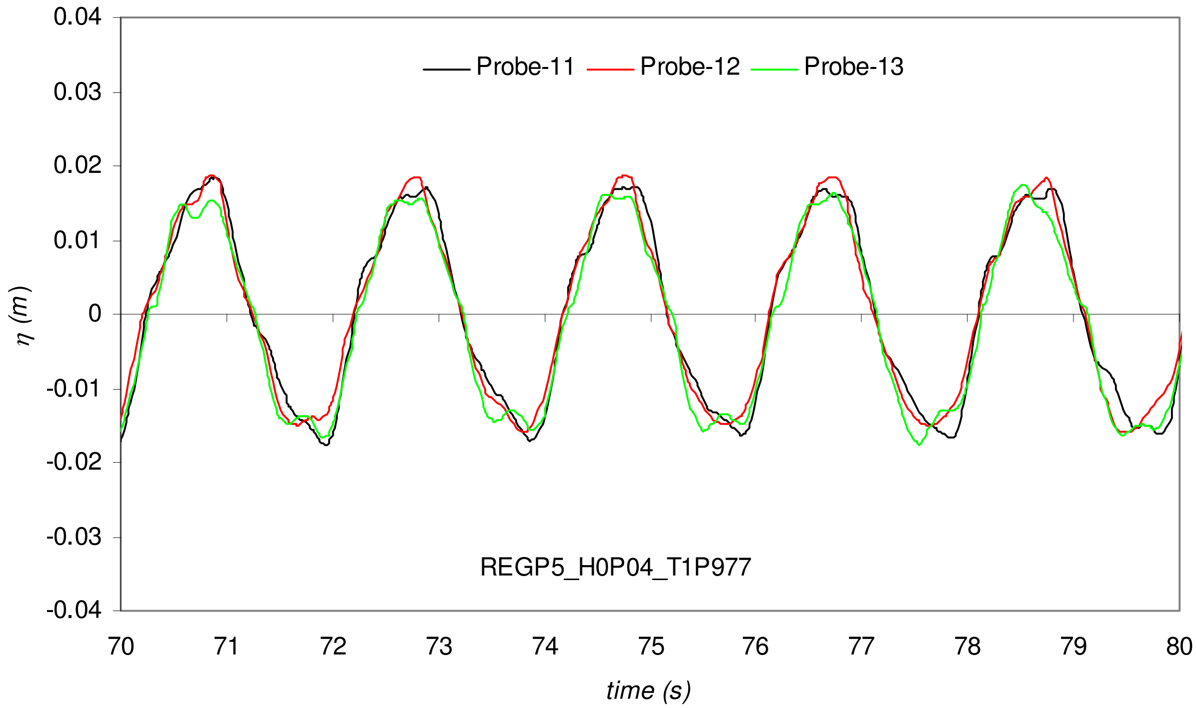

Fig. 24e Wave profile at Probes 11, 12 and 13 for First-order generation
(C5-4, *h = 0.5m, T = 1.977s and H = 0.04m*)

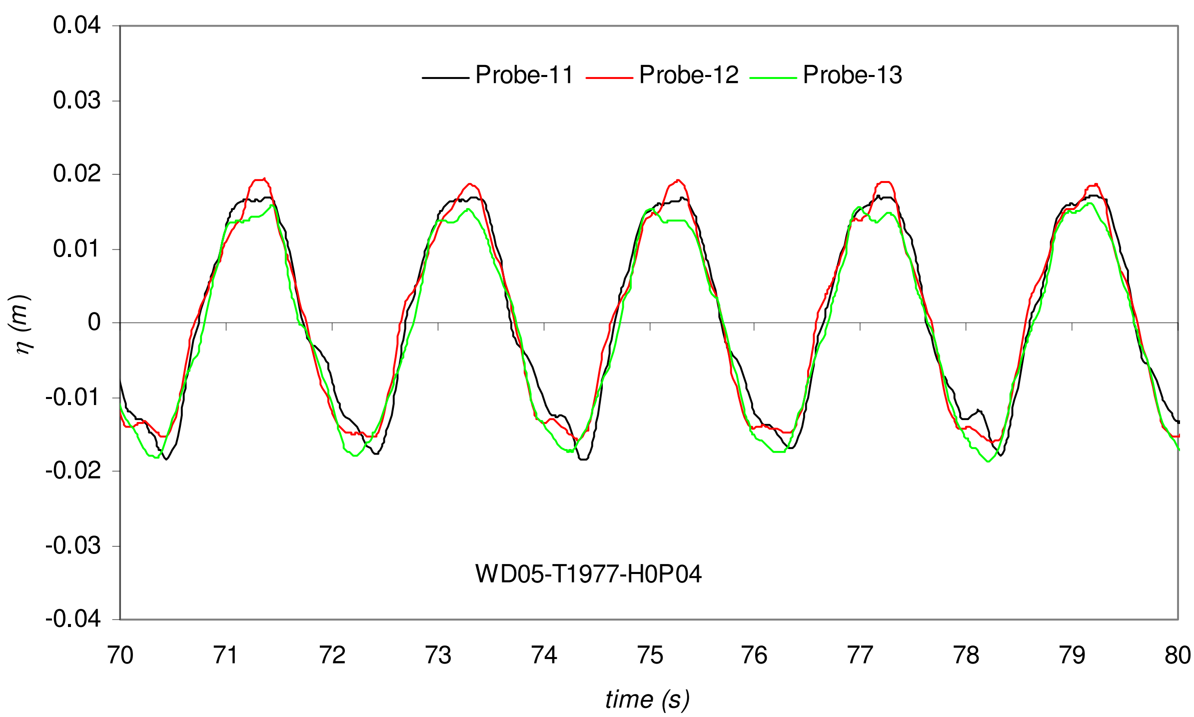

Fig. 24f Wave profile at Probes 11, 12 and 13 for Second-order generation
(C5-4, *h = 0.5m, T = 1.977s and H = 0.04m*)

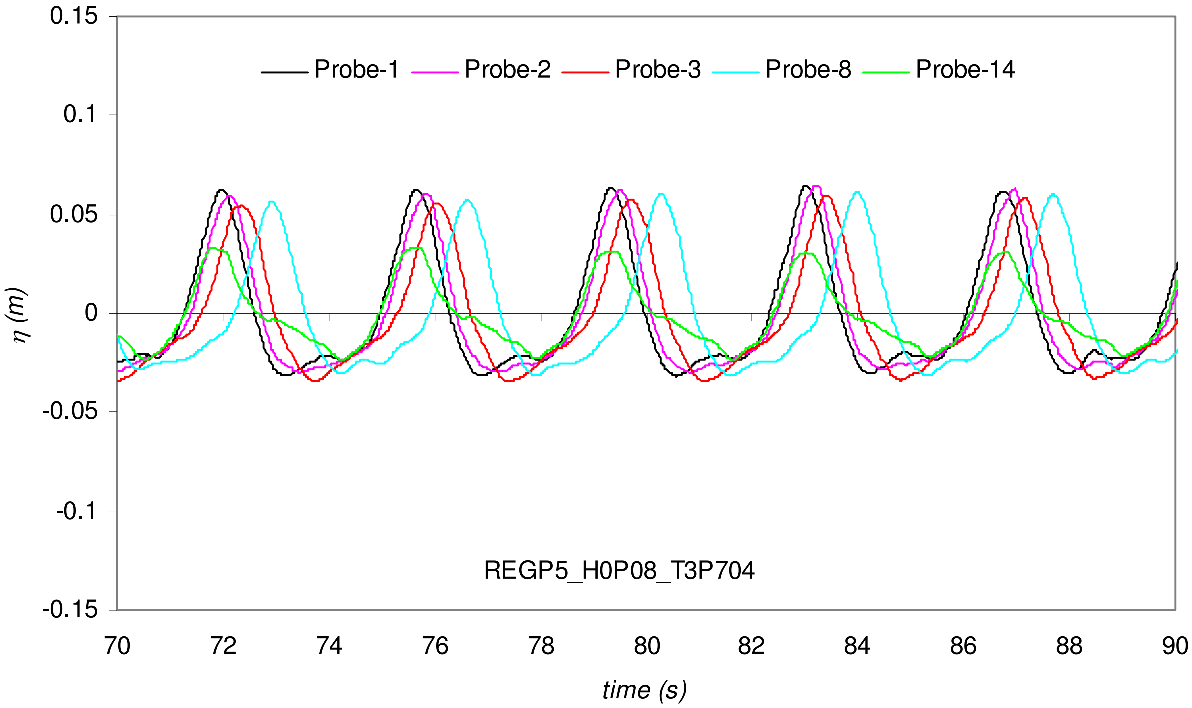

Fig. 25a Wave profile at Probes 14, 1, 2, 3 and 8 for First-order generation
(C5-7, $h = 0.5m$, $T = 3.704s$ and $H = 0.08m$)

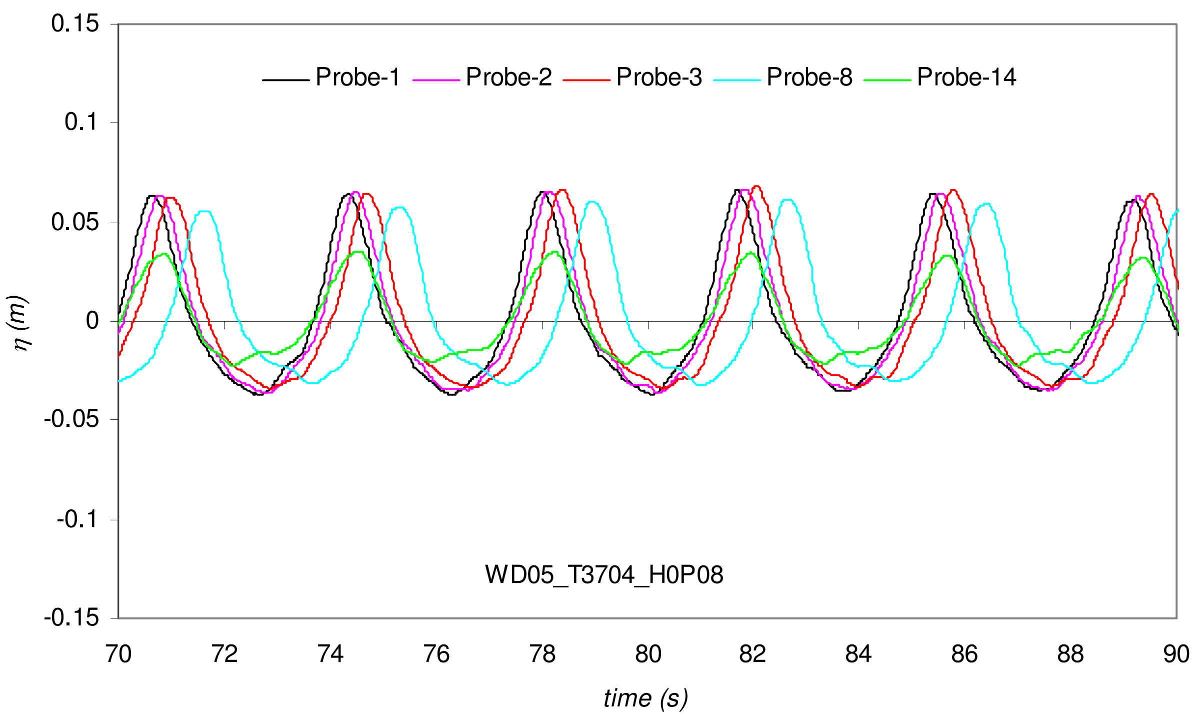

Fig. 25b Wave profile at Probes 14, 1, 2, 3 and 8 for Second-order generation
(C5-7, $h = 0.5m$, $T = 3.704s$ and $H = 0.08m$)

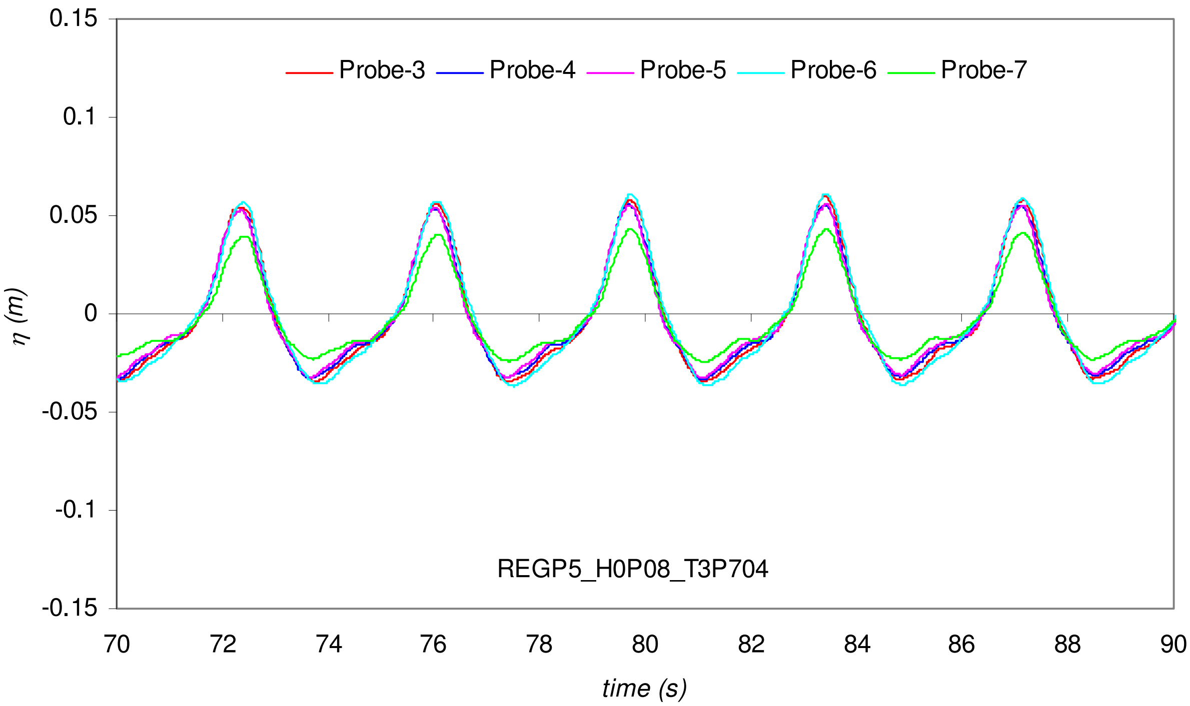

Fig. 25c Wave profile at Probes 3, 4, 5, 6 and 7 for First-order generation
(C5-7, $h = 0.5m$, $T = 3.704s$ *and* $H = 0.08m$)

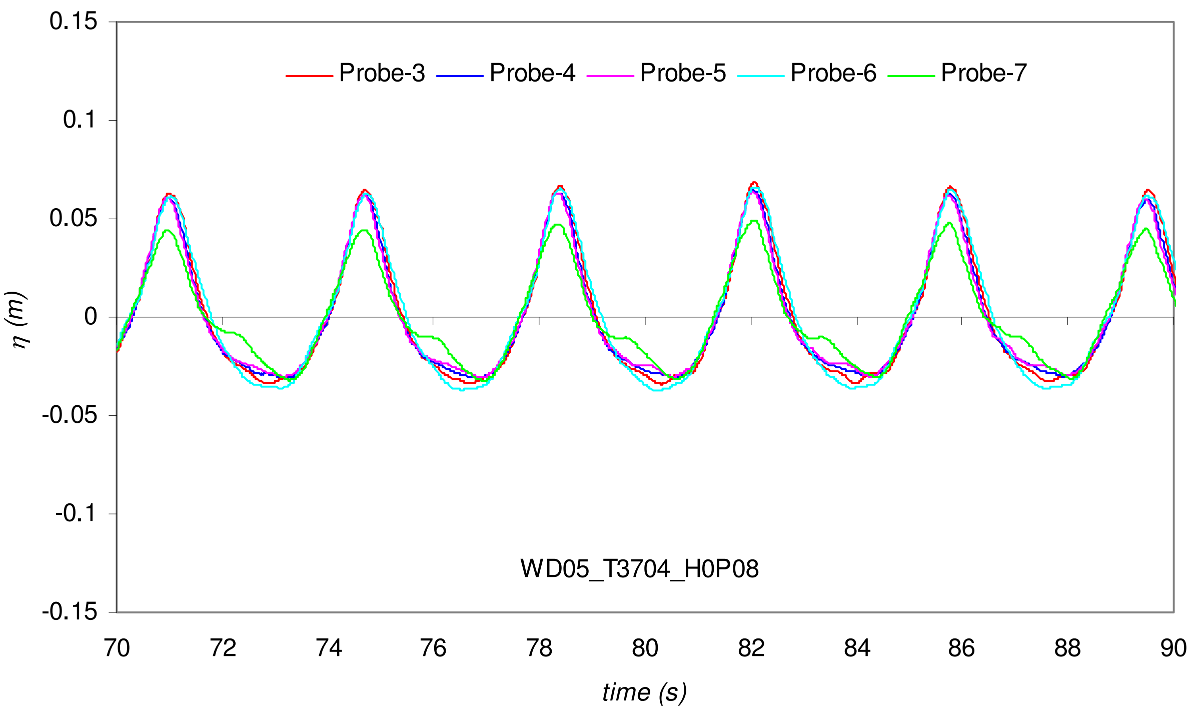

Fig. 25d Wave profile at Probes 3, 4, 5, 6 and 7 for Second-order generation
(C5-7, $h = 0.5m$, $T = 3.704s$ *and* $H = 0.08m$)

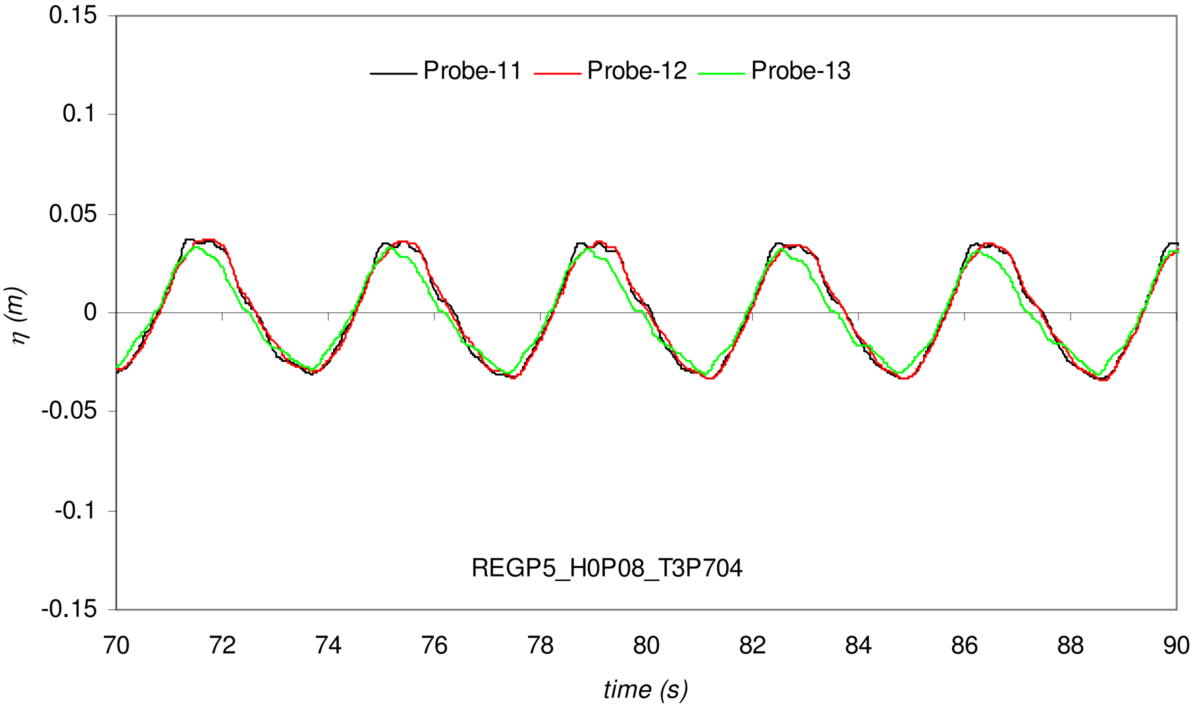

Fig. 25e Wave profile at Probes 11, 12 and 13 for First-order generation
(C5-7, *h = 0.5m, T = 3.704s and H = 0.08m*)

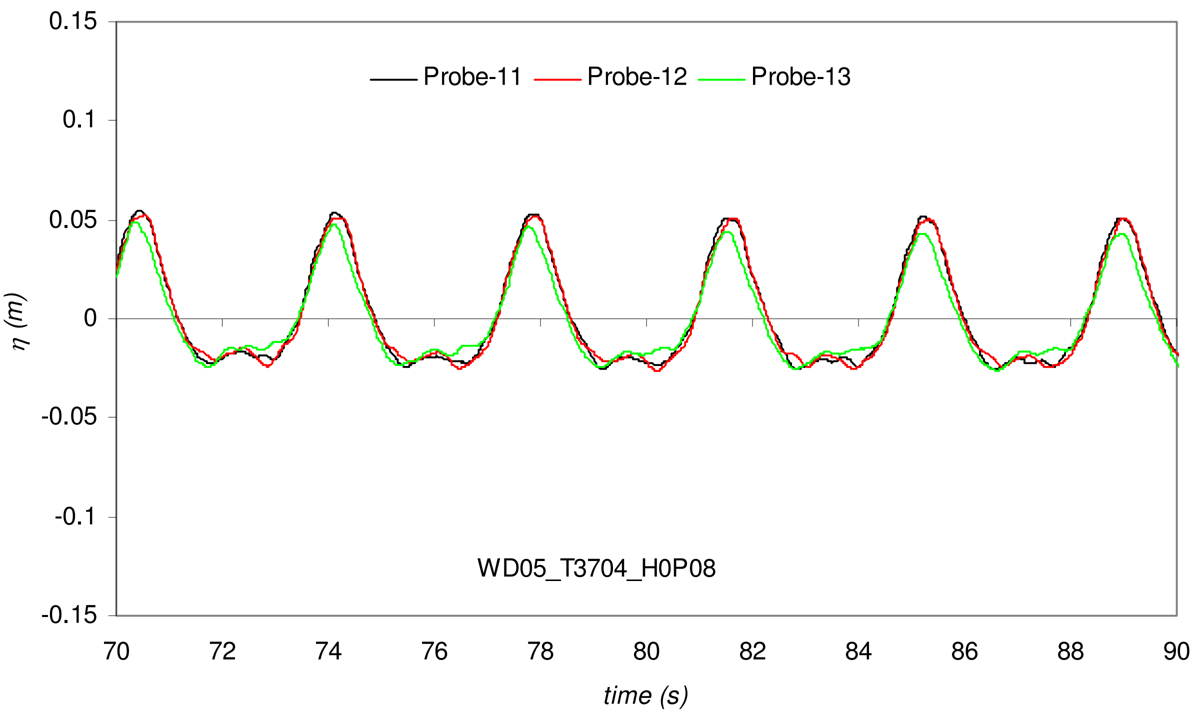

Fig. 25f Wave profile at Probes 11, 12 and 13 for Second-order generation
(C5-7, *h = 0.5m, T = 3.704s and H = 0.08m*)

APPENDIX – II

Figures for Bichromatic waves

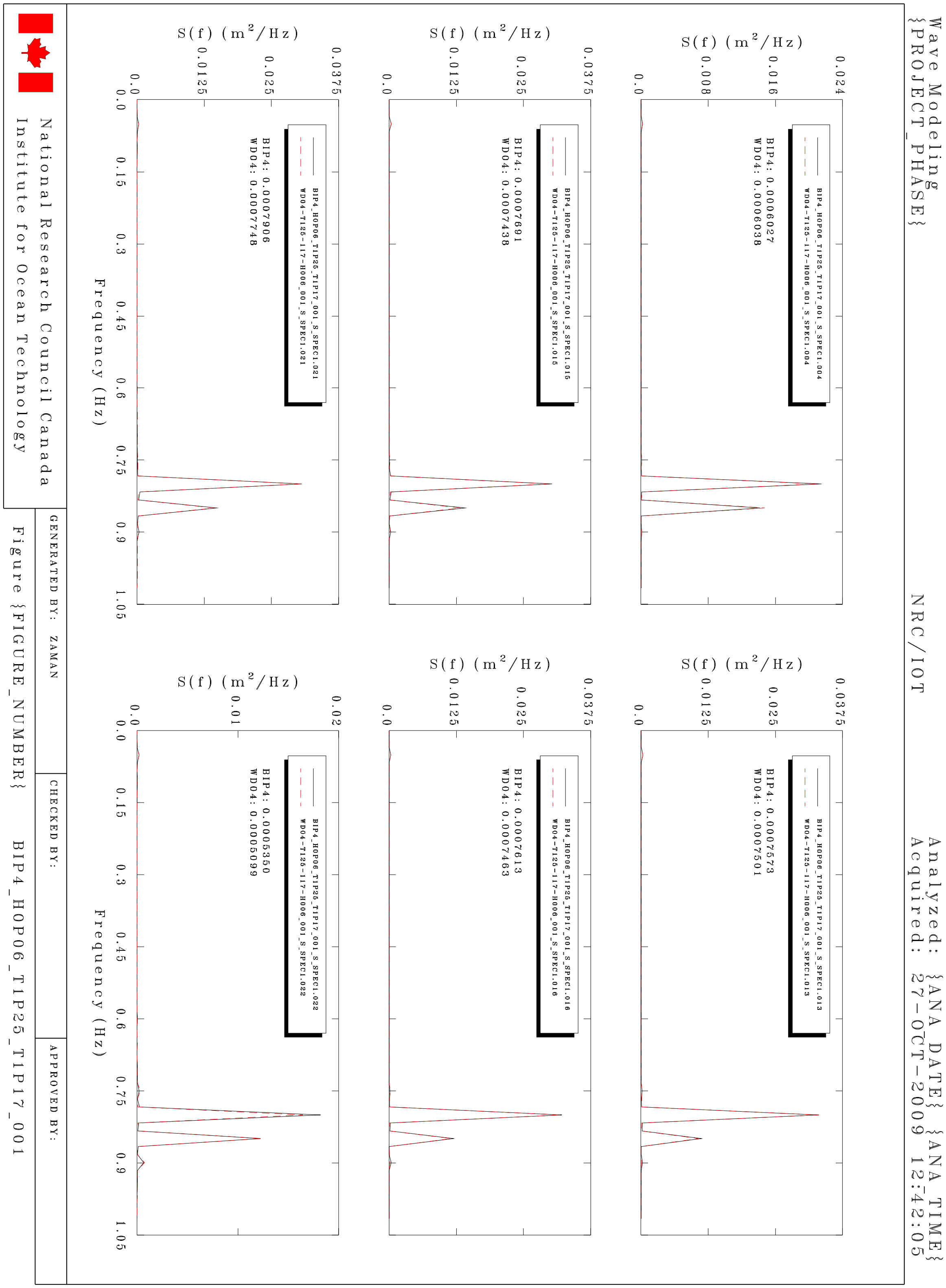

Fig. 26 Comparisons of the energy density between First- and Second-order generations (*Case-1, h=0.4m,* T_1*=1.25s,* T_2*=1.17s,* H_1*=0.06m and* H_2*=0.06m*)

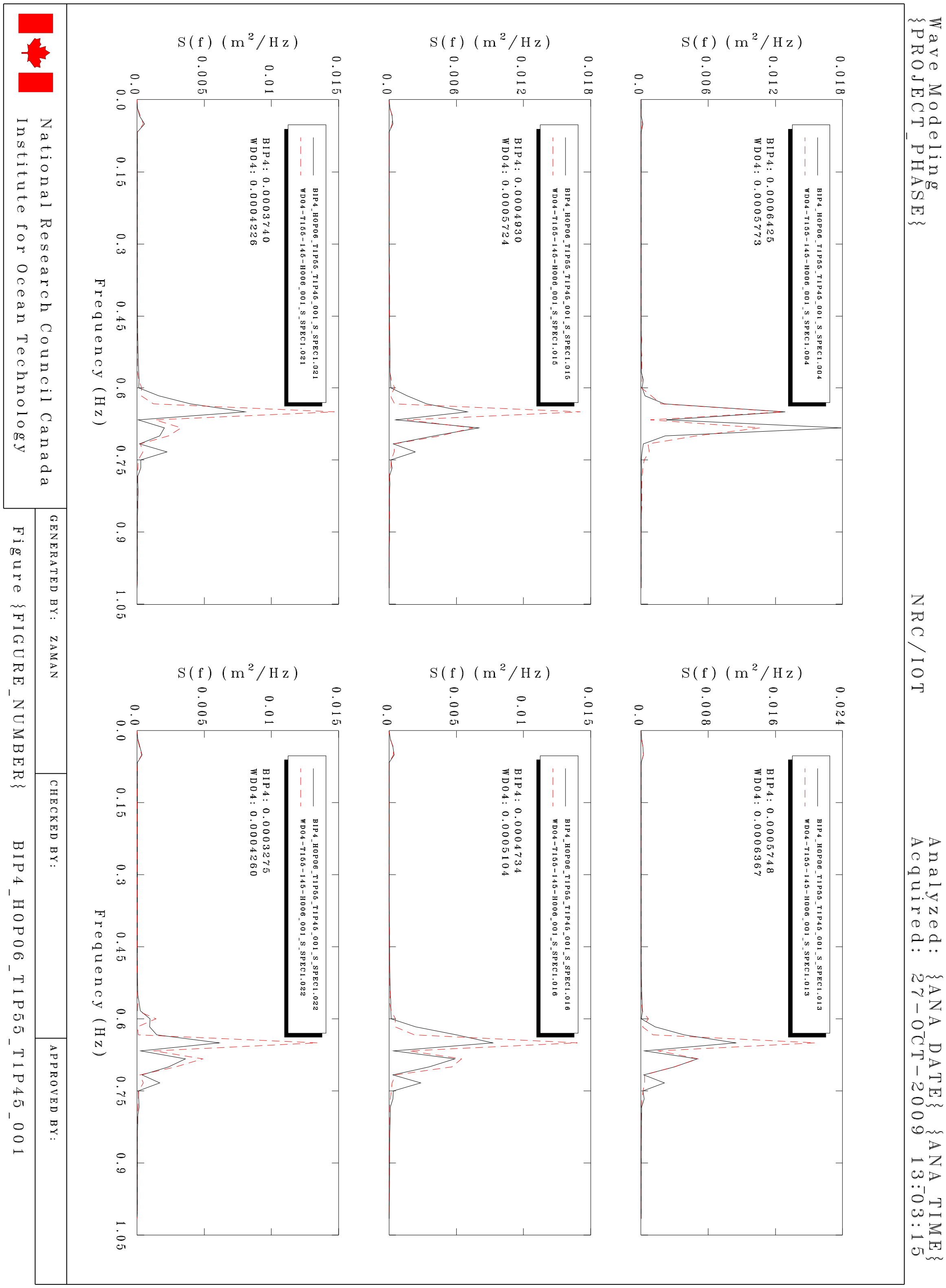

Fig. 27 Comparisons of the energy density between First- and Second-order generations
(*Case-2, $h=0.4m$, $T_1=1.55s$, $T_2=1.45s$, $H_1=0.06m$ and $H_2=0.06m$*)

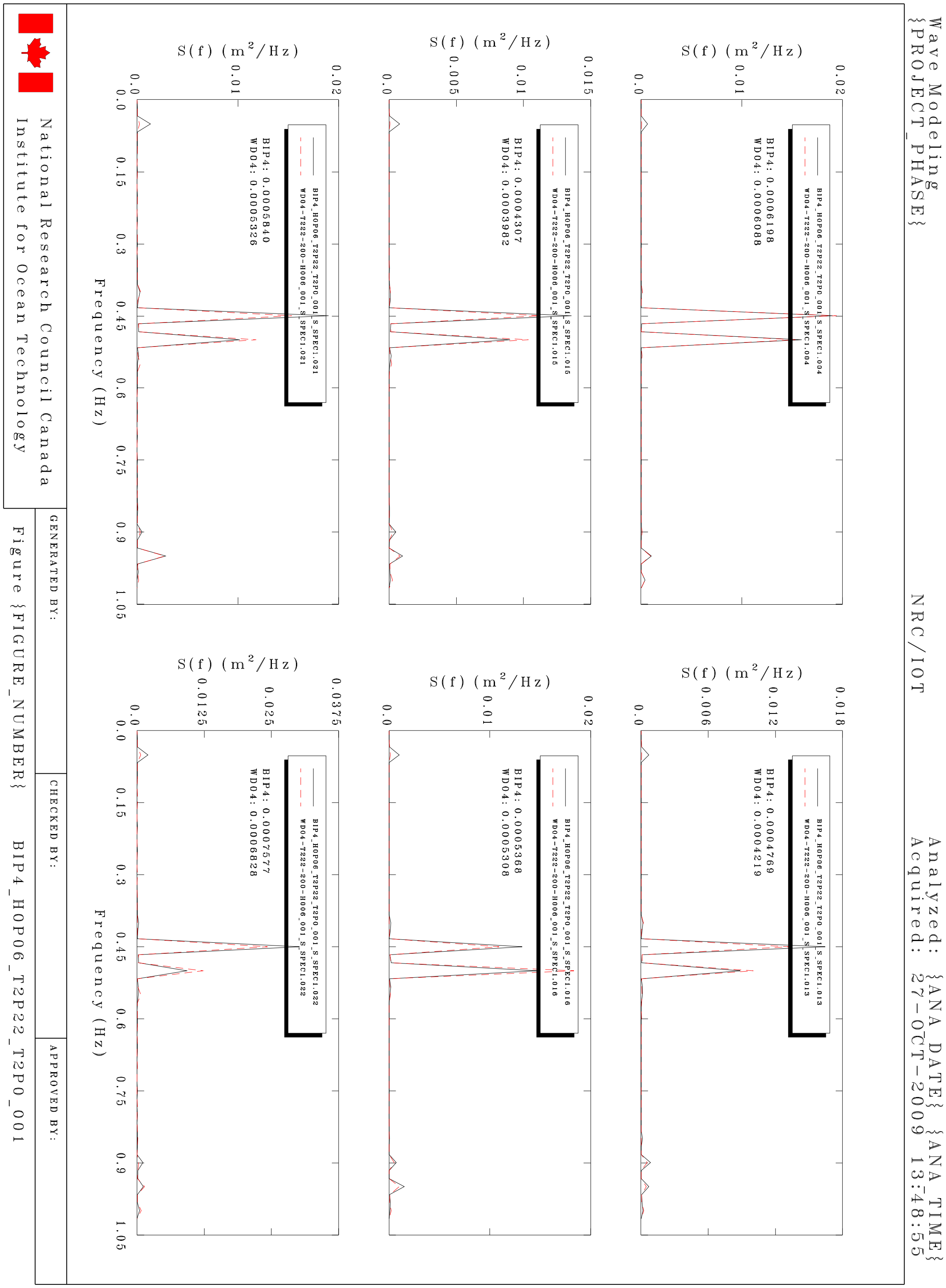

Fig. 28 Comparisons of the energy density between First- and Second-order generations
(*Case-3, h=0.4m,* T_1*=2.22s,* T_2*=2.0s,* H_1*=0.06m and* H_2*=0.06m*)

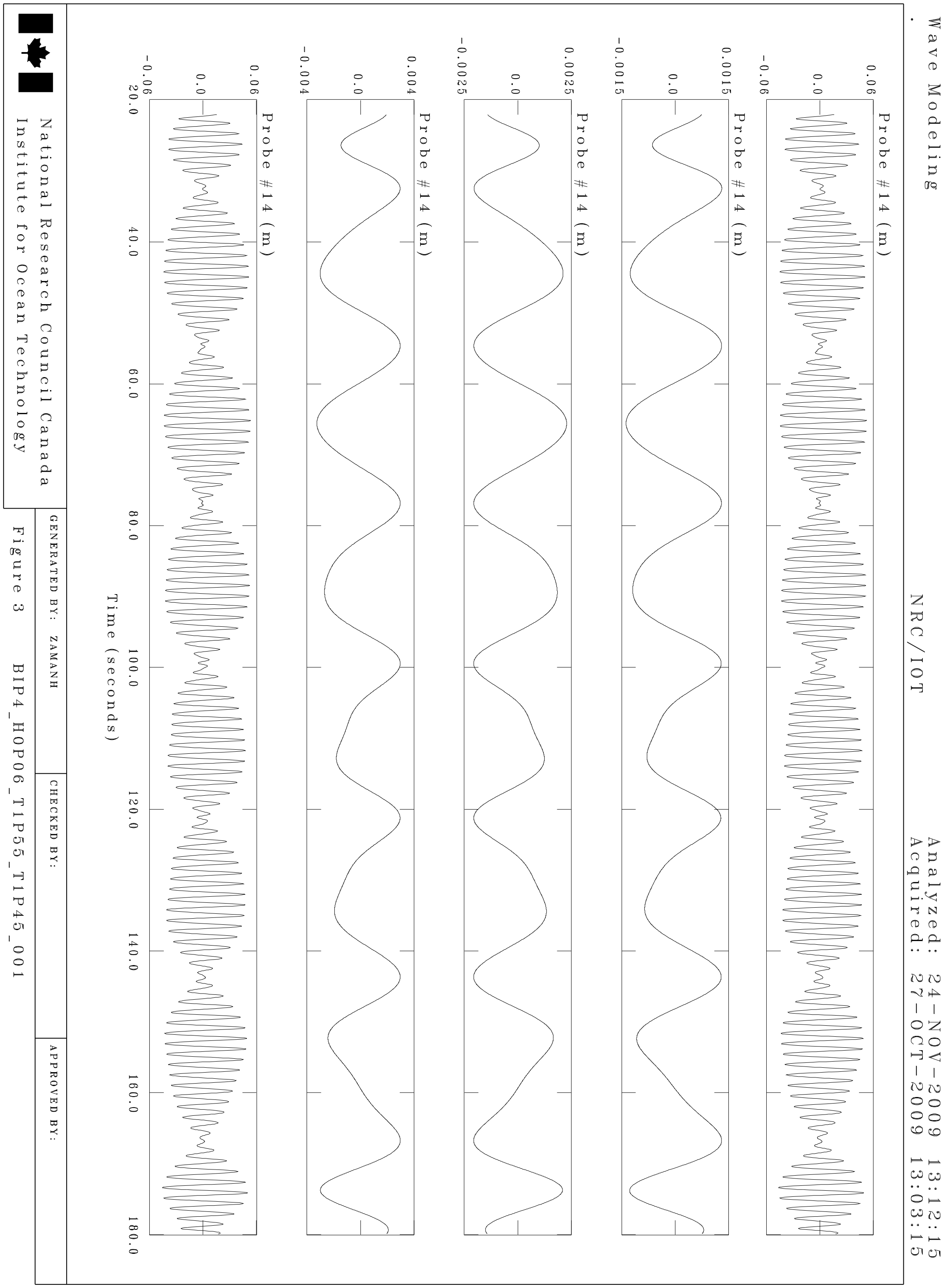

Fig. 29a LWAVE analysis of measured eta at Probe-14; First-order generation
(*Case-2,* $h=0.4m$*,* $T_1=1.55s$*,* $T_2=1.45s$*,* $H_1=0.06m$ *and* $H_2=0.06m$)

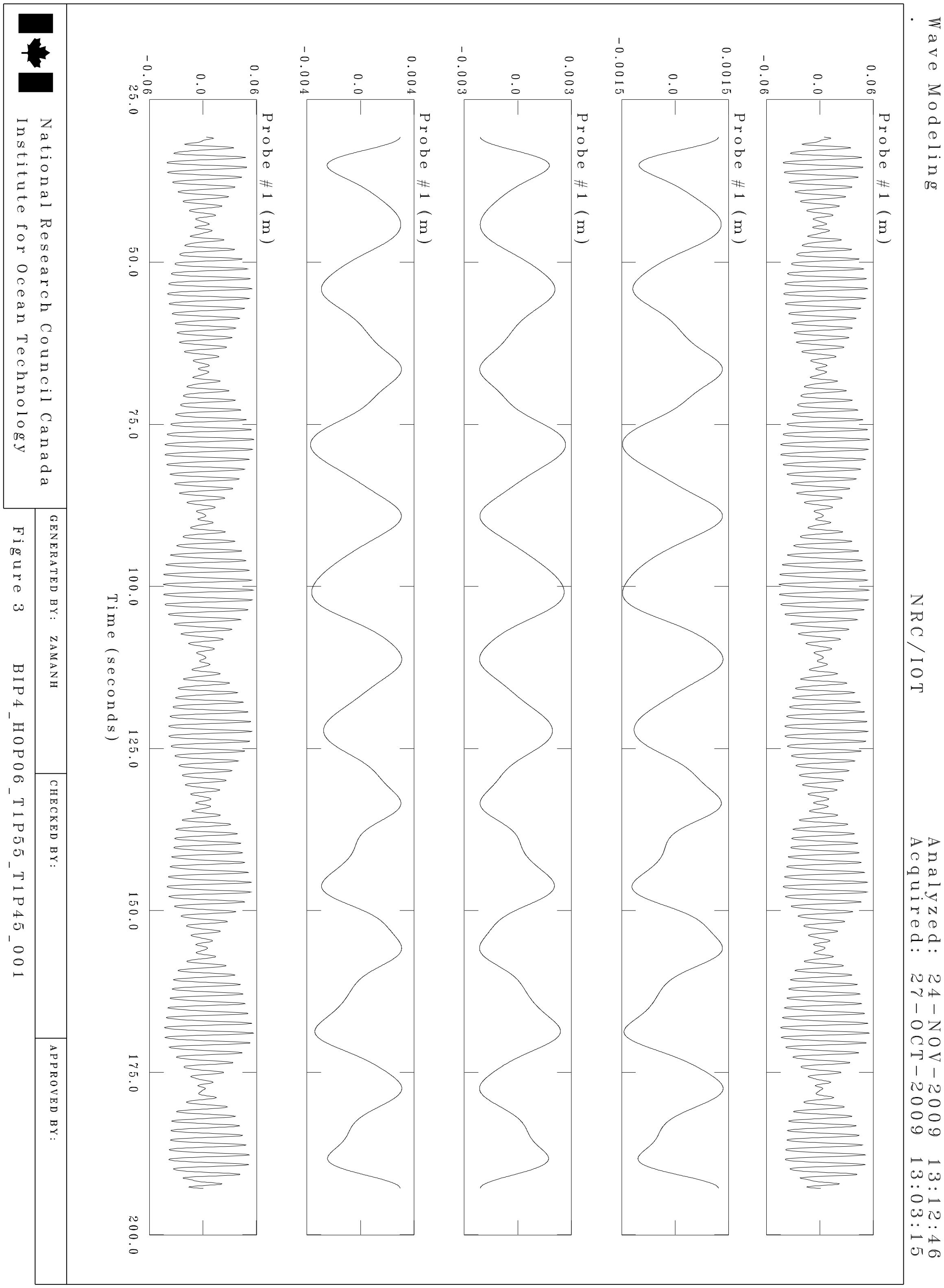

Fig. 29b LWAVE analysis of measured eta at Probe-1; First-order generation
(*Case-2, h=0.4m,* T_1*=1.55s,* T_2*=1.45s,* H_1*=0.06m and* H_2*=0.06m*)

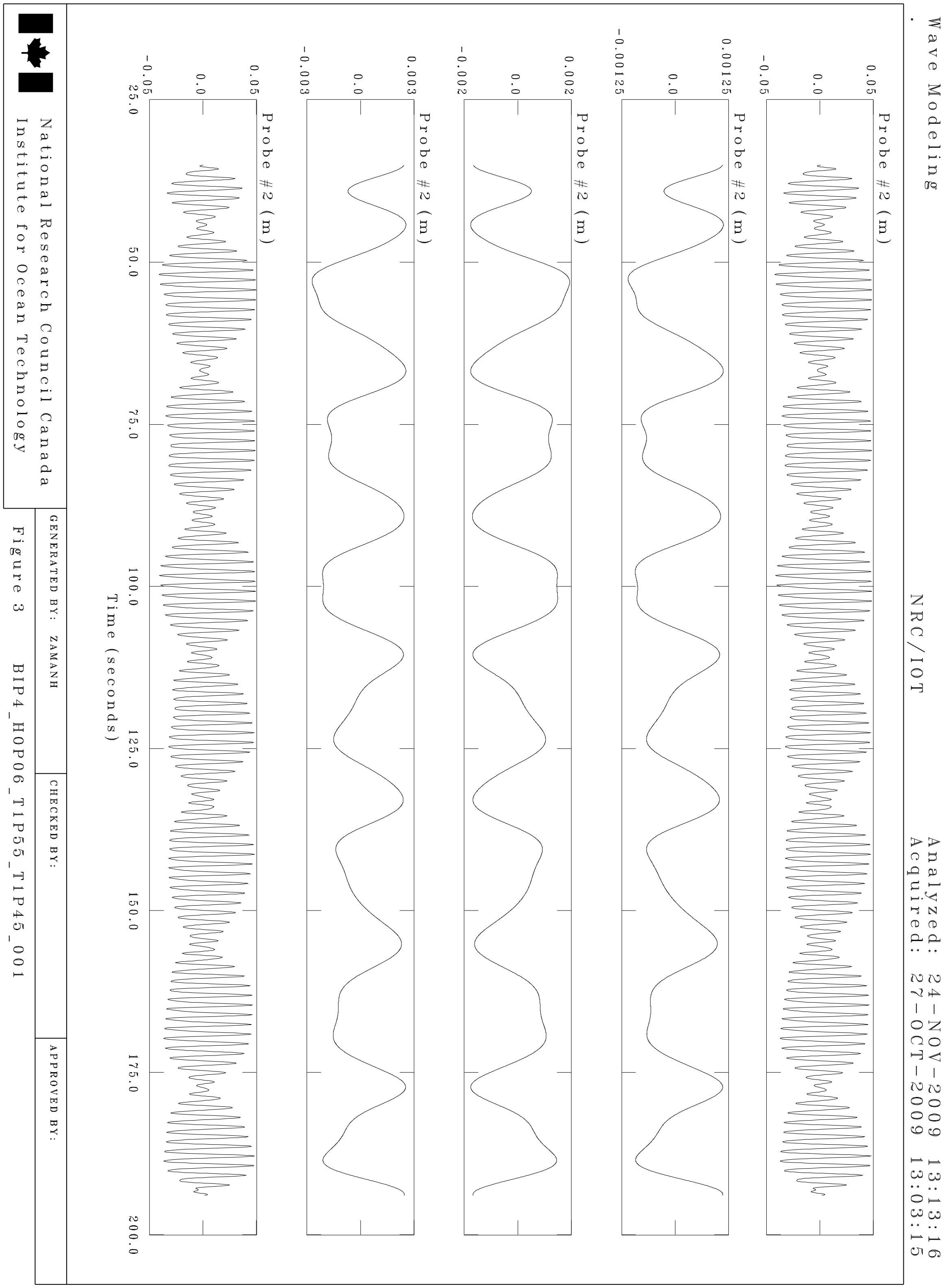

Fig. 29c LWAVE analysis of measured eta at Probe-2; First-order generation
(*Case-2, h=0.4m,* T_1*=1.55s,* T_2*=1.45s,* H_1*=0.06m and* H_2*=0.06m*)

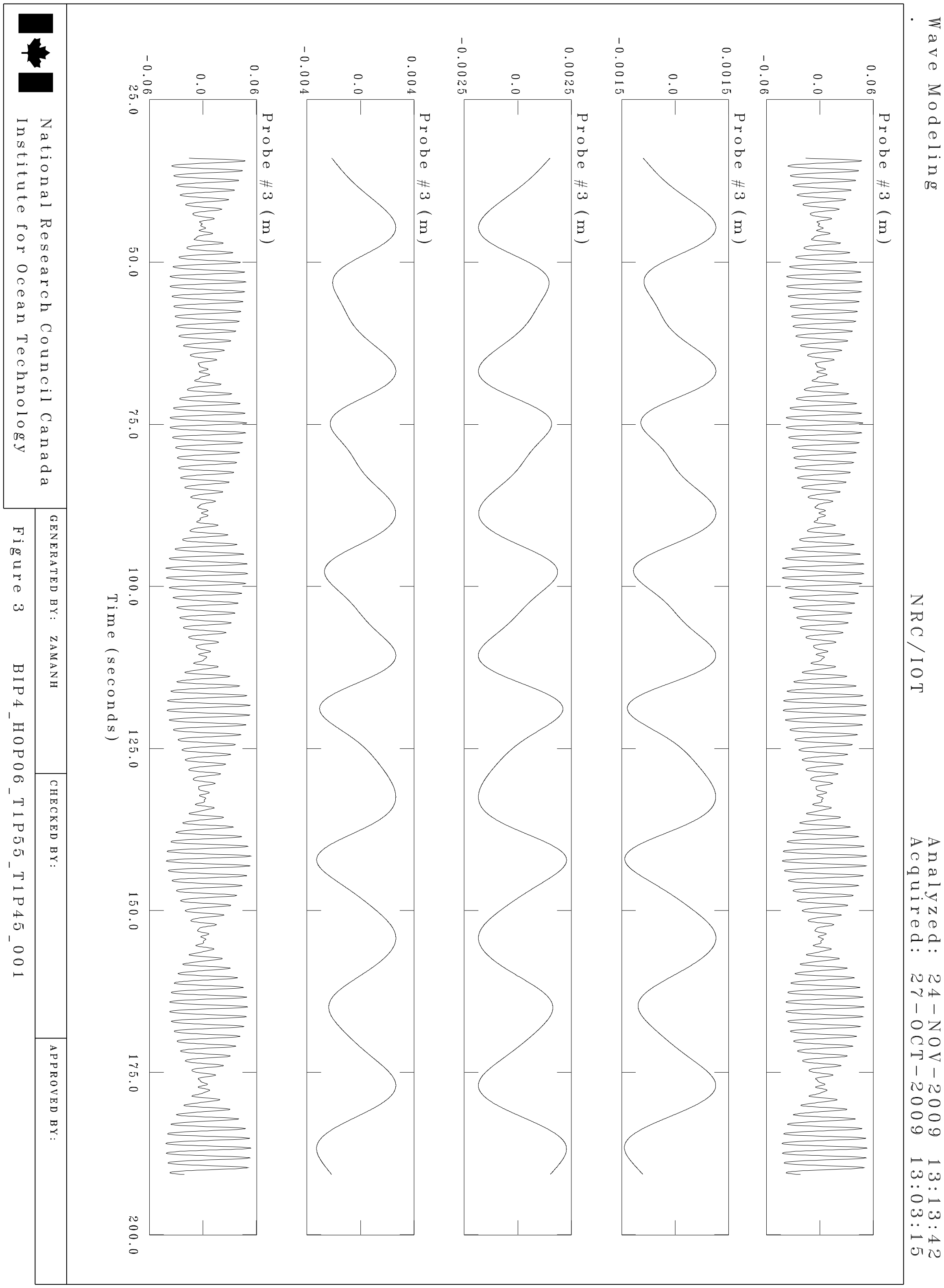

Fig. 29d LWAVE analysis of measured eta at Probe-3; First-order generation
(*Case-2,* $h=0.4m$, $T_1=1.55s$, $T_2=1.45s$, $H_1=0.06m$ *and* $H_2=0.06m$)

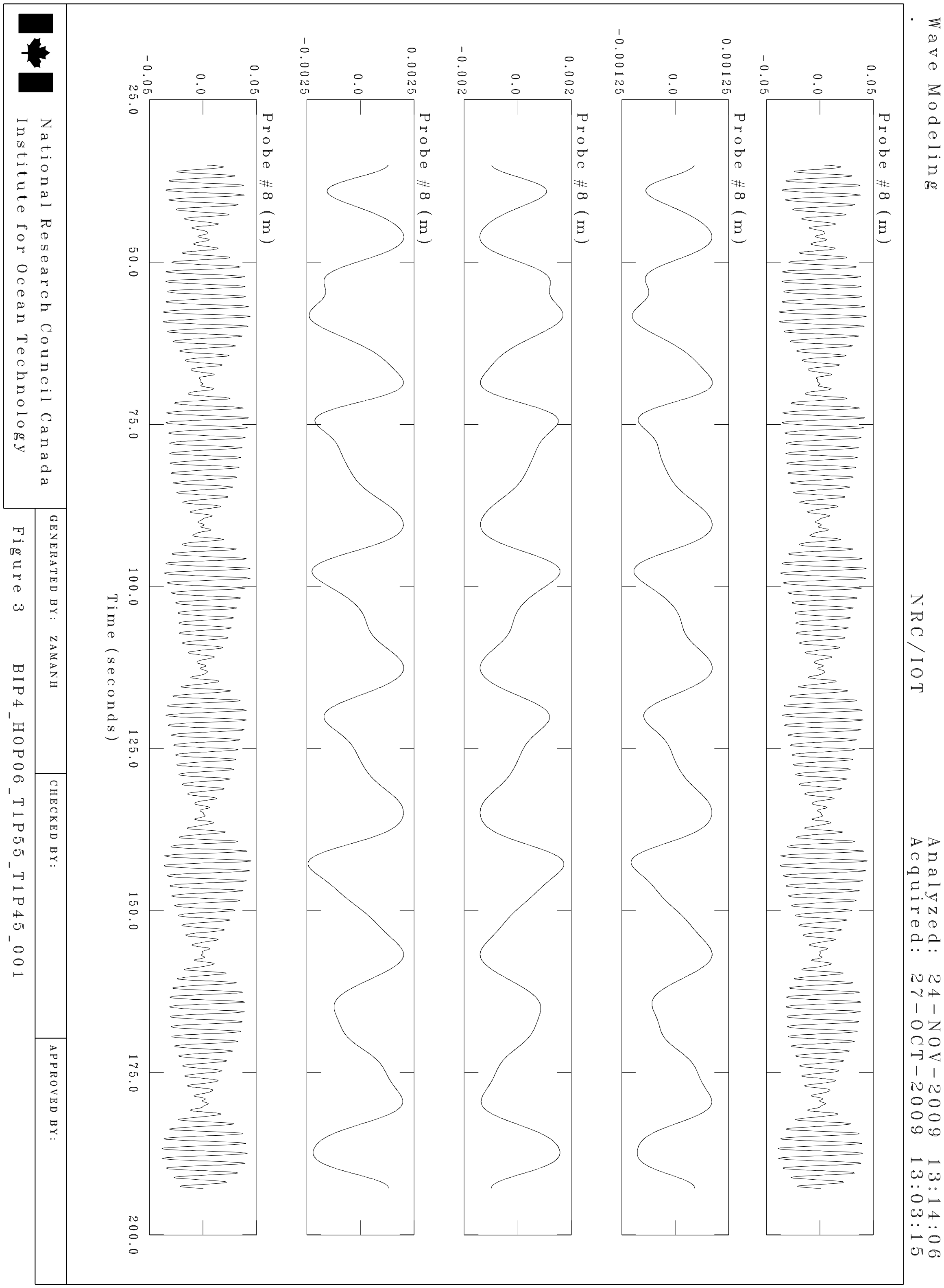

Fig. 29e LWAVE analysis of measured eta at Probe-8; First-order generation
(*Case-2, h=0.4m,* T_1*=1.55s,* T_2*=1.45s,* H_1*=0.06m and* H_2*=0.06m*)

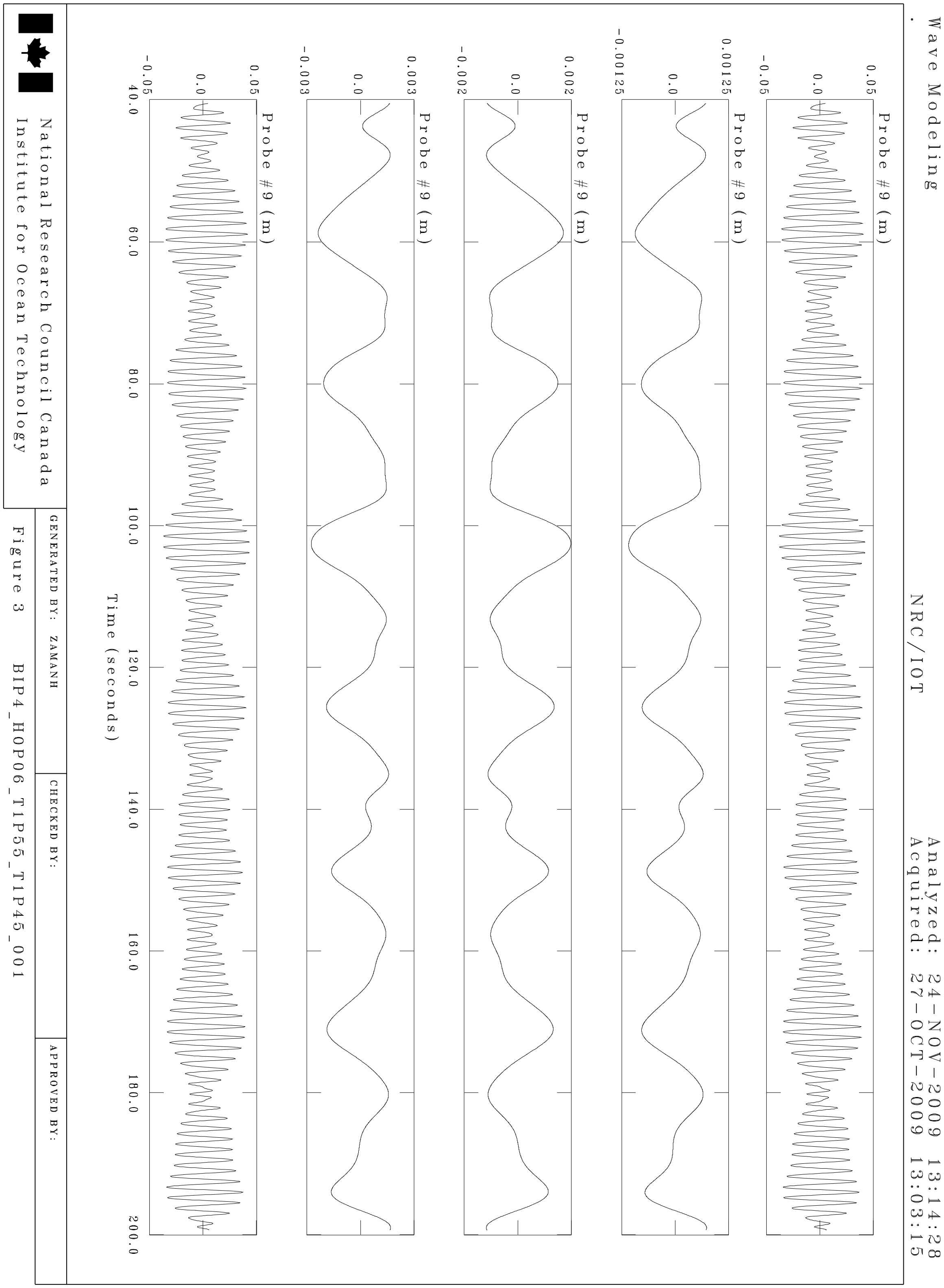

Fig. 29f LWAVE analysis of measured eta at Probe-9; First-order generation
(*Case-2, h=0.4m,* T_1*=1.55s,* T_2*=1.45s,* H_1*=0.06m and* H_2*=0.06m*)

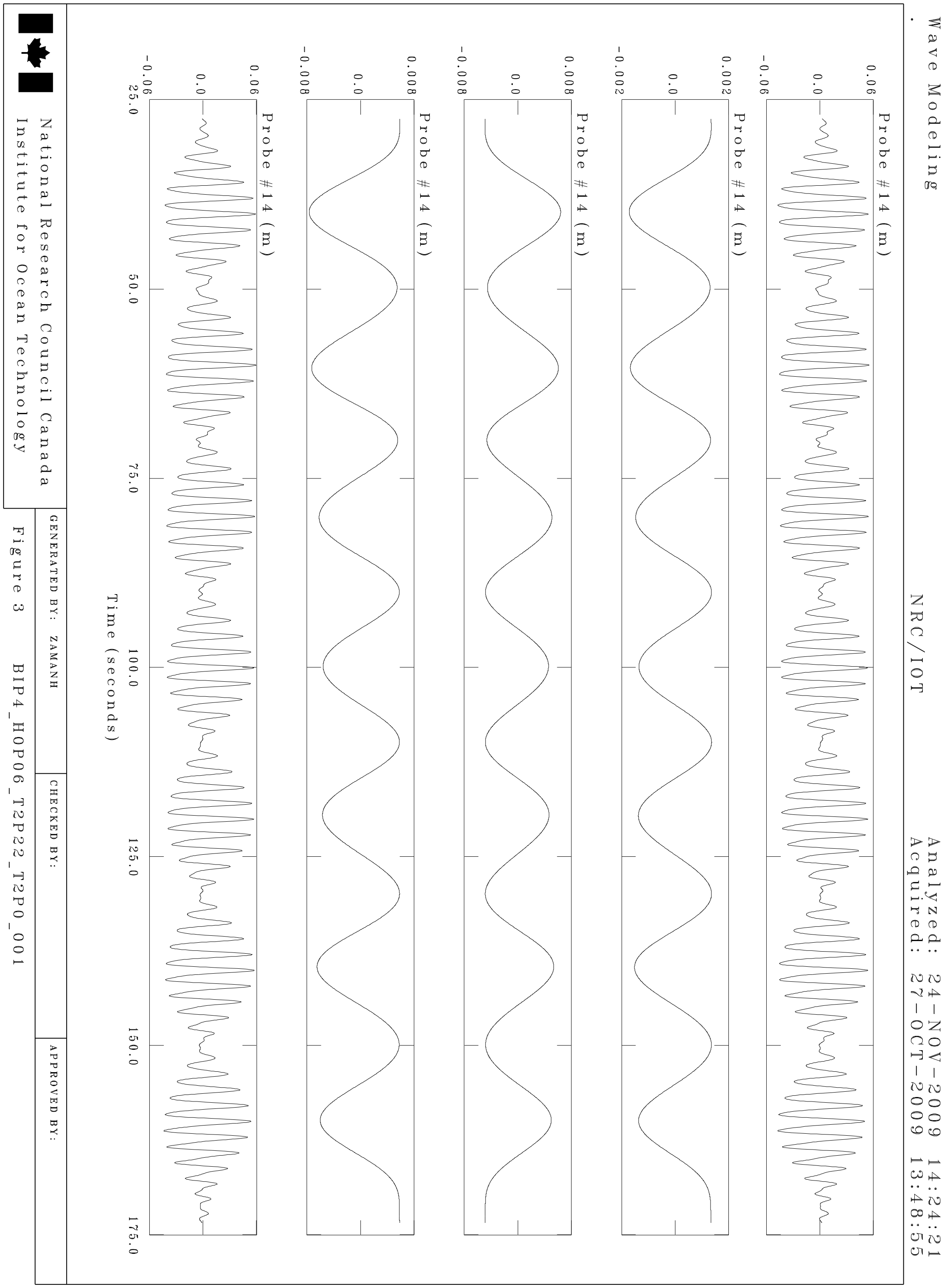

Fig. 30a LWAVE analysis of measured eta at Probe-14; First-order generation (*Case-3, h=0.4m,* T_1*=2.22s,* T_2*=2.0s,* H_1*=0.06m and* H_2*=0.06m*)

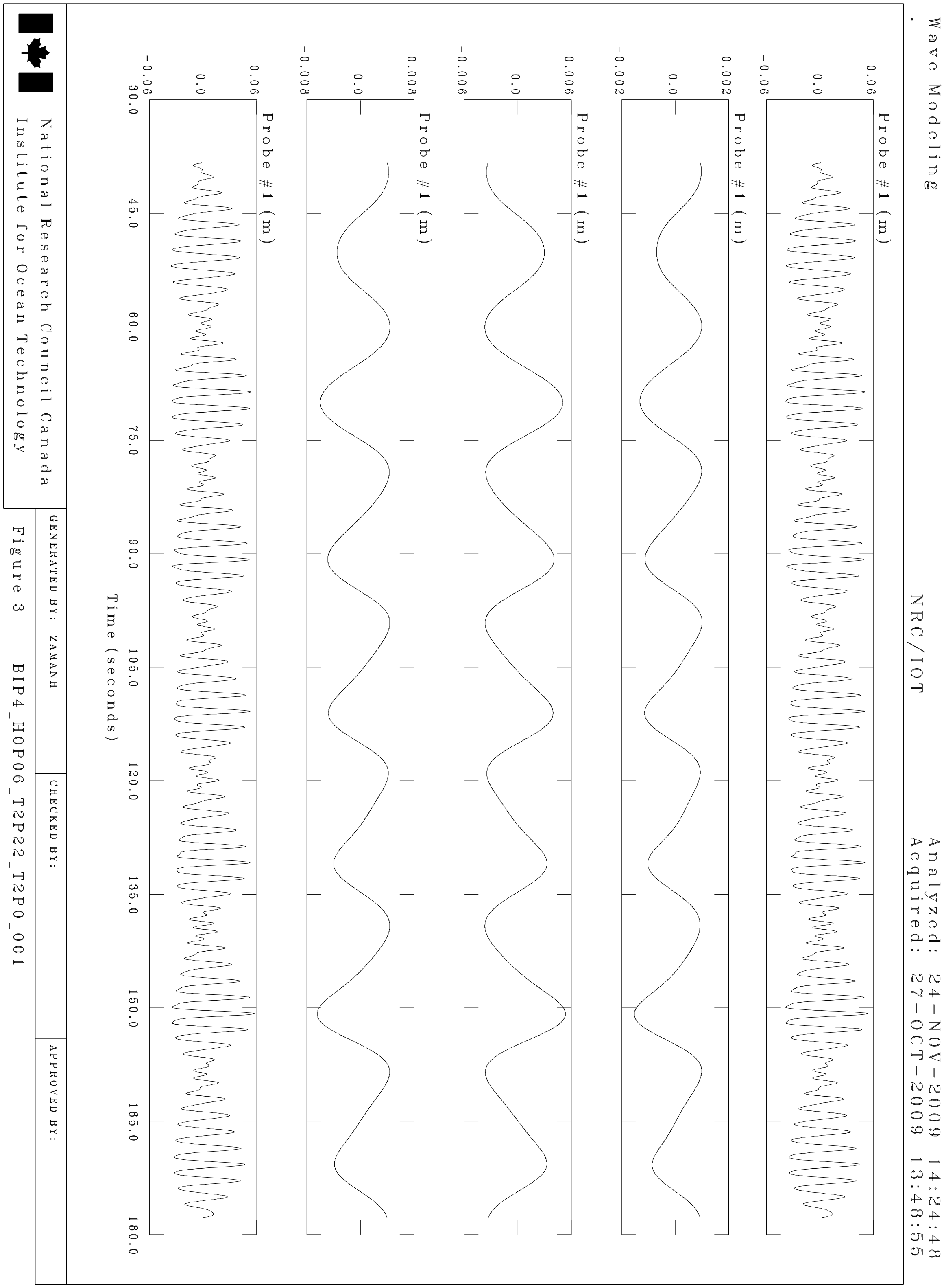

Fig. 30b LWAVE analysis of measured eta at Probe-1; First-order generation
(*Case-3, h=0.4m,* T_1*=2.22s,* T_2*=2.0s,* H_1*=0.06m and* H_2*=0.06m*)

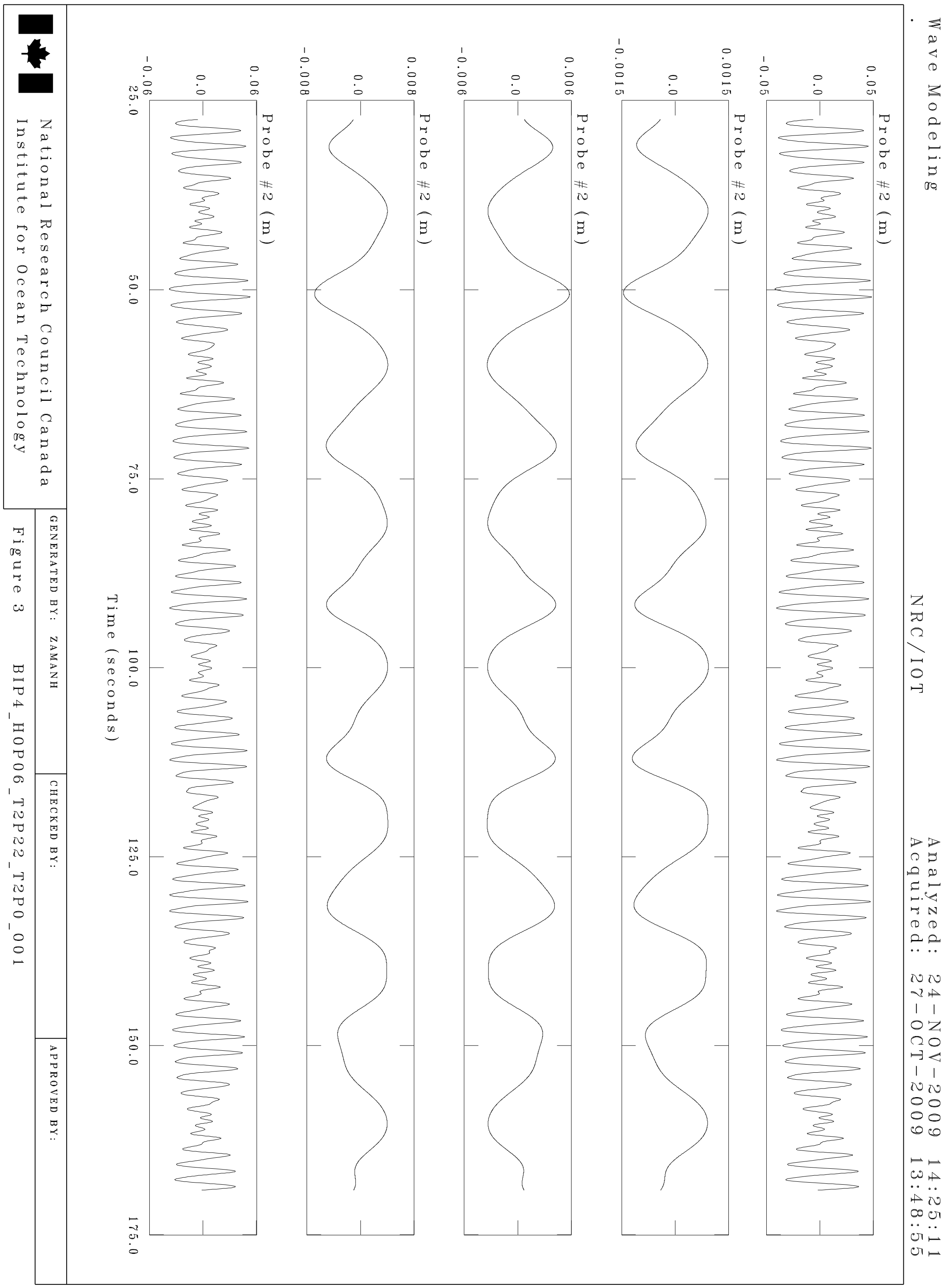

Fig. 30c LWAVE analysis of measured eta at Probe-2; First-order generation (Case-3, h=0.4m, T1=2.22s, T2=2.0s, H1=0.06m and H2=0.06m)

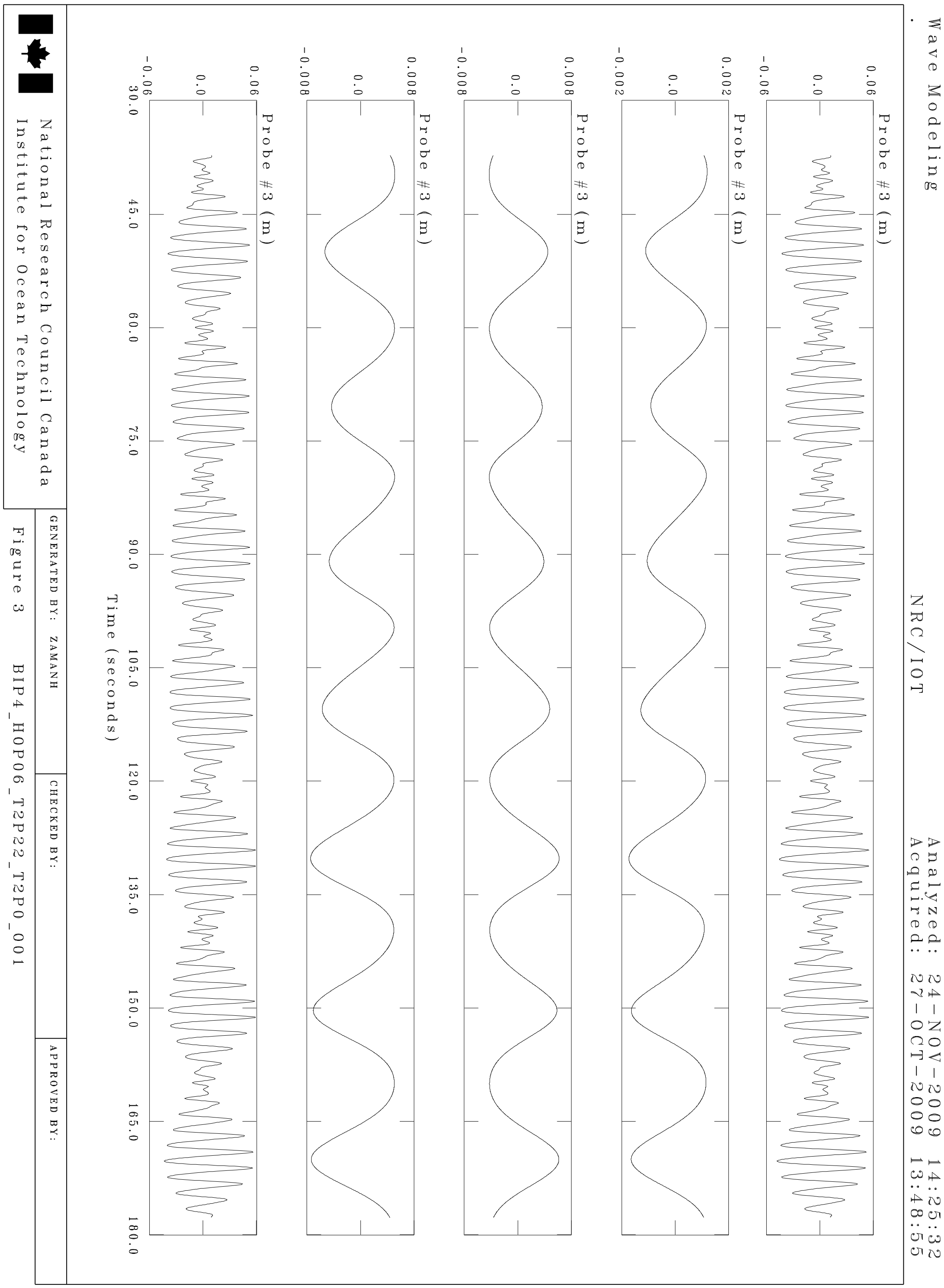

Fig. 30d LWAVE analysis of measured eta at Probe-3; First-order generation
(*Case-3, h=0.4m,* T_1*=2.22s,* T_2*=2.0s,* H_1*=0.06m and* H_2*=0.06m*)

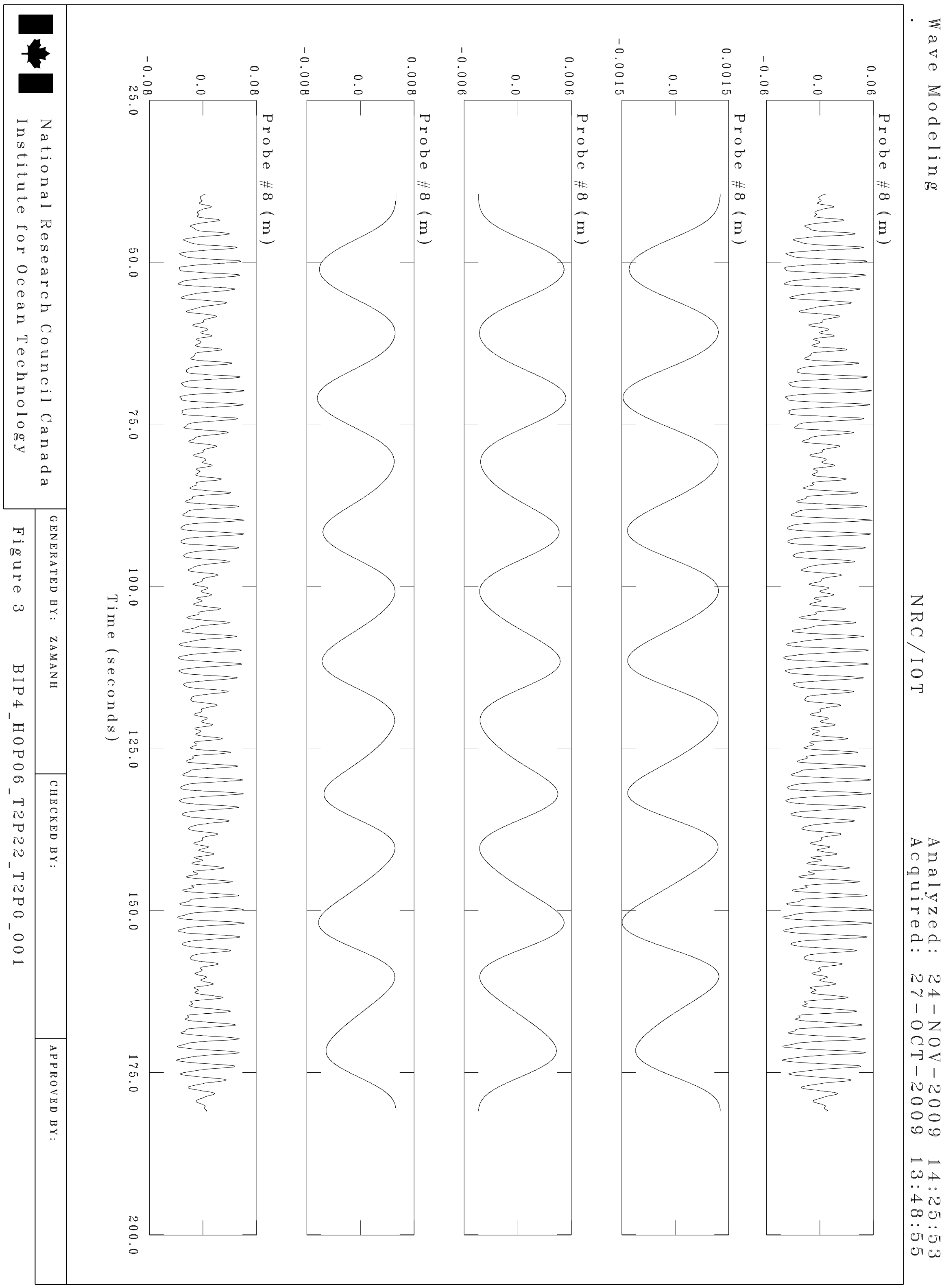

Fig. 30e LWAVE analysis of measured eta at Probe-8; First-order generation
(*Case-3, h=0.4m,* T_1*=2.22s,* T_2*=2.0s,* H_1*=0.06m and* H_2*=0.06m*)

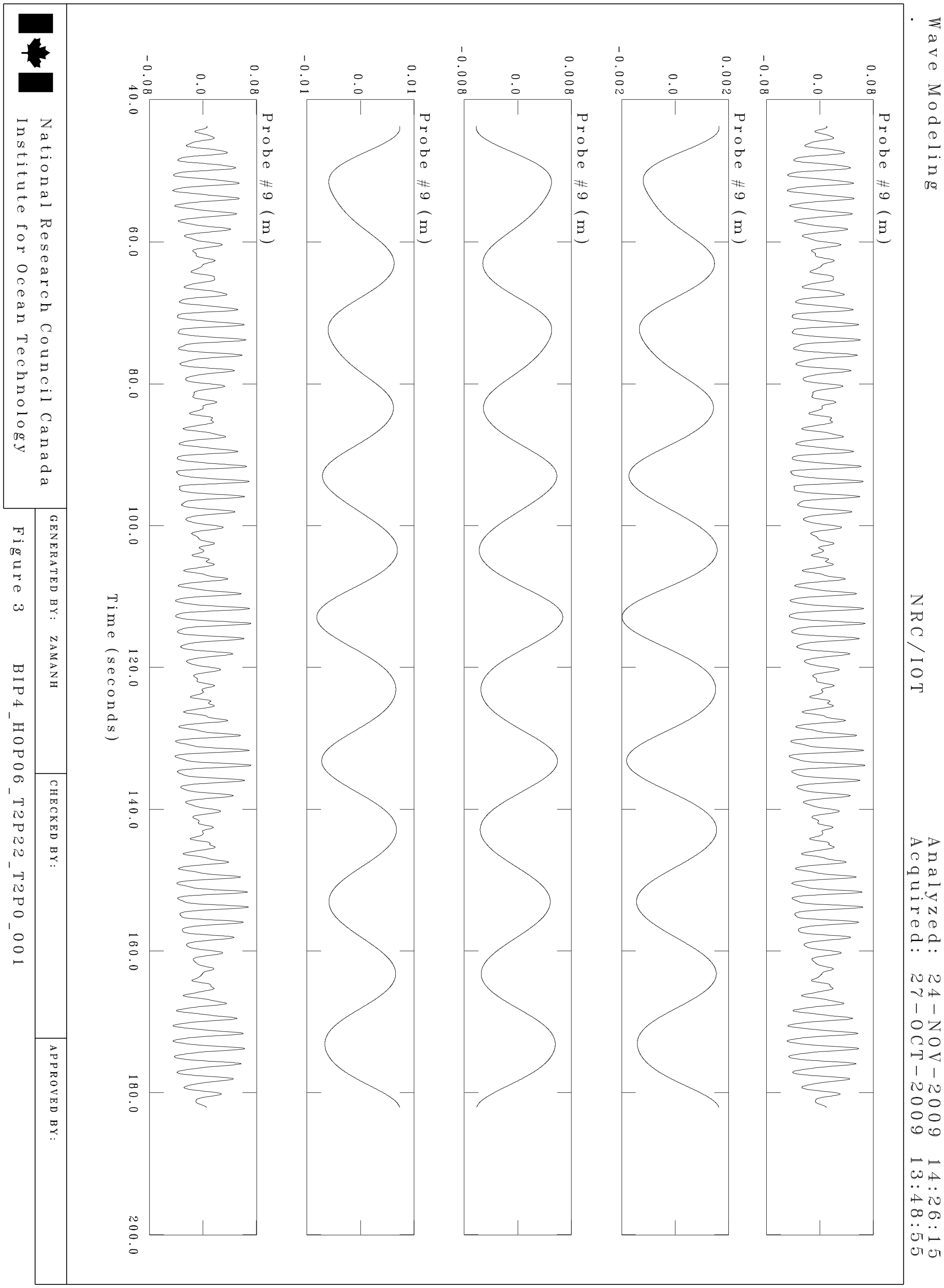

Fig. 30f LWAVE analysis of measured eta at Probe-9; First-order generation
(*Case-3, h=0.4m,* T_1*=2.22s,* T_2*=2.0s,* H_1*=0.06m and* H_2*=0.06m*)

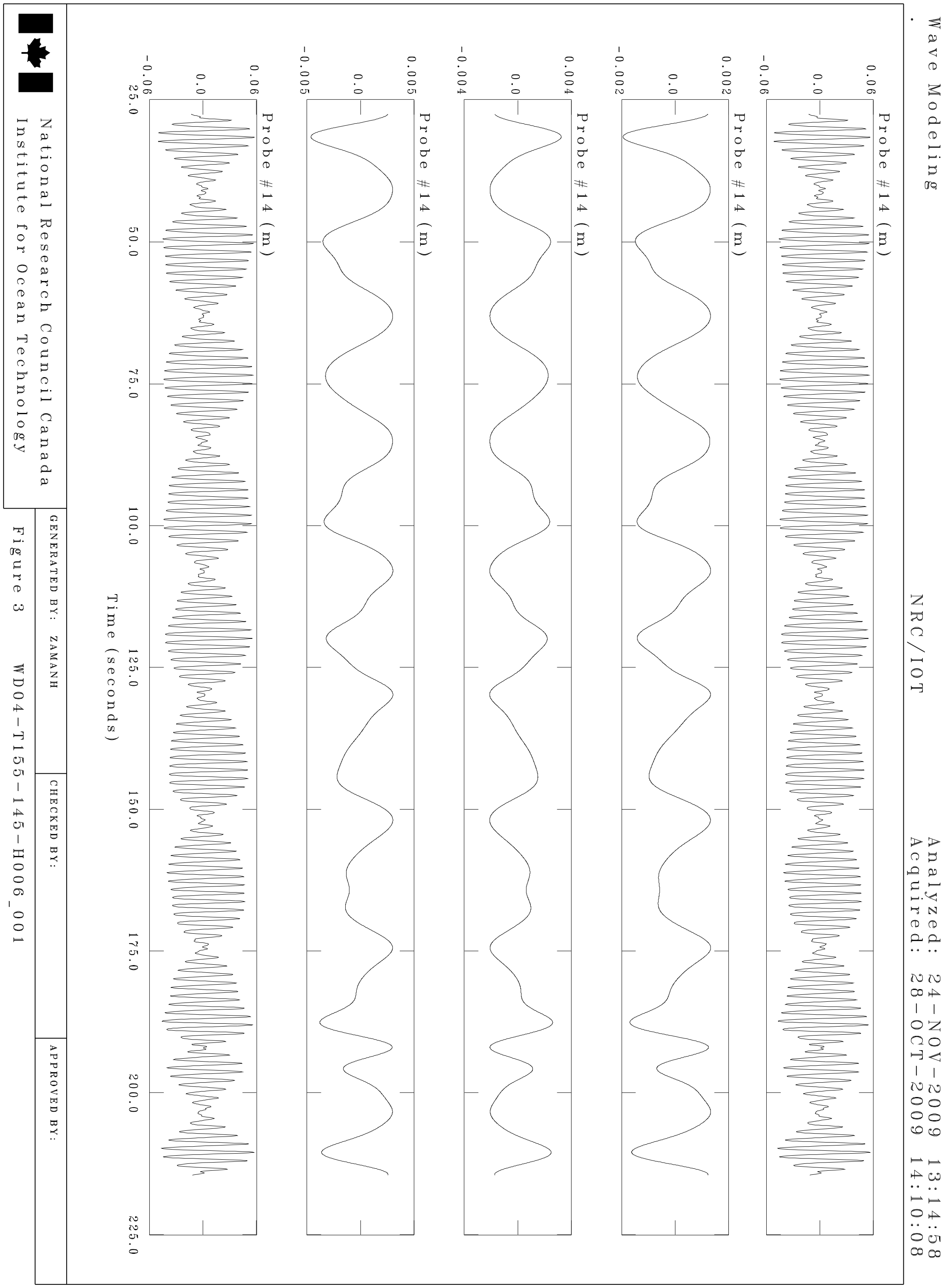

Fig. 31a LWAVE analysis of measured eta at Probe-14; Second-order generation (*Case-2, h=0.4m,* T_1*=1.55s,* T_2*=1.45s,* H_1*=0.06m and* H_2*=0.06m*)

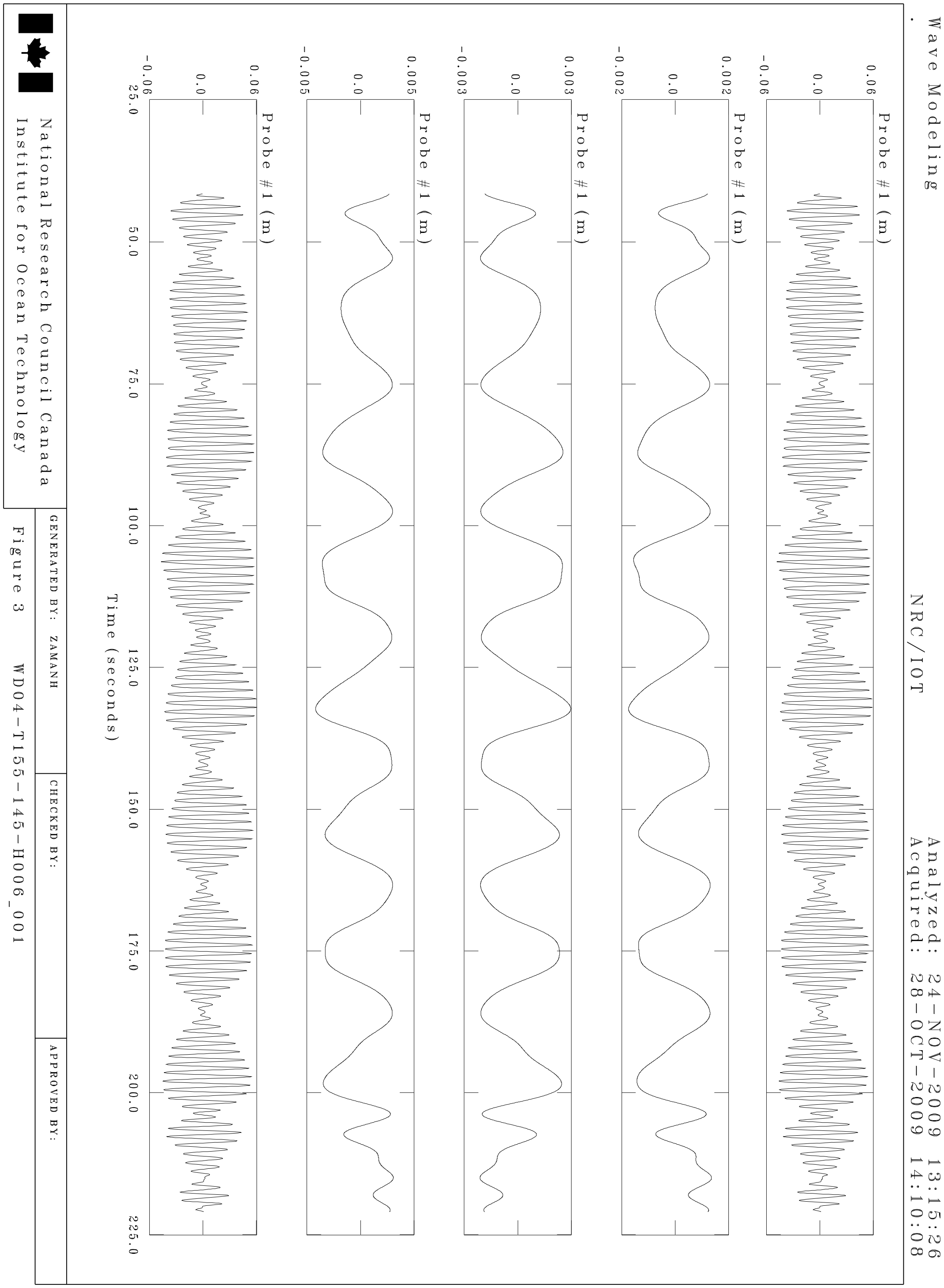

Fig. 31b LWAVE analysis of measured eta at Probe-1; Second-order generation (*Case-2, h=0.4m, T_1=1.55s, T_2=1.45s, H_1=0.06m and H_2=0.06m*)

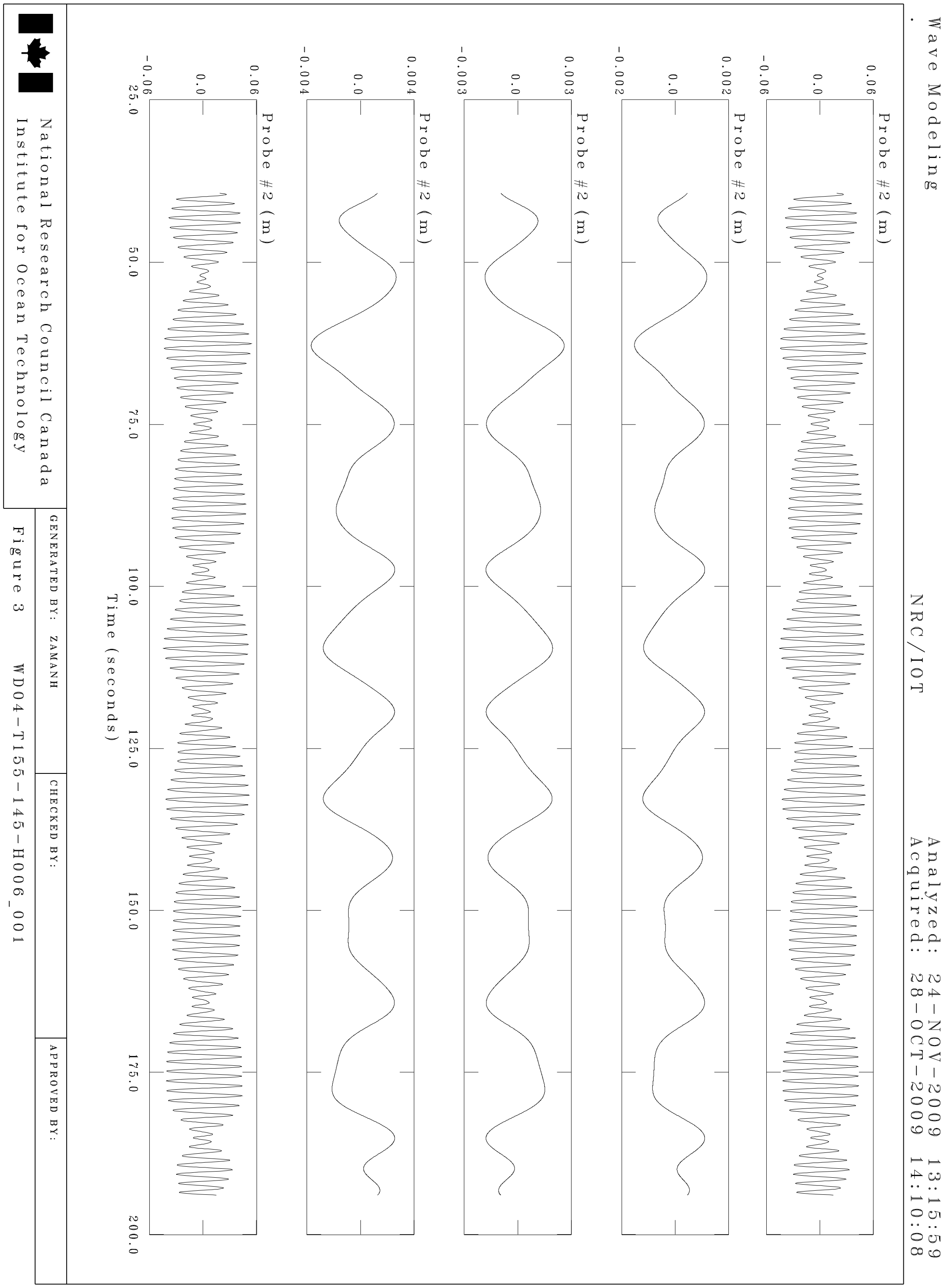

Fig. 31c LWAVE analysis of measured eta at Probe-2; Second-order generation (*Case-2, h=0.4m,* T_1*=1.55s,* T_2*=1.45s,* H_1*=0.06m and* H_2*=0.06m*)

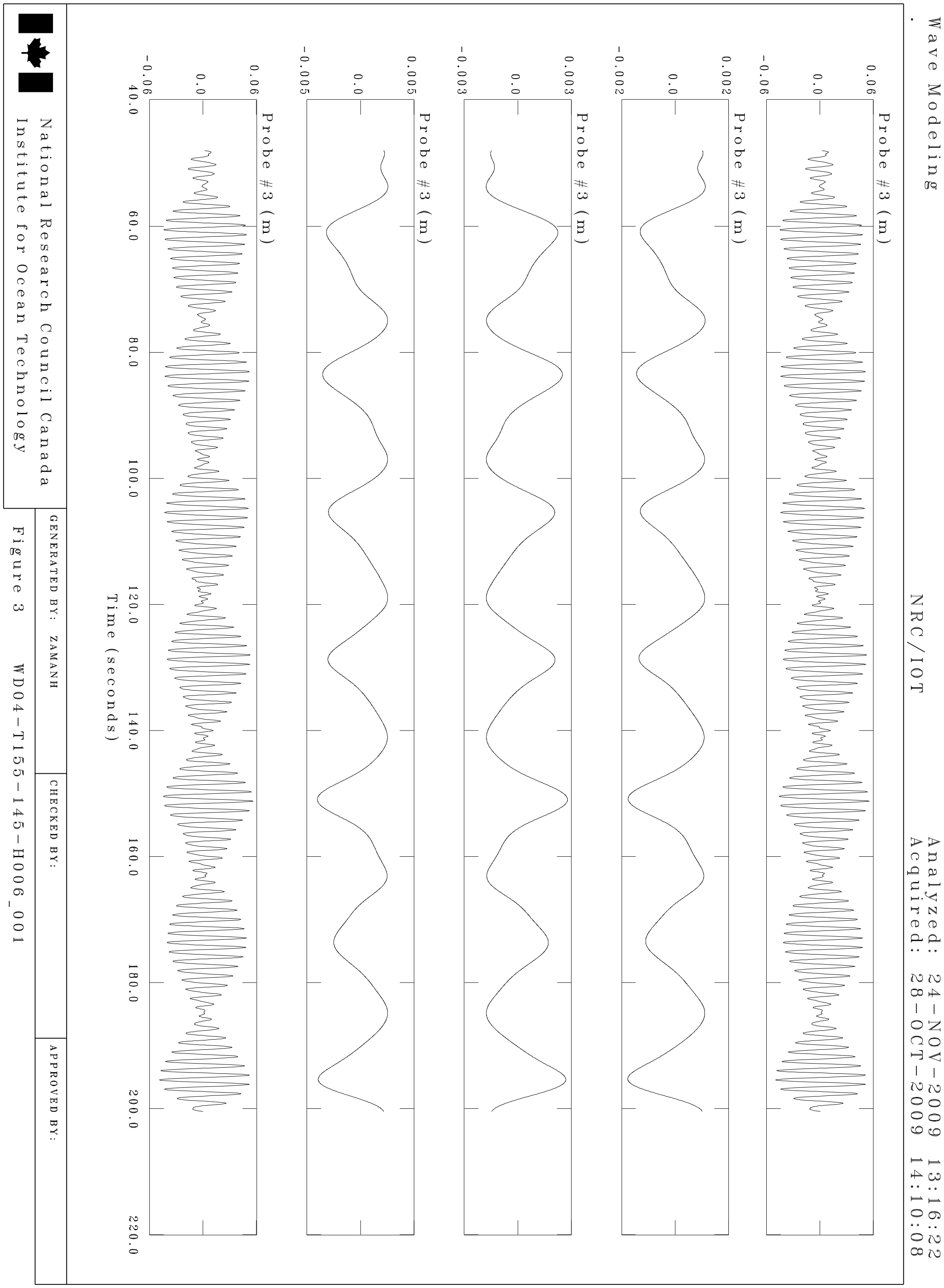

Fig. 31d LWAVE analysis of measured eta at Probe-3; Second-order generation (*Case-2, h=0.4m, T_1=1.55s, T_2=1.45s, H_1=0.06m and H_2=0.06m*)

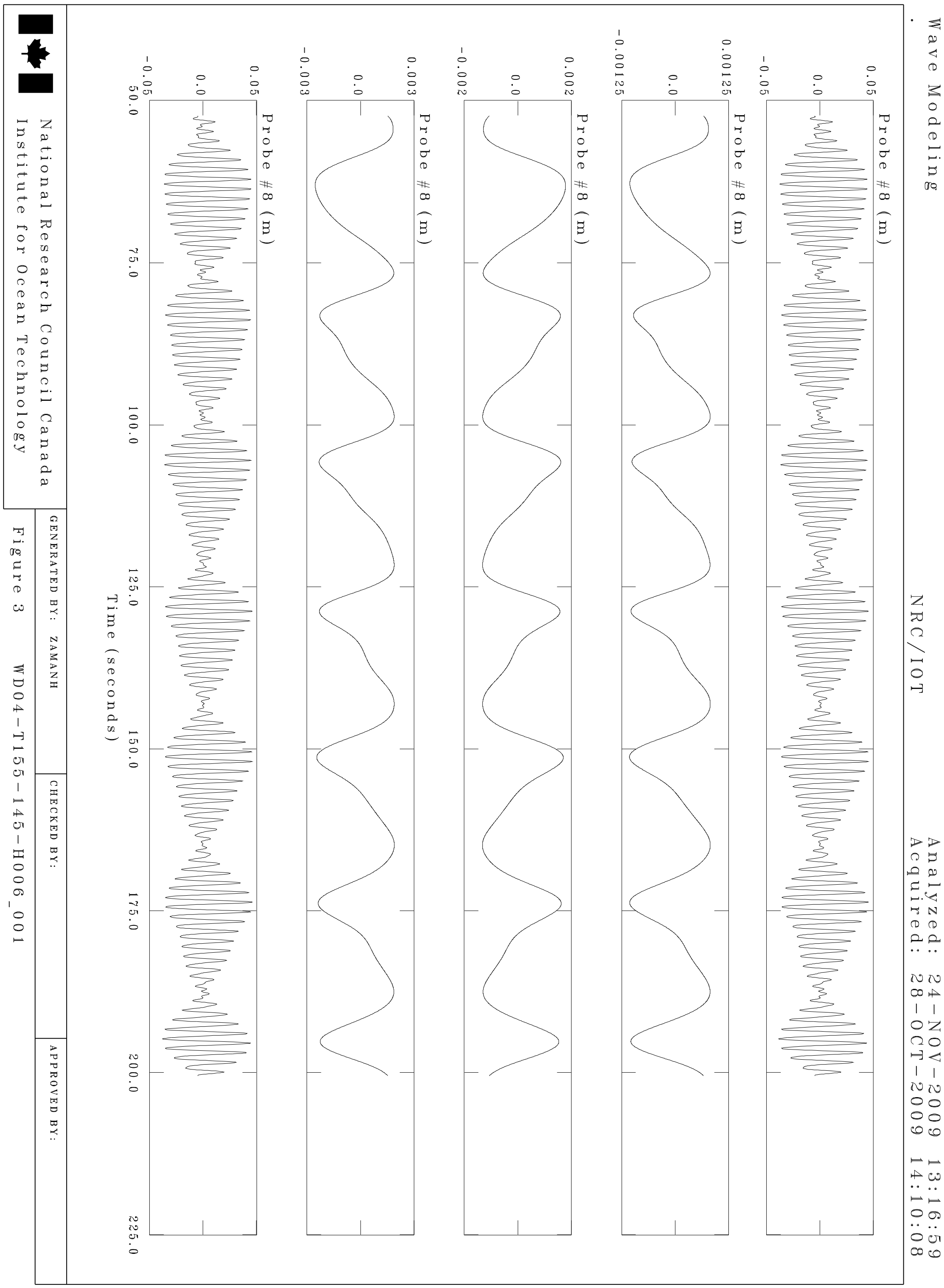

Fig. 31e LWAVE analysis of measured eta at Probe-8; Second-order generation (*Case-2, h=0.4m,* T_1*=1.55s,* T_2*=1.45s,* H_1*=0.06m and* H_2*=0.06m*)

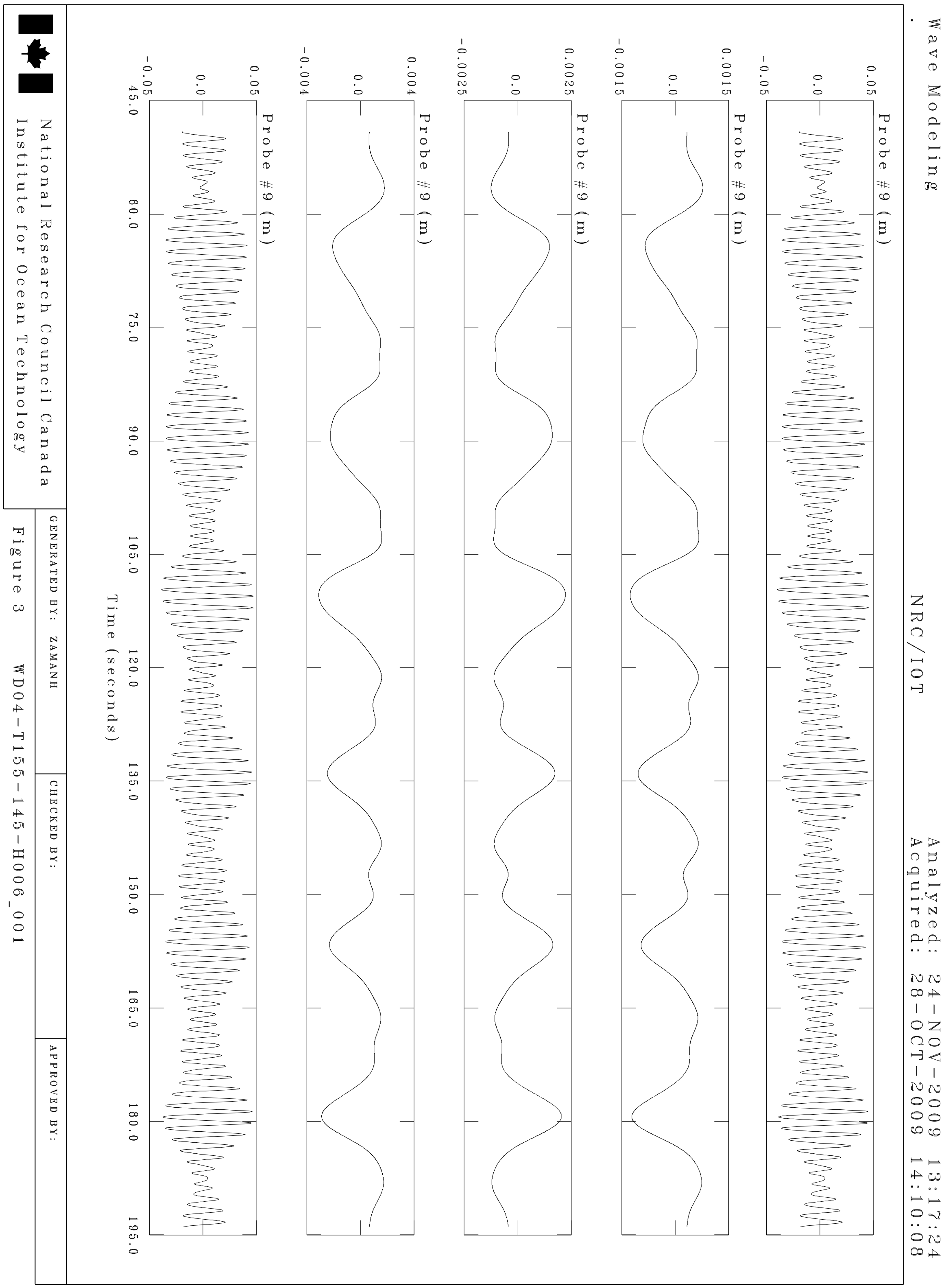

Fig. 31f LWAVE analysis of measured eta at Probe-9; Second-order generation
(*Case-2, h=0.4m,* T_1*=1.55s,* T_2*=1.45s,* H_1*=0.06m and* H_2*=0.06m*)

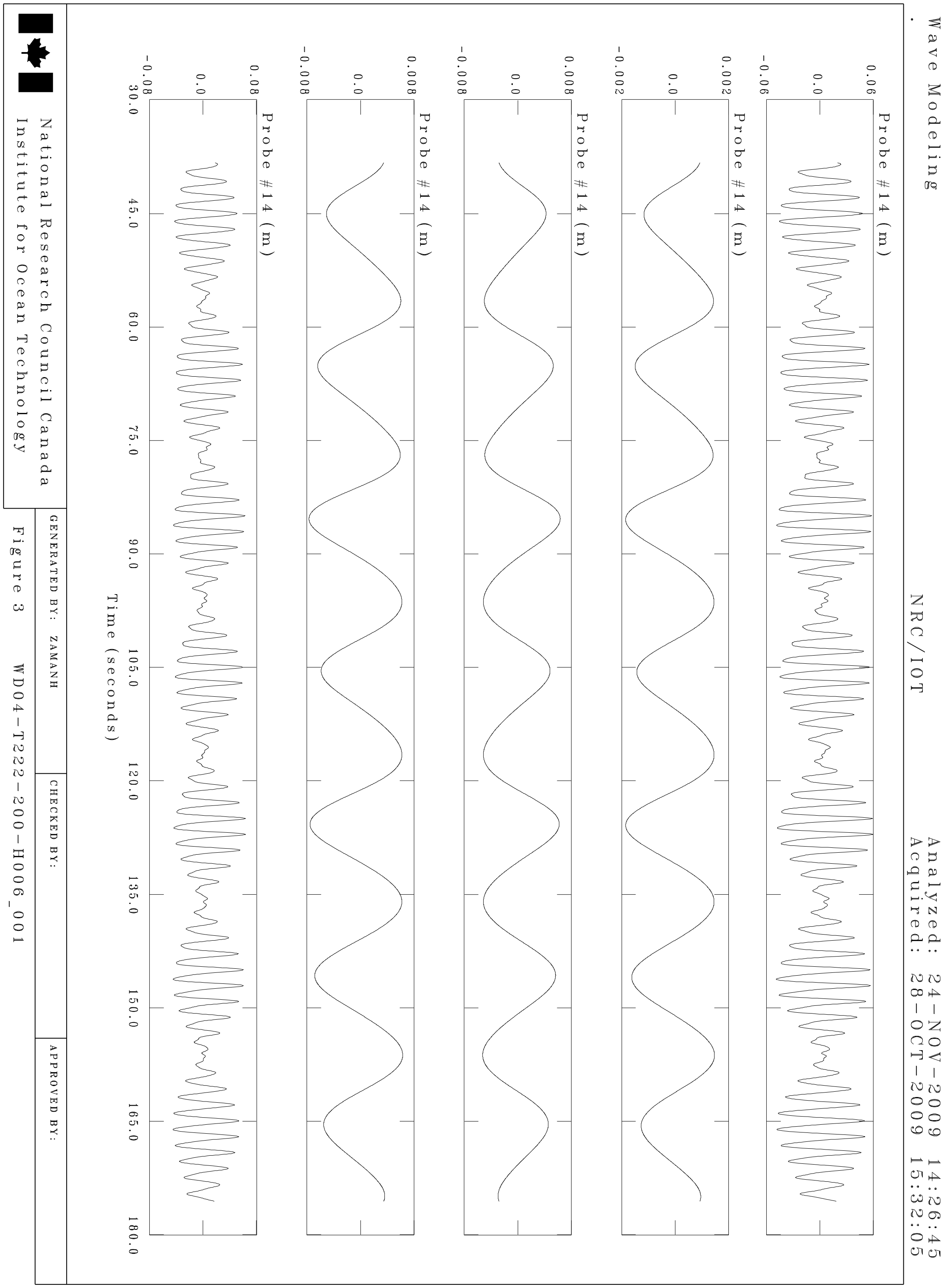

Fig. 32a LWAVE analysis of measured eta at Probe-14; Second-order generation
(*Case-3, h=0.4m,* T_1*=2.22s,* T_2*=2.0s,* H_1*=0.06m and* H_2*=0.06m*)

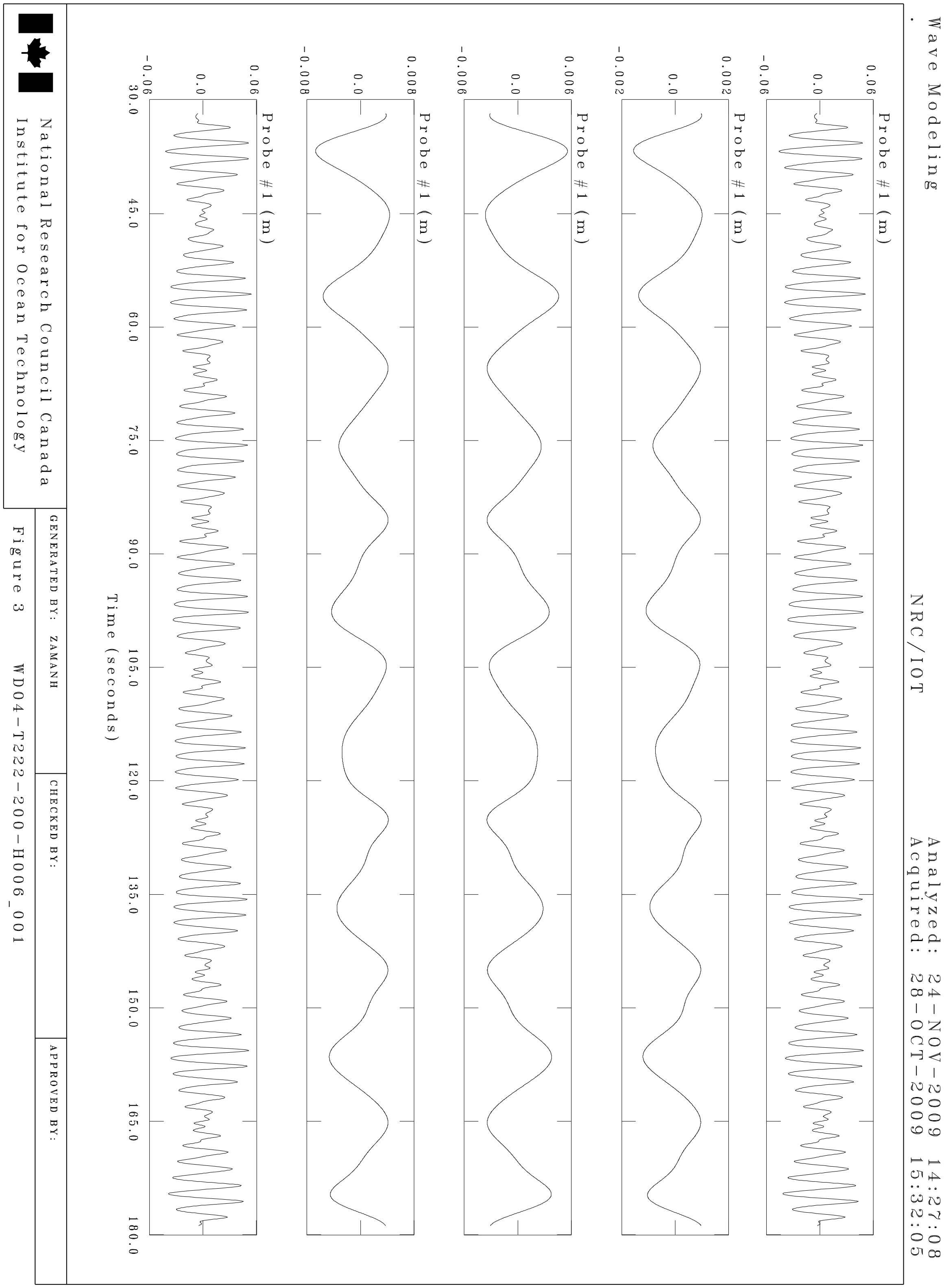

Fig. 32b LWAVE analysis of measured eta at Probe-1; Second-order generation (*Case-3, h=0.4m,* T_1*=2.22s,* T_2*=2.0s,* H_1*=0.06m and* H_2*=0.06m*)

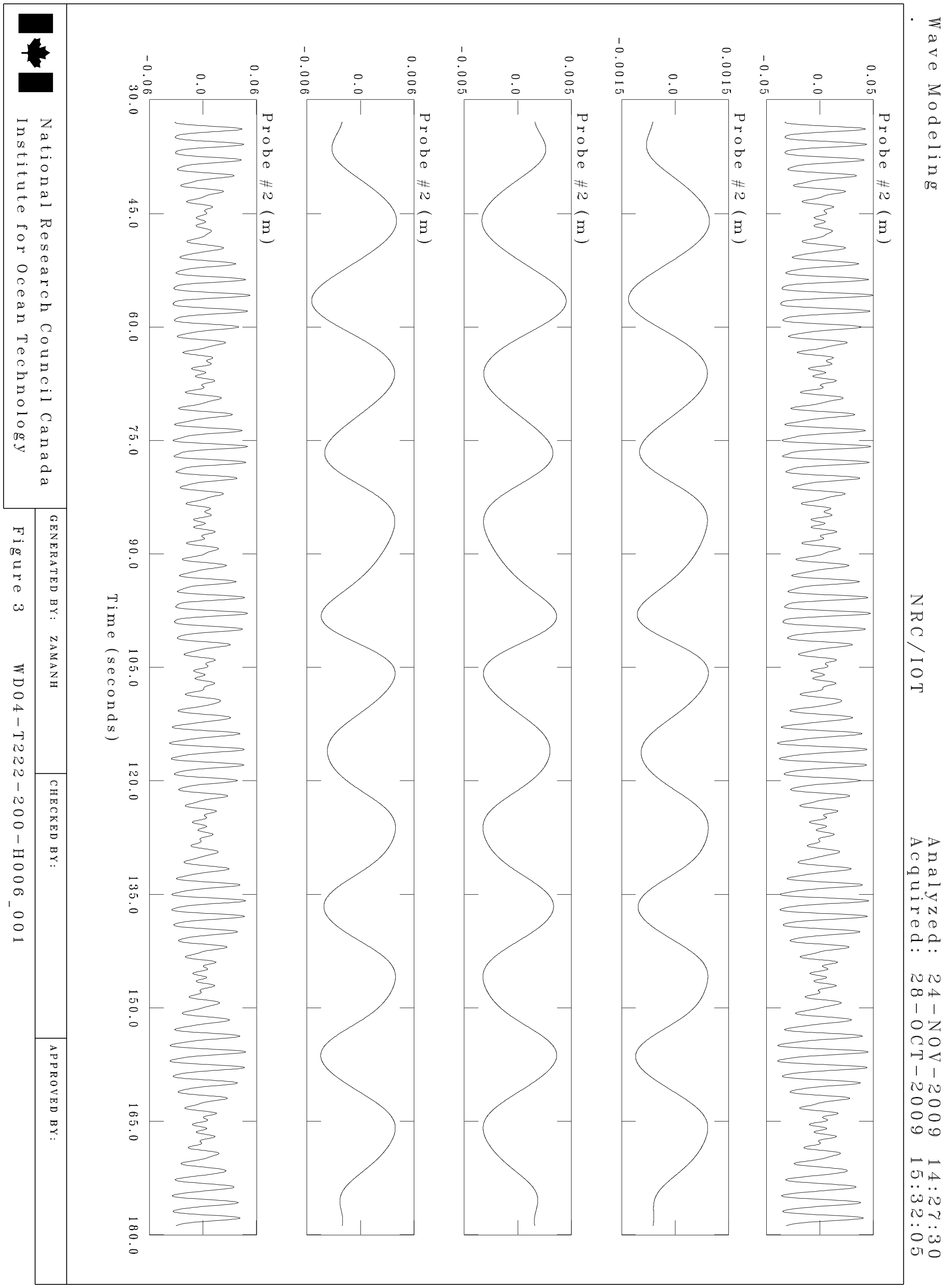

Fig. 32c LWAVE analysis of measured eta at Probe-2; Second-order generation (*Case-3, h=0.4m, T_1=2.22s, T_2=2.0s, H_1=0.06m and H_2=0.06m*)

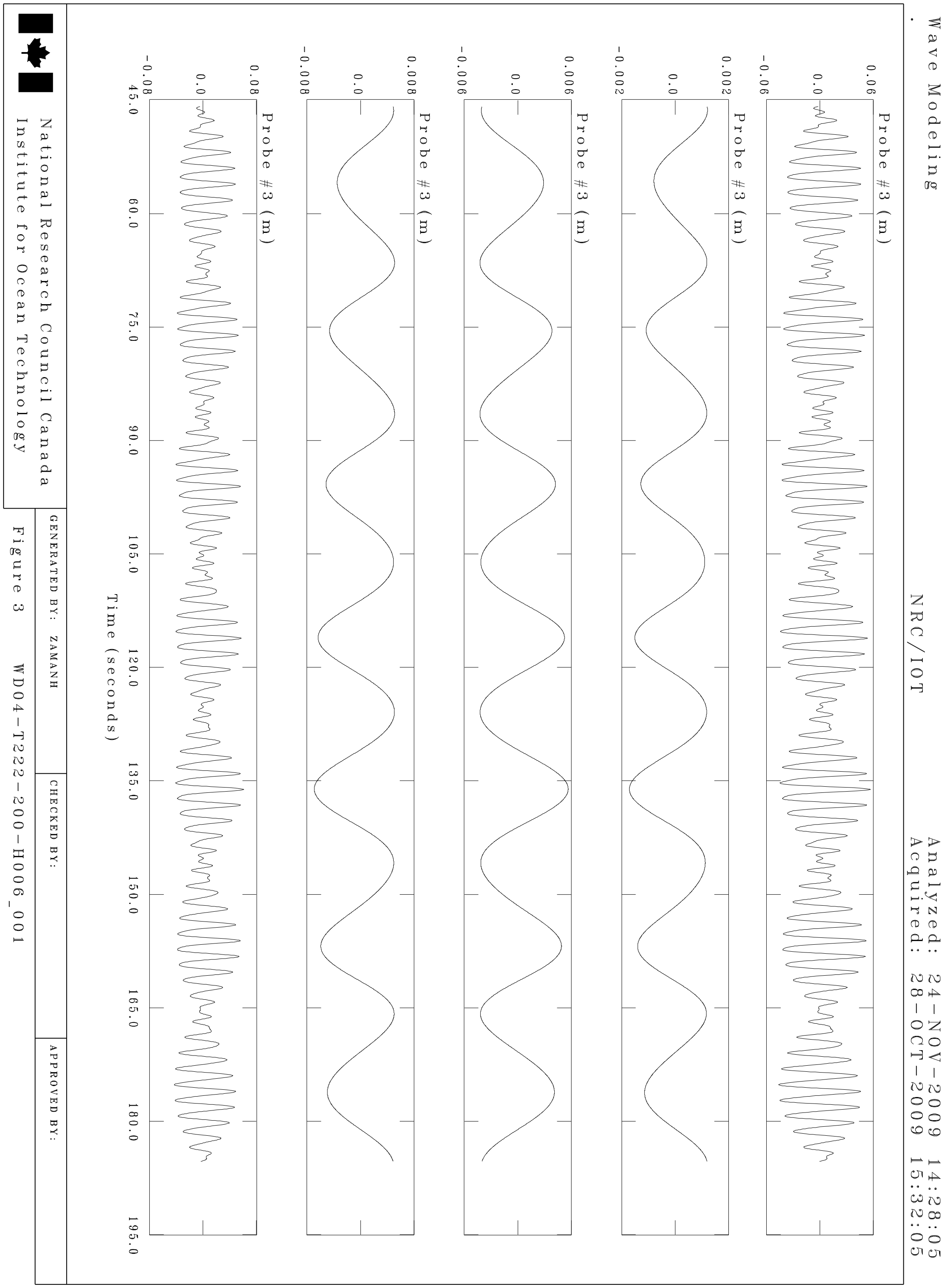

Fig. 32d LWAVE analysis of measured eta at Probe-3; Second-order generation
(*Case-3, h=0.4m,* T_1*=2.22s,* T_2*=2.0s,* H_1*=0.06m and* H_2*=0.06m*)

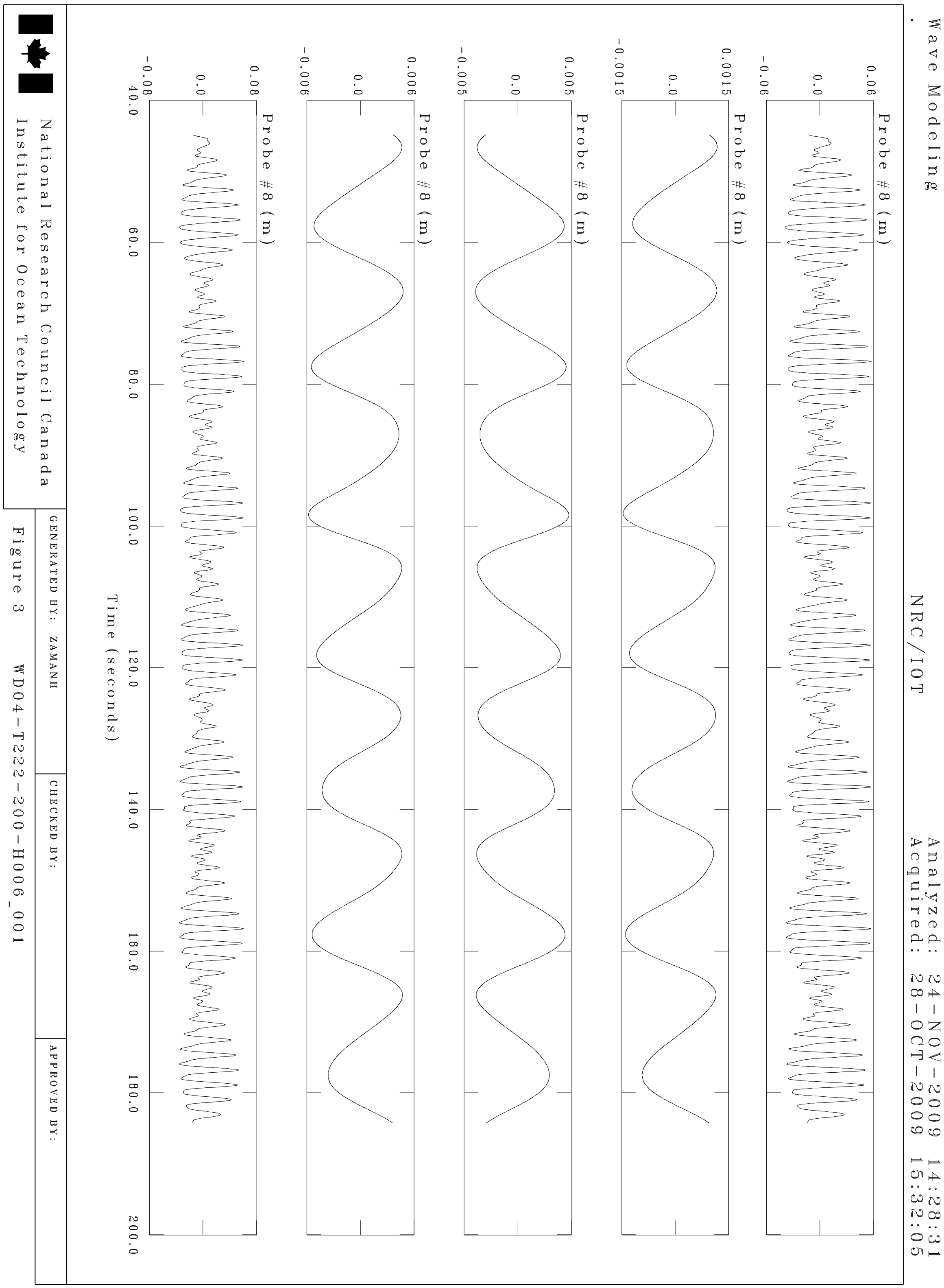

Fig. 32e LWAVE analysis of measured eta at Probe-8; Second-order generation
(*Case-3, h=0.4m,* T_1*=2.22s,* T_2*=2.0s,* H_1*=0.06m and* H_2*=0.06m*)

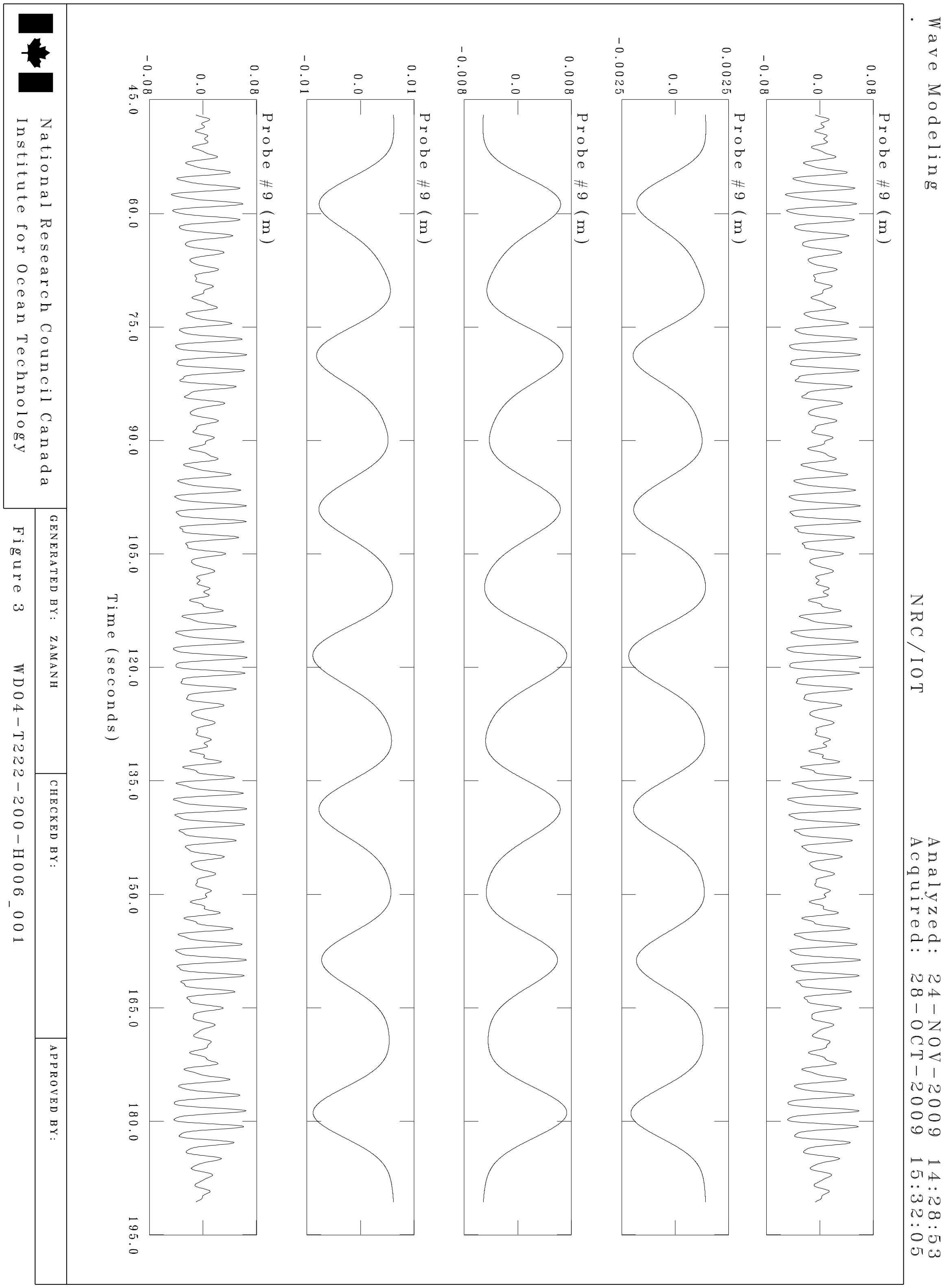

Fig. 32f LWAVE analysis of measured eta at Probe-9; Second-order generation (*Case-3, h=0.4m,* T_1*=2.22s,* T_2*=2.0s,* H_1*=0.06m and* H_2*=0.06m*)

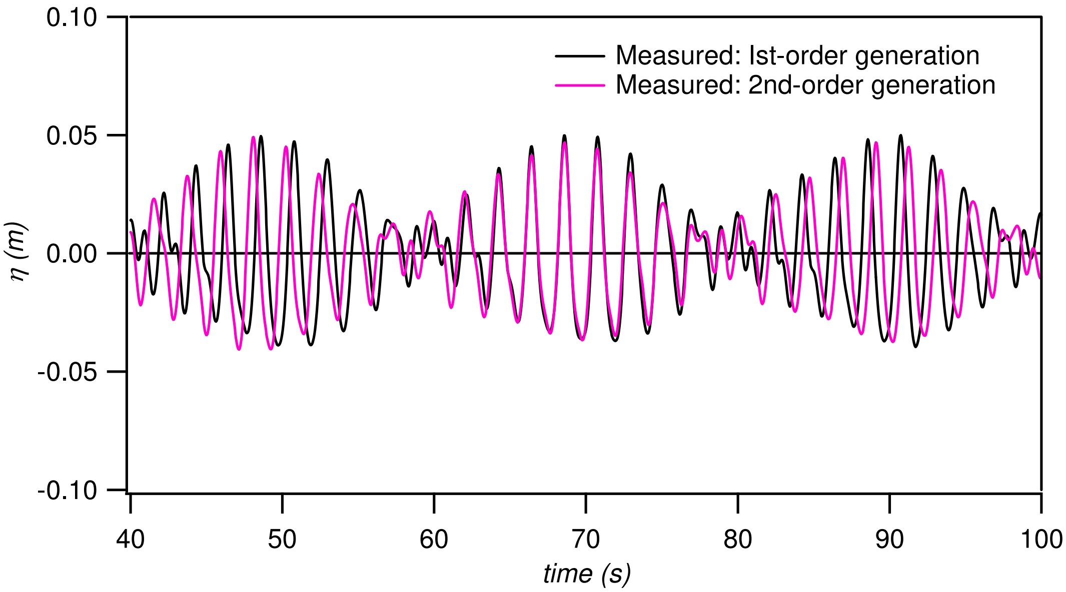

Fig. 33a: Comparisons of the measured waves amplitudes at Probe-1
(h=0.4m, T1=2.22s, H1=0.06m, T2=2.0s and H2=0.06m)

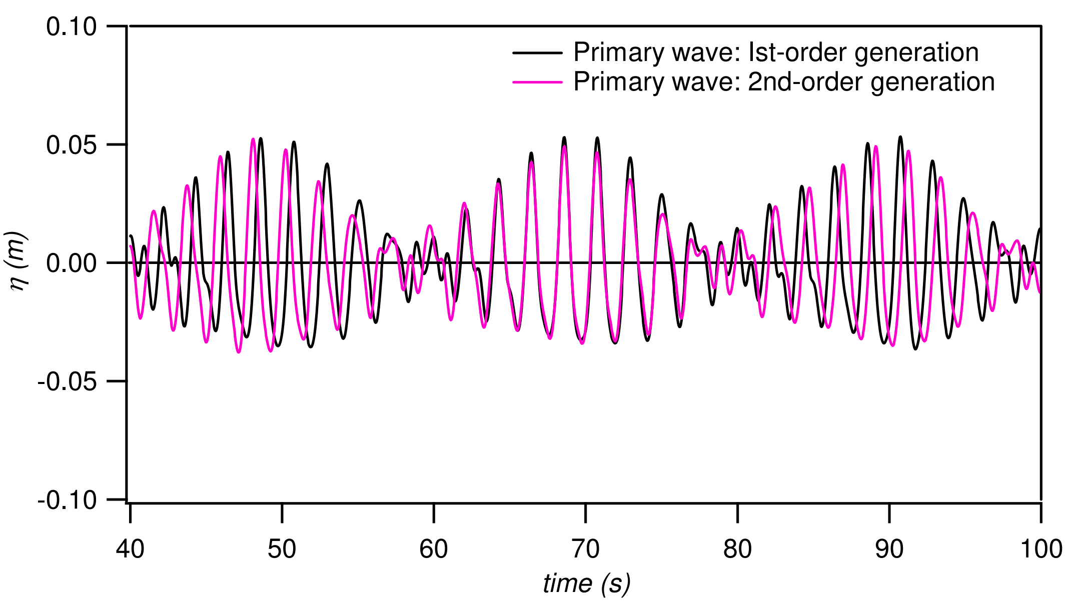

Fig. 33b: Comparisons of the primary waves amplitudes at Probe-1
($h=0.4m$, $T_1=2.22s$, $H_1=0.06m$, $T_2=2.0s$ and $H_2=0.06m$

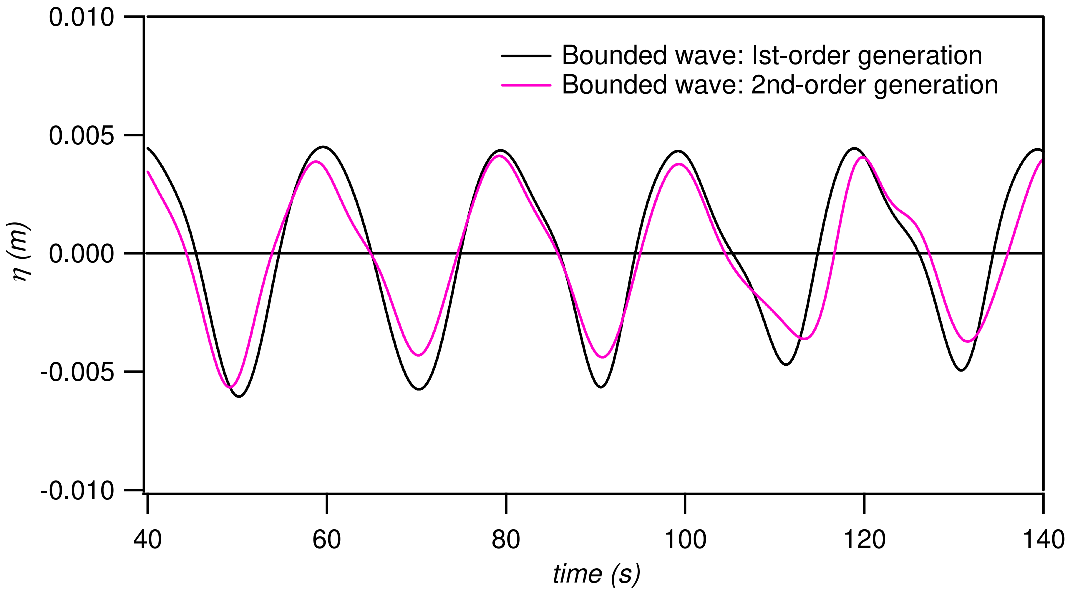

Fig. 33c: Comparisons of the bounded waves amplitudes at Probe-1
(*h=0.4m, T_1=2.22s, H_1=0.06m, T_2=2.0s and H_2=0.06m*)

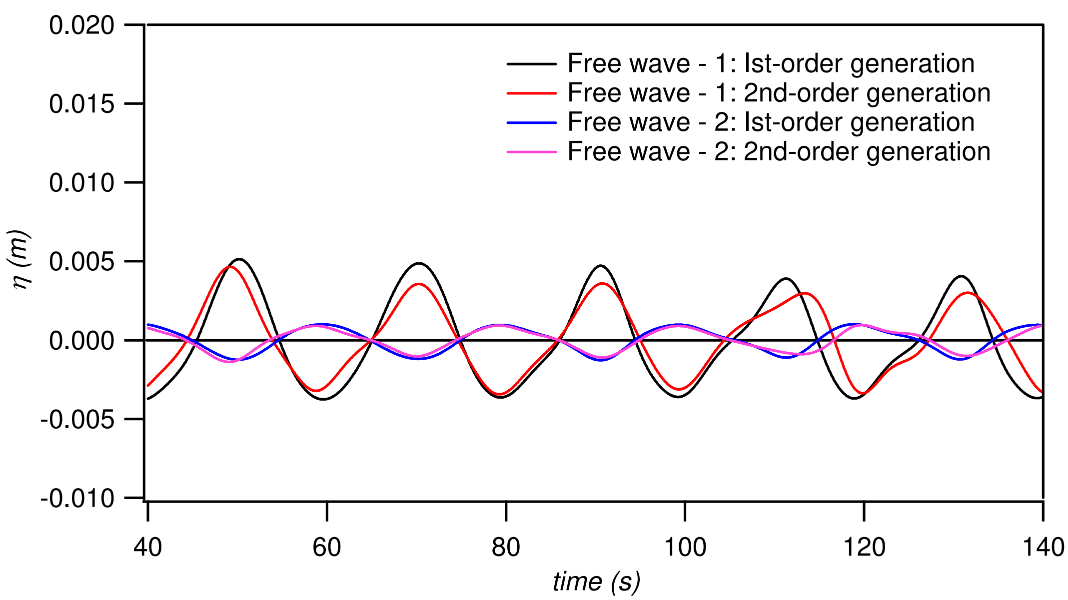

Fig. 33d: Comparisons of the free waves amplitudes at Probe-1
(*h=0.4m, T_1=2.22s, H_1=0.06m, T_2=2.0s and H_2=0.06m*)

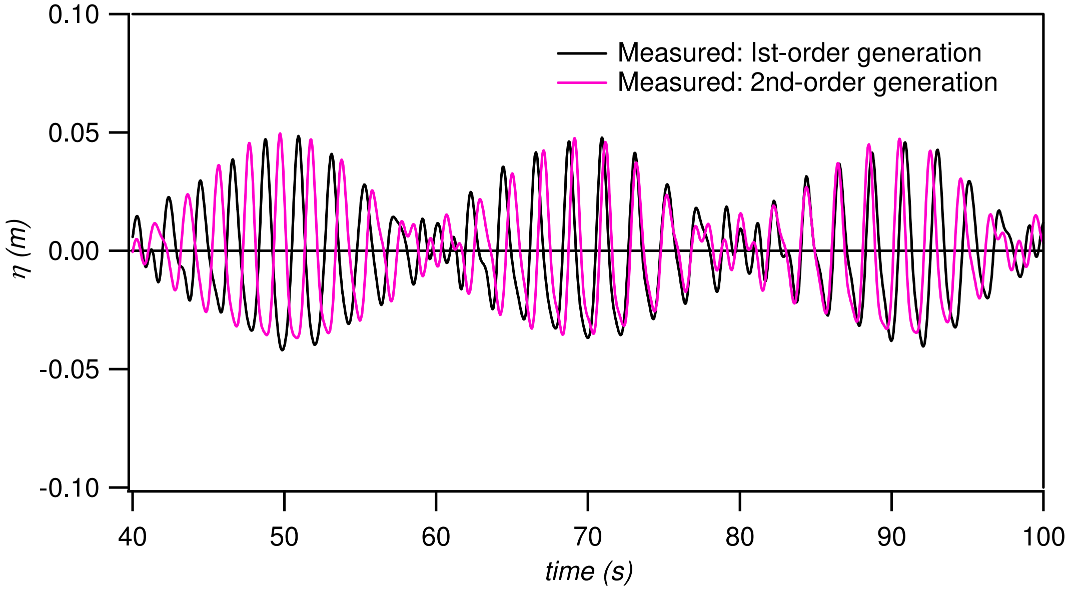

Fig. 34a: Comparisons of the measured waves amplitudes at Probe-2
(*h=0.4m*, T_1*=2.22s*, H_1*=0.06m*, T_2*=2.0s and* H_2*=0.06m*)

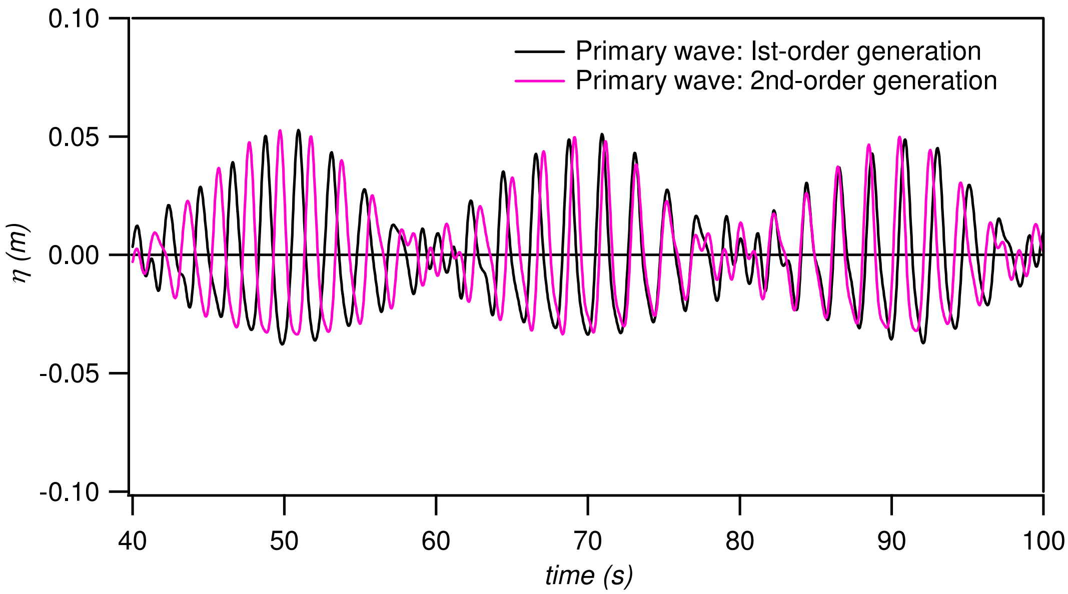

Fig. 34b: Comparisons of the primary waves amplitudes at Probe-2
(*h=0.4m*, T_1*=2.22s*, H_1*=0.06m*, T_2*=2.0s and* H_2*=0.06m*)

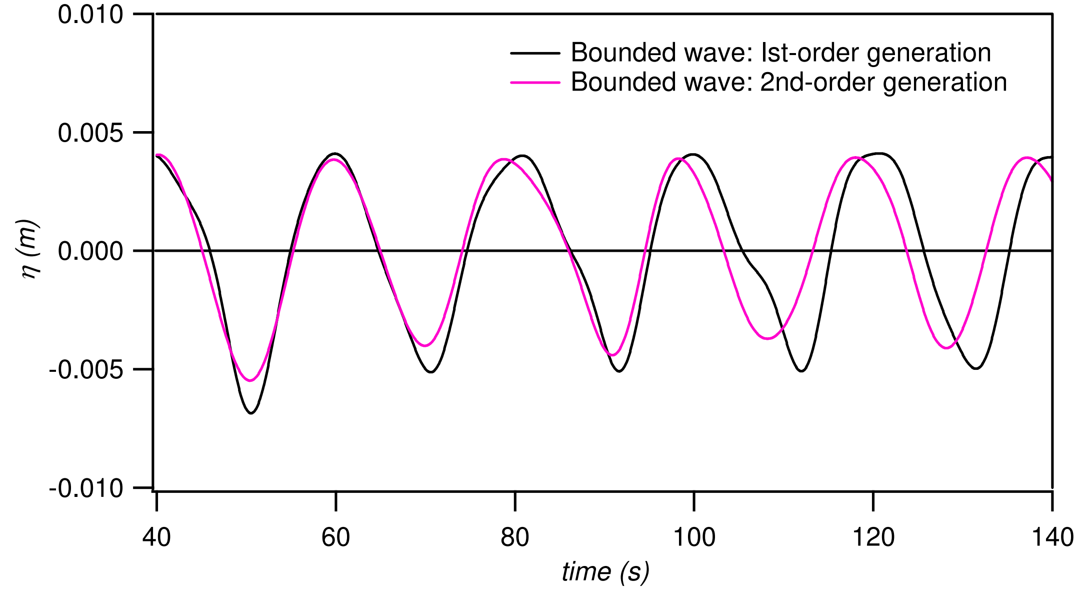

Fig. 34c: Comparisons of the bounded waves amplitudes at Probe-2
(*h=0.4m, T_1=2.22s, H_1=0.06m, T_2=2.0s and H_2=0.06m*)

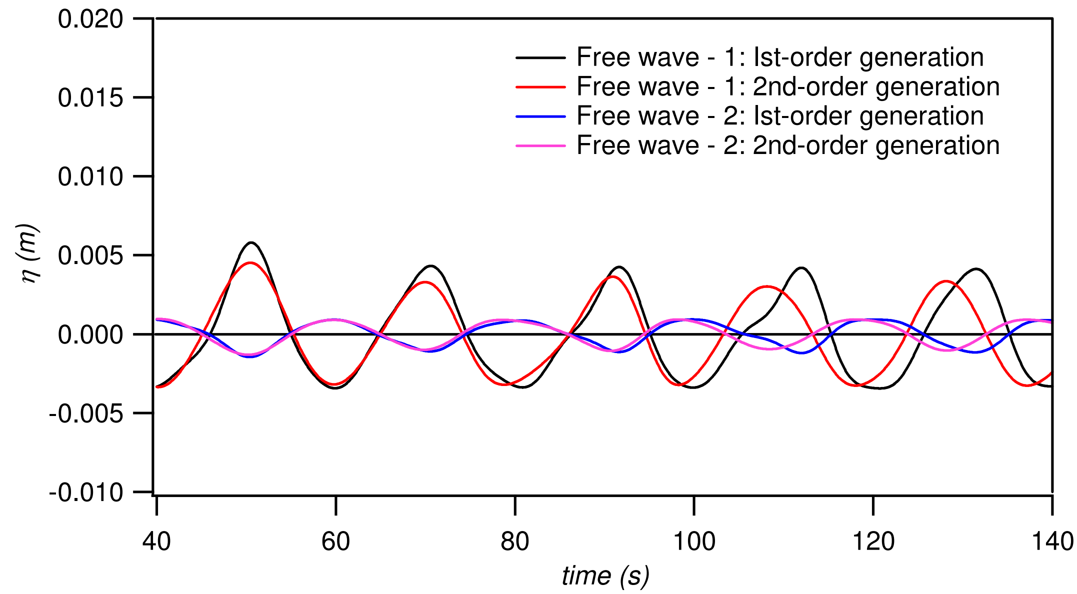

Fig. 34d: Comparisons of the free waves amplitudes at Probe-2
(*h=0.4m, T_1=2.22s, H_1=0.06m, T_2=2.0s and H_2=0.06m*)

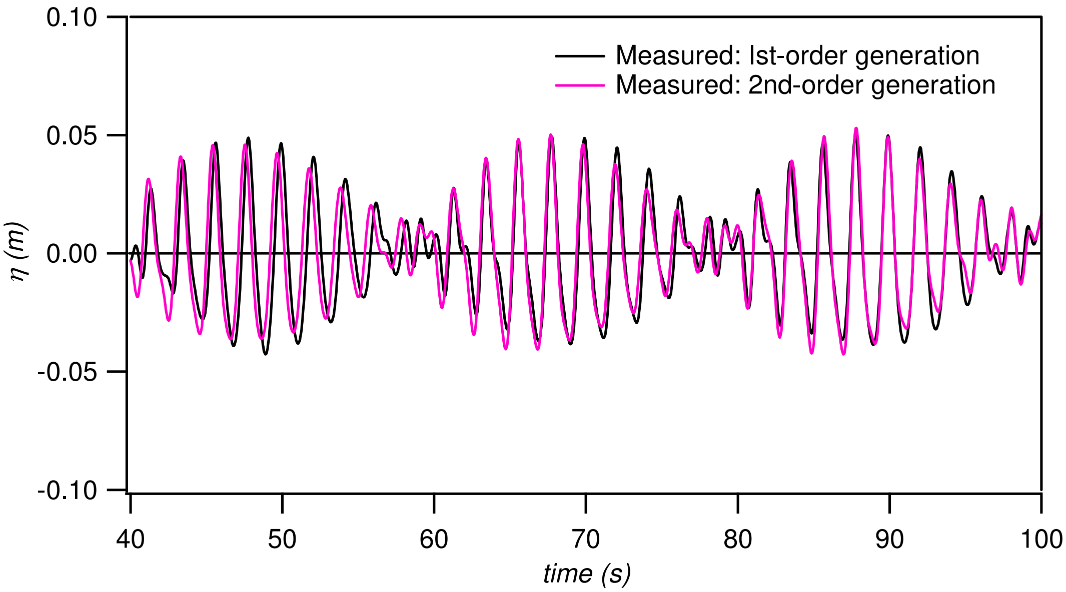

Fig. 35a: Comparisons of the measured waves amplitudes at Probe-3
(*h=0.4m, T1=2.22s, H1=0.06m, T2=2.0s and H2=0.06m*)

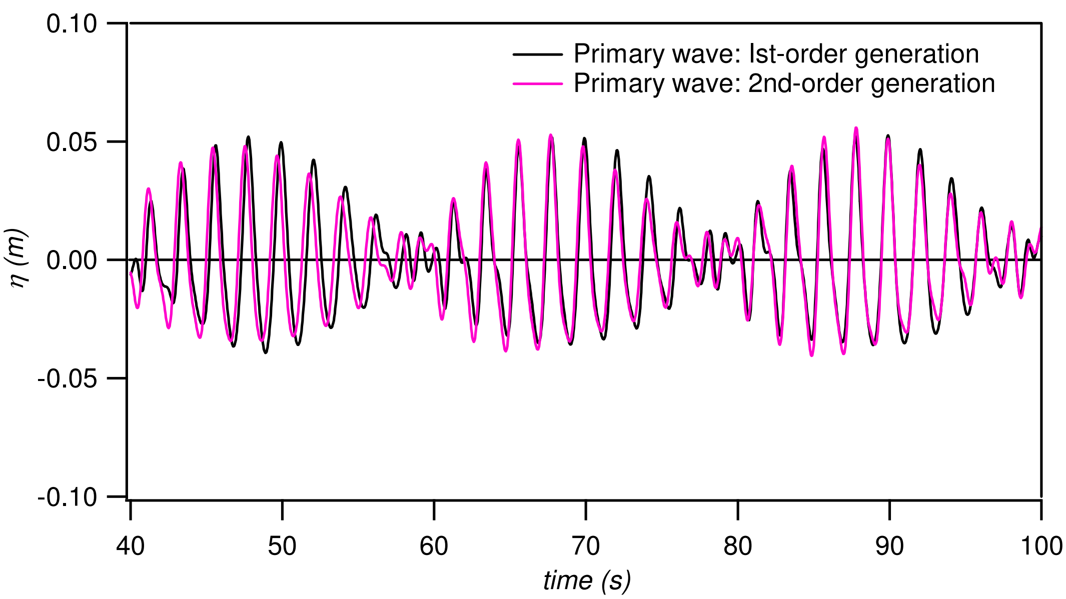

Fig. 35b: Comparisons of the primary waves amplitudes at Probe-3
($h=0.4m$, $T_1=2.22s$, $H_1=0.06m$, $T_2=2.0s$ and $H_2=0.06m$)

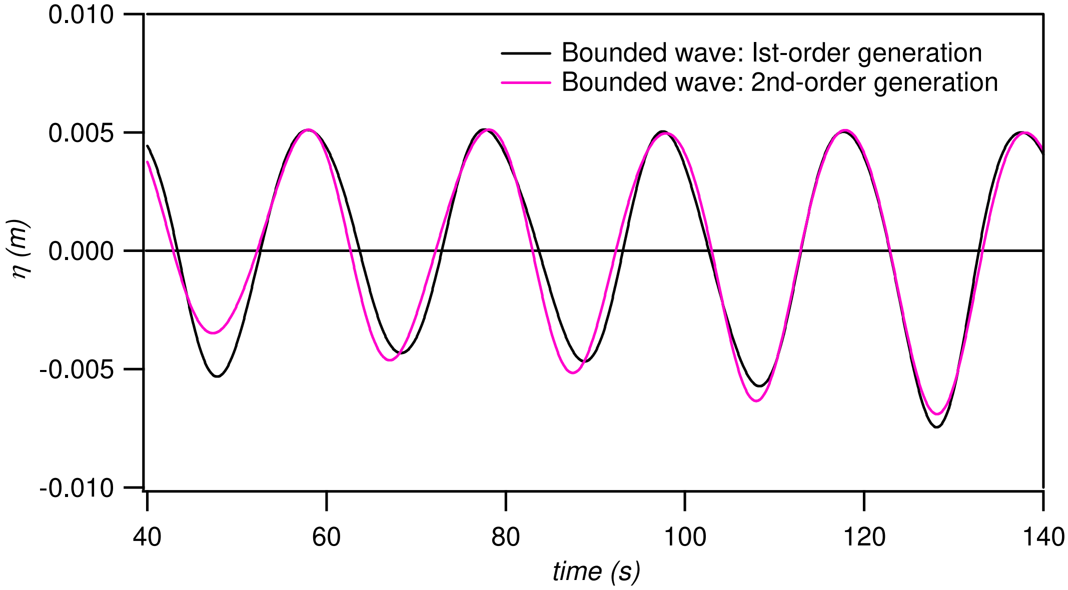

Fig. 35c: Comparisons of the bounded waves amplitudes at Probe-3
(*h=0.4m, T_1=2.22s, H_1=0.06m, T_2=2.0s and H_2=0.06m*)

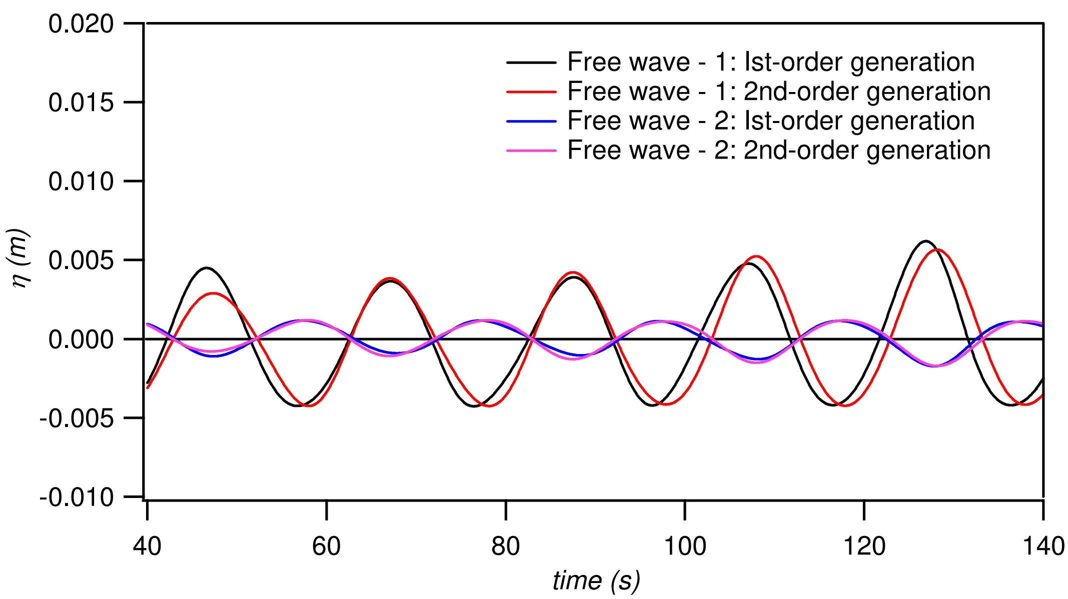

Fig. 35d: Comparisons of the free waves amplitudes at Probe-3
(*h=0.4m, T_1=2.22s, H_1=0.06m, T_2=2.0s and H_2=0.06m*)

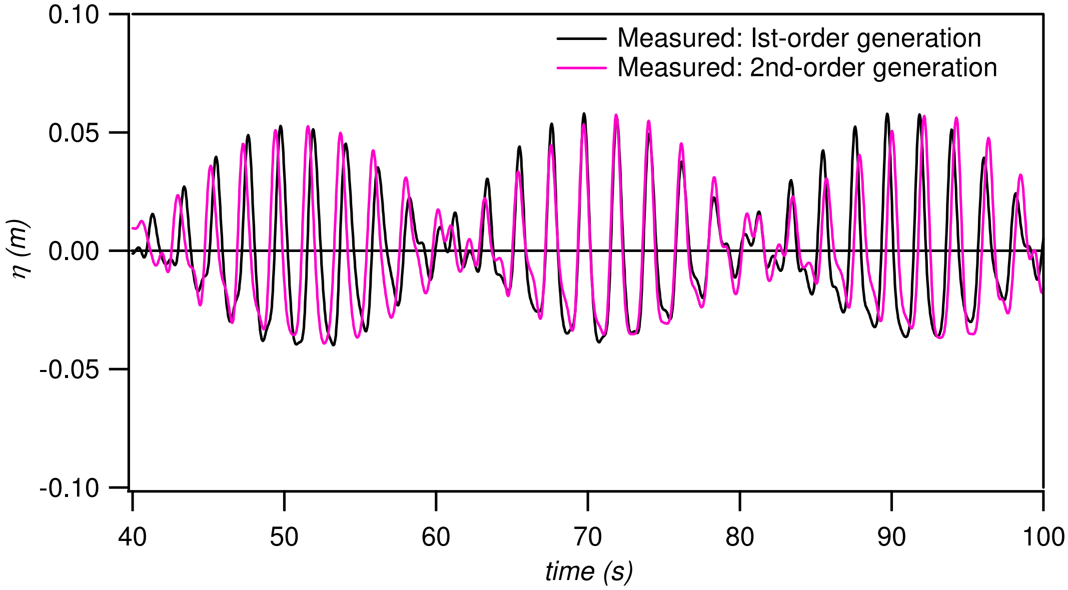

Fig. 36a: Comparisons of the measured waves amplitudes at Probe-8
(*h=0.4m, T_1=2.22s, H_1=0.06m, T_2=2.0s and H_2=0.06m*)

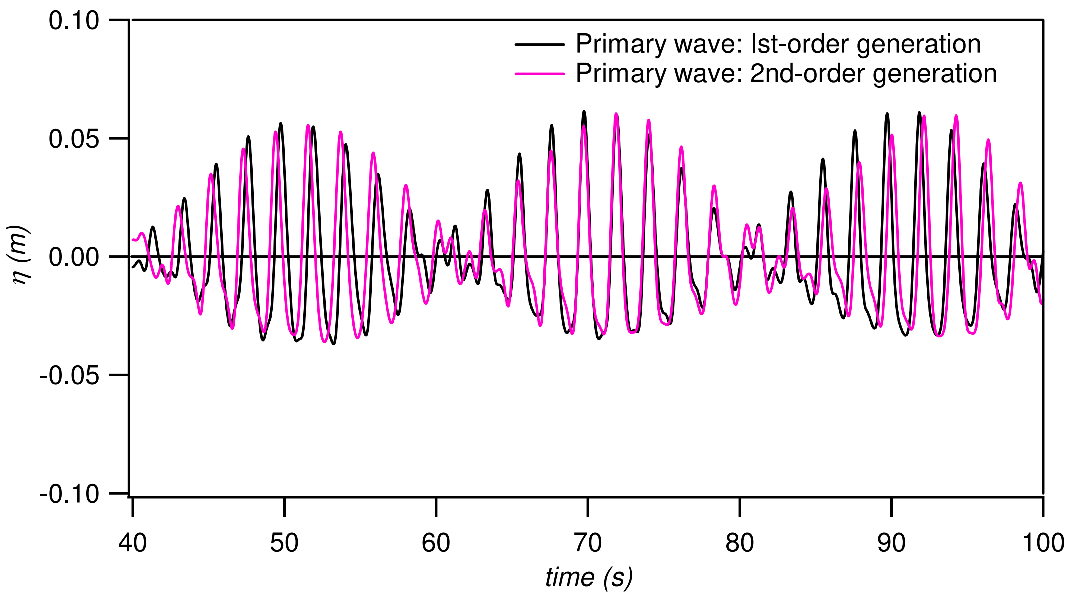

Fig. 36b: Comparisons of the primary waves amplitudes at Probe-8
(*h=0.4m, T_1=2.22s, H_1=0.06m, T_2=2.0s and H_2=0.06m*)

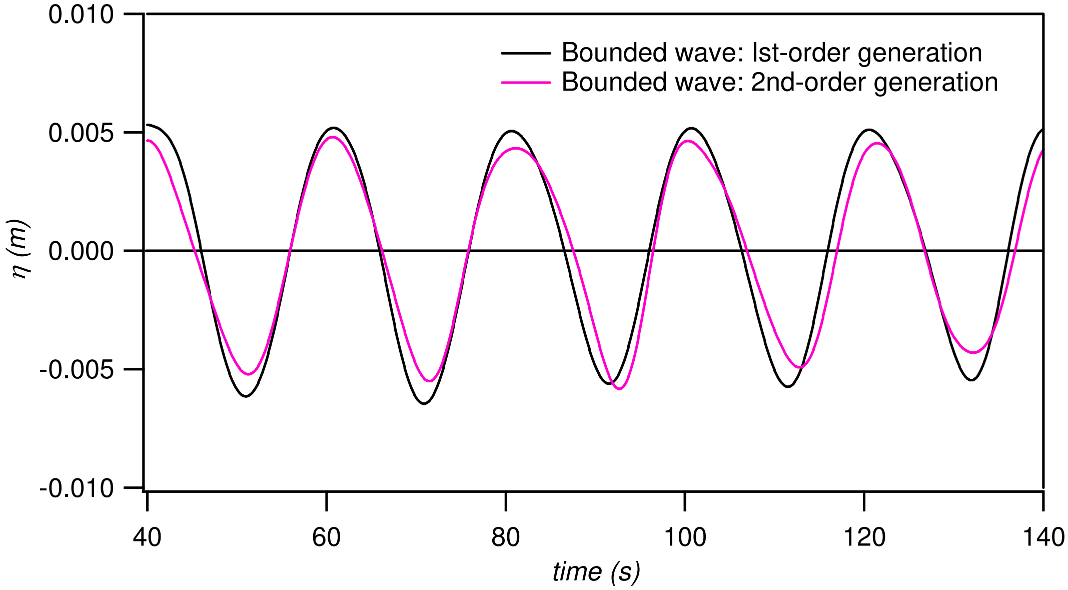

Fig. 36c: Comparisons of the bounded waves amplitudes at Probe-8
(*h=0.4m, T_1=2.22s, H_1=0.06m, T_2=2.0s and H_2=0.06m*)

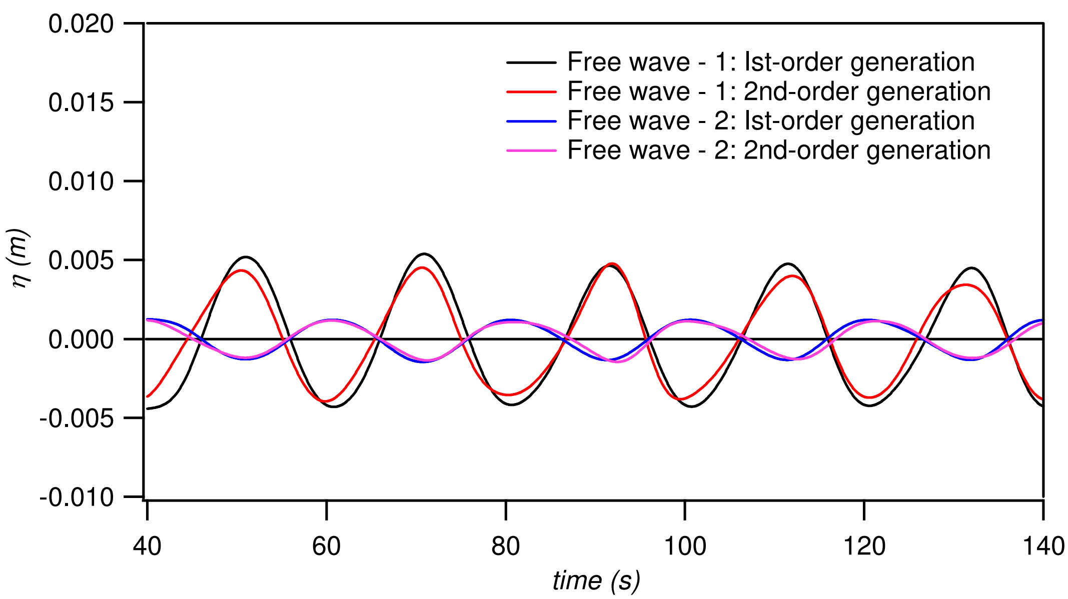

Fig. 36d: Comparisons of the free waves amplitudes at Probe-8
(h=0.4m, T_1=2.22s, H_1=0.06m, T_2=2.0s and H_2=0.06m)

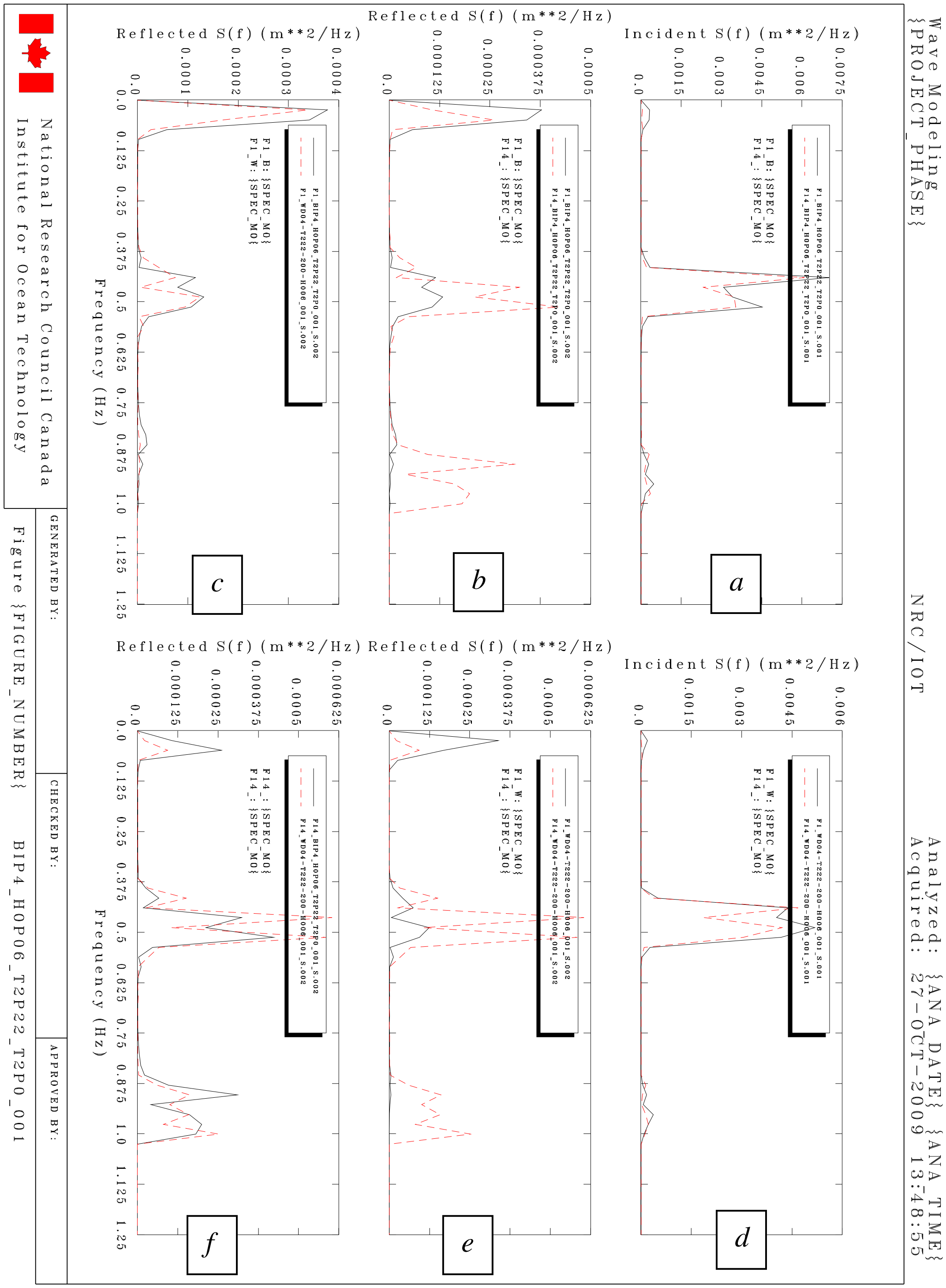

Fig. 37 Reflection analysis with respect to Probe-1 and Probe-14 for Case-3. Comparisons of: (a) incident waves and (b) reflected waves for First-order generation at Probe-1 and Probe-14, (c) reflected waves for First- and Second-order generation a Probe-1, (d) incident waves and (e) reflected waves for Second-order generation at Probe-1 and Probe-14, (f) reflected waves for First- and Second-order generation at Probe-14.

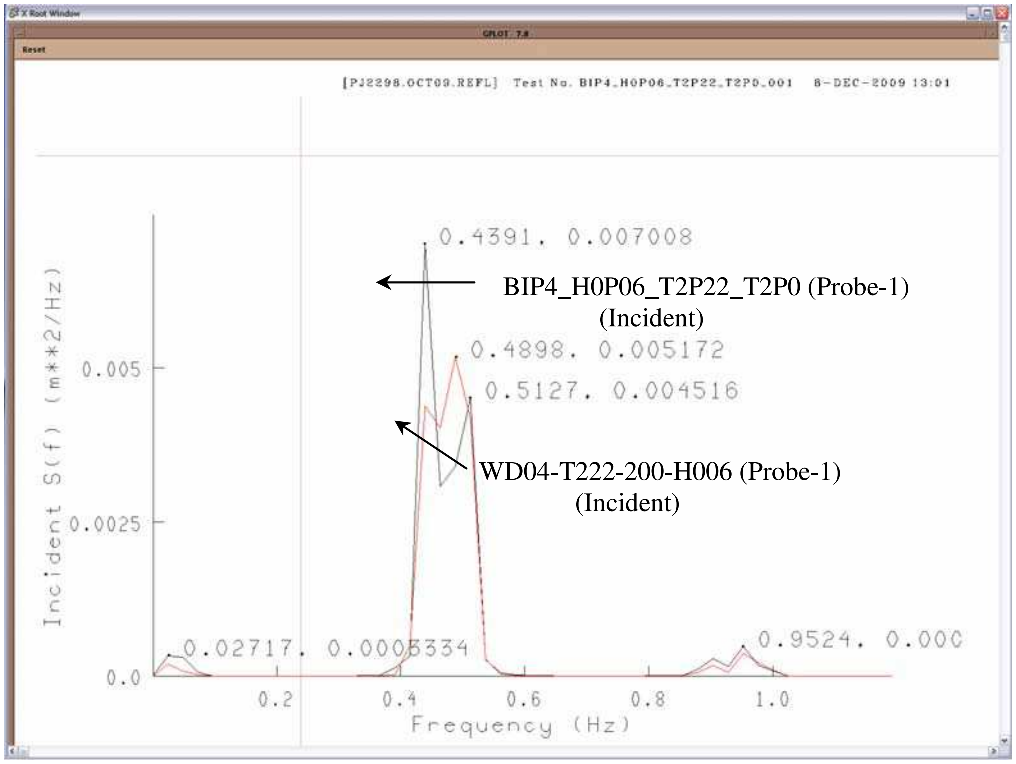

Fig. 38a Comparison of the First- and Second-order incident waves energies at Probe-1 for Case-3

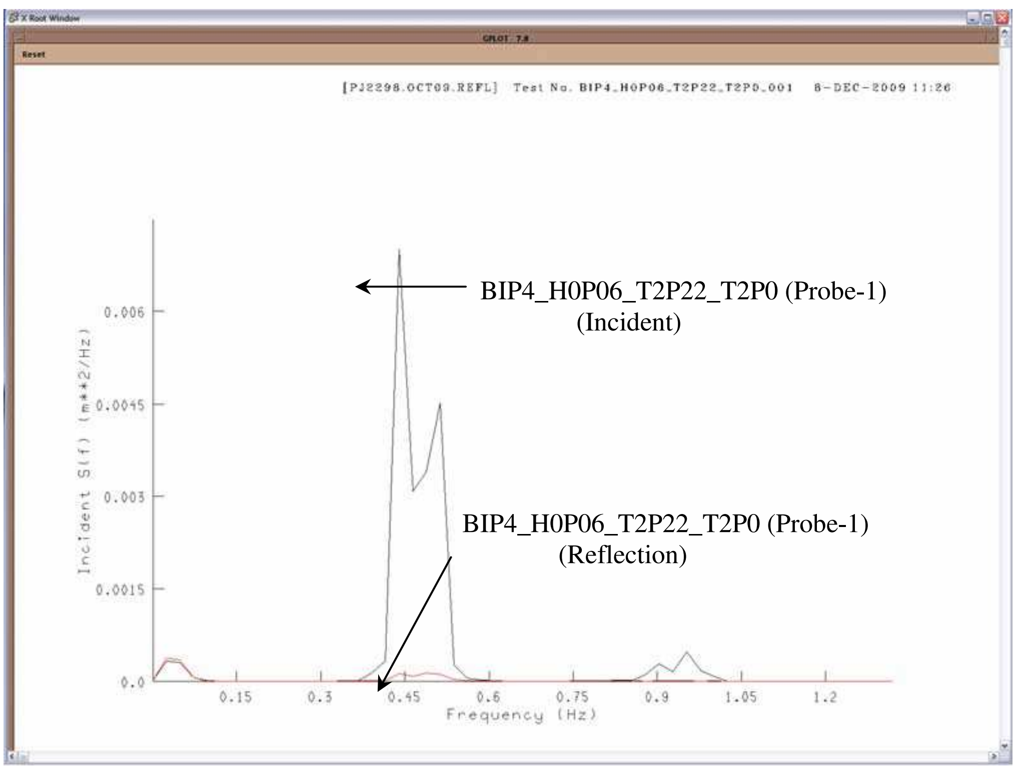

Fig. 38b First-order incident wave and reflected wave energies at Probe-1 for Case-3

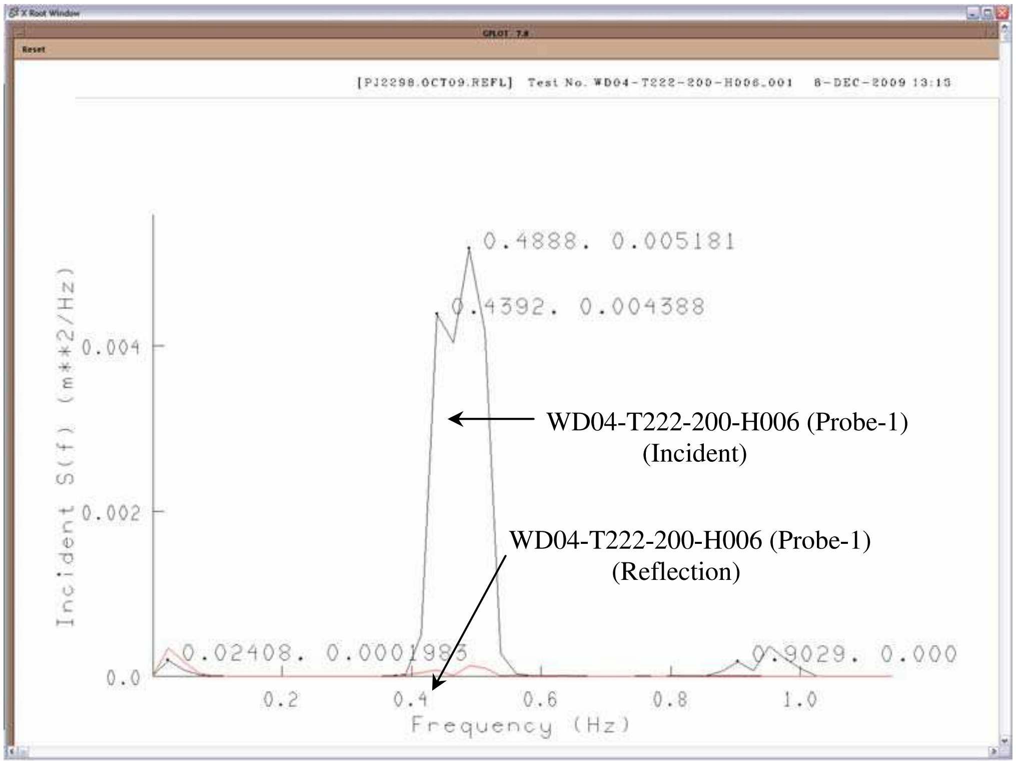

Fig. 38c Second-order incident wave and reflected wave energies at Probe-1 for Case-3

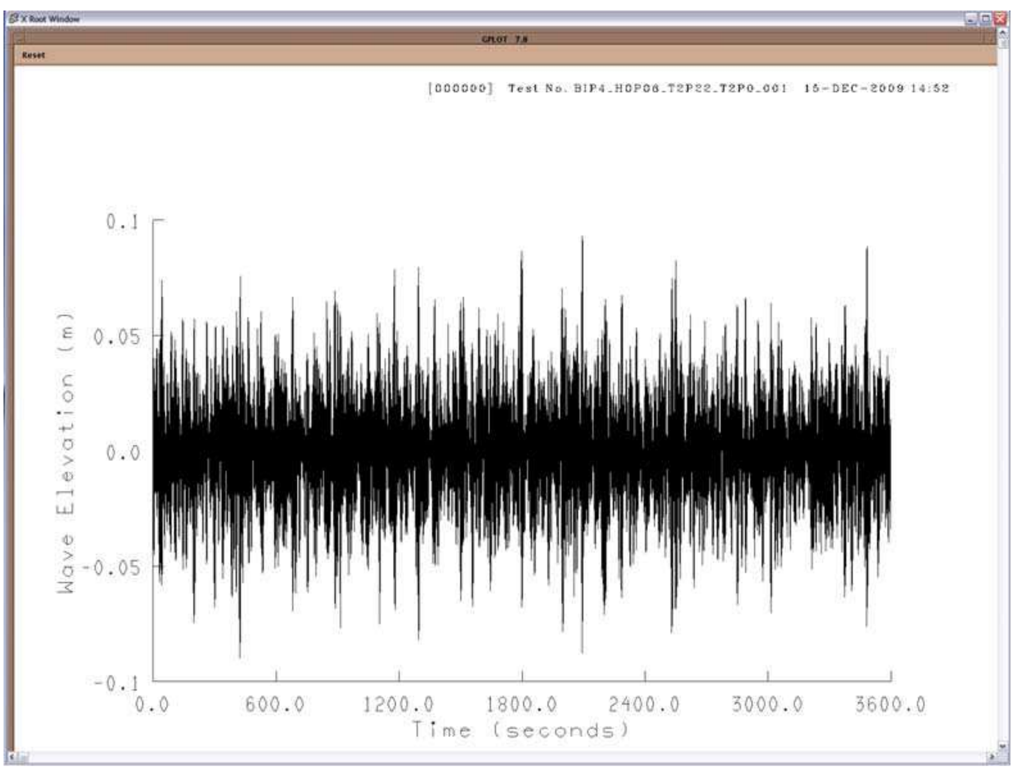

Fig. 38d Surface elevation from first-order incident wave spectrum at Probe-1 for Case-3
(Inverse FFT used)

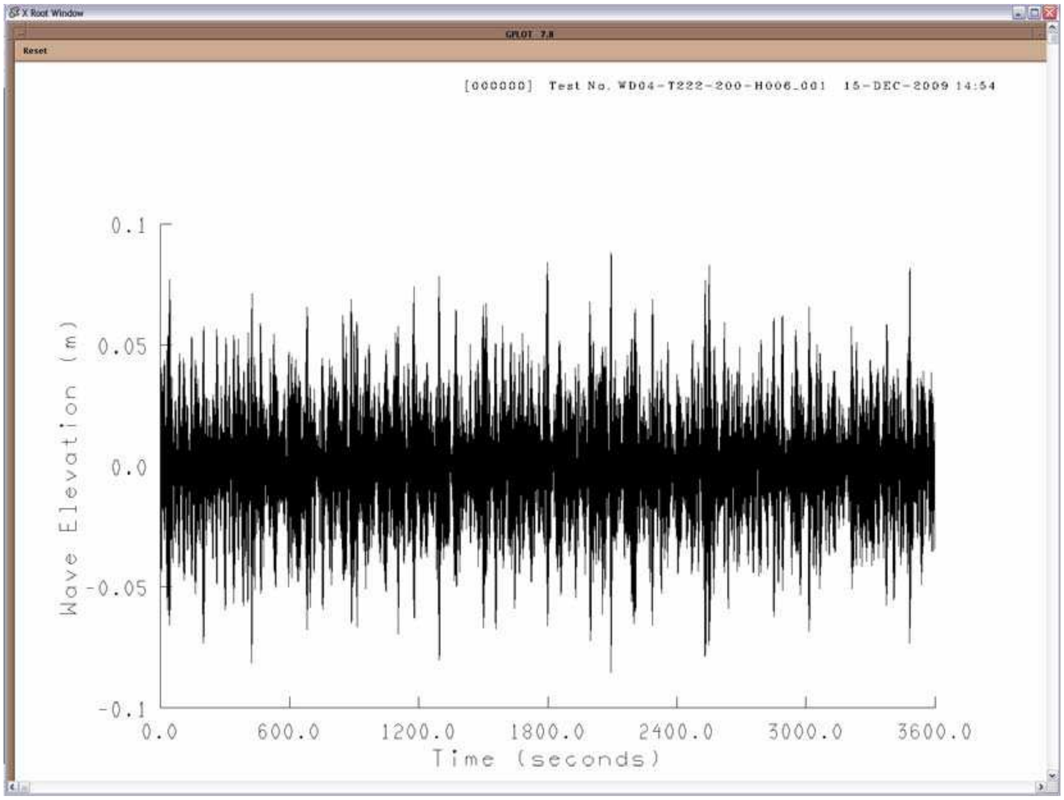

Fig. 38e Surface elevation from Second-order incident wave spectrum at Probe-1 for Case-3 (Inverse FFT used)

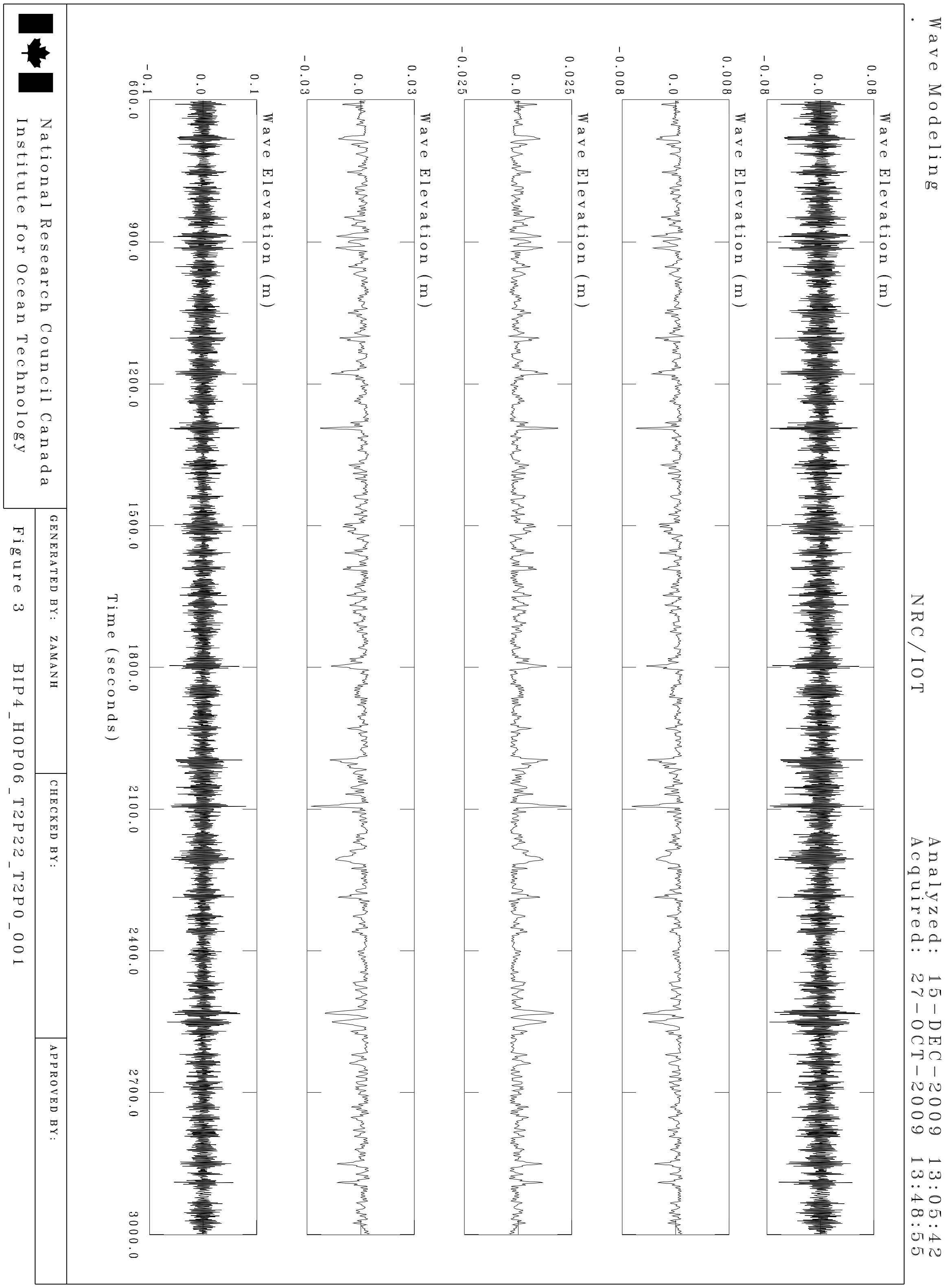

Fig. 38f LWAVE analysis on the surface elevation shown in Fig. 37e.
(Case-3, First-order generation, Probe-1)

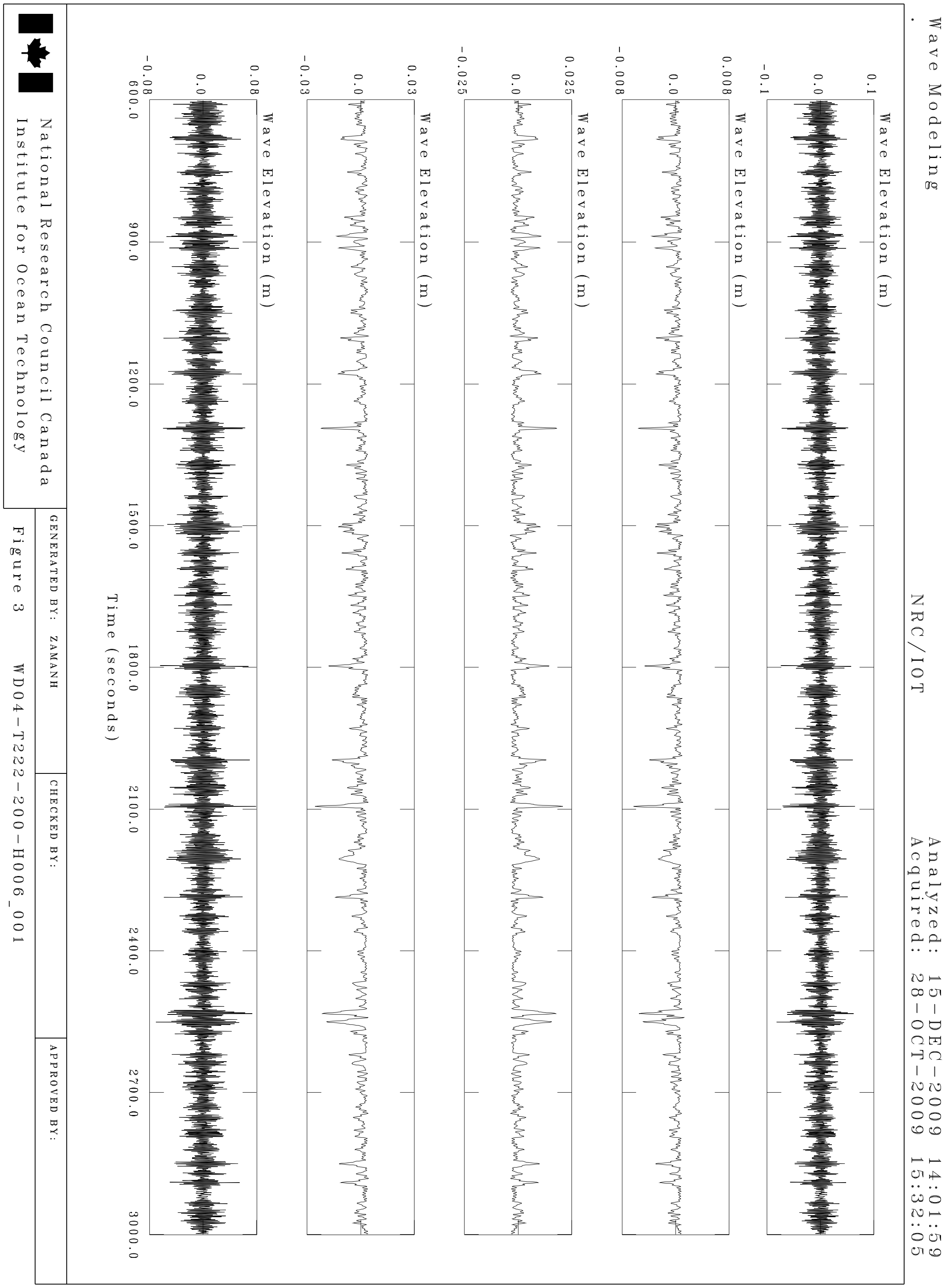

Fig. 38g LWAVE analysis on the surface elevation shown in Fig. 37f.
(Case-3, Second-order generation, Probe-1)